

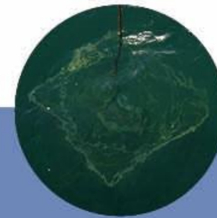

A modeling intercomparison for the North Sea with a view to methane dispersion

Janine Nauw and Henk de Haas

NIOZ Royal Netherlands Institute for Sea Research

A modeling intercomparison for the North Sea with a view to methane dispersion

Janine Nauw and Henk de Haas (Royal NIOZ, the Netherlands)

25 February, 2013

Executive summary

Stratification

As part of the methane released at site 22/4b will be dissolved locally, it will be transported by the local currents and therefore strongly dependent on the hydrodynamics of the North Sea. The hydrodynamics of the North Sea is dominated by tidally driven currents, but also determined by currents forced in the North Atlantic Ocean. Due to summertime heating the northern part of the North Sea becomes stratified. In autumn cooling to the atmosphere, causes the stratification to break down slowly until at a certain moment that the mixing induced by tides and storms mixes the entire water column. During the period of stratification, the water column is divided into two layers, which can and will move independently.

3D circulation

To be able to determine the fate of methane in the North Sea, it is imperative to accurately know the 3D circulation, not only at the site where methane is released, but also the entire surroundings (meaning the entire North Sea) as currents will transport the dissolved methane elsewhere. The most obvious way to determine the 3D circulation is by applying a numerical hydrodynamic model to the North Sea as a whole. The numerical model should be 3-dimensional; otherwise it is impossible to correctly simulate the seasonal stratification in the northern North Sea, which is essential to determine the currents in the lower layer in which the methane is being released from the sea floor.

Inter- and interannual variability

Besides the seasonal stratification, other complicated processes take place in the North Sea. Due to the tidal currents a long-term average anti-clockwise circulation arises. Wind forcing over the North Sea may strengthen this anti-cyclonic circulation; however, it can also have the opposing effect and halt this circulation, or even turn it around into a clockwise rotating flow, depending on the wind speed and direction. Wind driven storm surges may push water from the North into the southern part of the North Sea, which have led to a significant amount of flooding occurrences. Climate change or variability adds its part to the complexity of the circulation in the North Sea. The North Atlantic Oscillation (NAO) causes variability in the wind stress and direction over the North Sea due to variations in the large scale pressure system over the North Atlantic. A positive (negative) NAO is associated with stronger (weaker) than normal westerly winds. Under NAO+ situations the circulation in the North Sea strengthens and long-term mean currents at site 22/4b are stronger and directed eastward, whereas they weaken during NAO- conditions and are directed northeastward. Besides this, the NAO also influences the Sea Surface Temperature (SST) of the North Sea. High positive correlations were found between the SST at site 22/4b and the NAO index. Another source of variability on timescales from annual to interannual is brought about by the currents entering the northern part of the North Sea. Especially, the Fair Isle Current (FIC), entering the North Sea between the Orkney and the Shetland Islands, may be significant as it passes (on average) site 22/4b and displays strong variability in terms of temperature and salinity.

Numerical modeling

In general, 3D hydrodynamic models all solve the same basic equations. However, already in discretizing the equations differences occur. Both in the horizontal (Cartesian, Spherical, curvilinear), but mostly in the vertical (z-, σ-, hybrid or adaptive coordinates) different discretizations have been applied. Then, many different advection schemes have been developed. From comparison studies with different advection schemes, it was shown that the higher the order of the advection scheme, the better the horizontal, but also the vertical gradients were resolved. In fact, results with higher order advection schemes were qualitatively comparable to those with lower order advection schemes at higher resolution. Increasing the resolution or the order of the advection scheme are both at the cost of computational effort. Furthermore, subgrid scale processes need to be incorporated somehow to determine the transport of energy from larger to smaller scale currents to dissipation, in other words turbulence must be modeled. A suite of choices can be made with respect to the turbulence closure modeling, from simple parameterizations, relating turbulent processes to large scale mean flow variables, via one- and two-equation models, to second order models in which a large number of equation are solved to estimate the turbulent fluxes. Obviously, the more complex the turbulence closure, the higher the computational effort, but increasingly better results have been observed with the complexity of the turbulence closure model.

All of the above are characteristics of the core of each model and can in general not easily be changed, except if a model has a modular setup in which a choice for an advection scheme and/or turbulent closure model is built in, such as in the GETM-GOTM setup, but this approach is being applied more and more. Other differences between the models occur due to different horizontal and vertical resolution and in many cases a different source for the external forcing, such as the meteorological forcing, the river discharge and the forcing at the open boundary of the model.

Model comparison

In total 16 different 3D numerical models have been discussed, which were involved in one or more intercomparison studies; a list is provided in Table 1. Nine models were compared in the NOMADS 1 (NOrth Sea Model Advection-Dispersion Study). The main conclusion from this study was, that all models reproduced acceptable features of the circulation, that the variability in the hydrodynamics was large and that the major variation could be attributed to the different forcing sets applied in the different models. Besides this, the NOMADS 1 study showed that it proved extremely difficult to quantify the difference between model results. Particularly, errors in tidal and storm surge predictions are not useful, because sea level elevation is an integrated quantity and is therefore not representative for the 3d circulation. Mean volume fluxes and (passive) tracer (e.g. temperature and salinity) variations are more favorable quantities to assess. In NOMADS 2, the differences in forcing sets have been removed as much as possible. The main result was that the higher resolution models did a slightly better job than the coarser ones, but that the model simulations were much more comparable then during NOMADS 1.

From three other intercomparison studies with HAMSOM, which was suggested to be ranked amongst the best models in NOMADS, it could be concluded that model results from ISPRAMIX and GETM were comparable to those of HAMSOM. GETM showed improvements with respect to HAMSOM in terms of reproducing the observed seasonal stratification, due to its higher order turbulence closure scheme and even showed additional improvements, if higher order advection schemes were chosen in the simulation.

Another comparison study between FOAM and POLCOMS showed that FOAM was significantly better in representing the tides and in reproducing the observed seasonal tidal fronts in the North Sea. Moreover, FOAM simulates the observed surface – bed temperature difference in summer well, or in other words the seasonal stratification.

In the CONMAN project, the ROMS and HYCOM model on the one hand were compared with MIPOM on the other hand in order to assess which of the former could replace the latter as operational model at met.no. Since December 1, 2012, ROMS is the operational model at met.no, which summarizes the main conclusions from the CONMAN project. ROMS results had similar current strengths and variability in the northern North Sea as MIPOM, where HYCOM significantly underestimated these. Also observations of surface and near-bed salinity and temperature were reproduced best by ROMS. In a follow-up comparison between ROMS and MIPOM, it was shown that it is necessary to have an eddy-resolving resolution model to capture the mesoscale eddy activity properties, which may be essential to simulate the pathways of particles.

Methane

Methane dispersion in the North Sea is complicated due to the seasonal stratification. Most of the methane released in bubbles dissolves in the water column; estimates are that only 4% of the initially released methane reaches the surface in the gas phase. The flux of dissolved methane to the surface and the subsequent release to the atmosphere is high during well-mixed stormy autumn of winter conditions. However, methane that is trapped under the summer thermocline may be transferred horizontally over long distances to shallower areas and exchanged with the atmosphere elsewhere.

Results from particle tracking models in the North Sea essentially show that the underlying 3D hydrodynamic model dictates the outcome of the pathways. In coarse resolution time-averaged models, transport paths are unrealistically smooth. Whereas, in more complicated settings, transport paths compare more-and-more to observed tracks of in-situ released drifter buoys.

Conclusion

Based on this literature review, this lists the state-of-the-art models to be GETM, FOAM and ROMS (not necessarily in that order). Moreover, as computer power increases, modelers can run on increasingly higher resolution. A group at CEFAS is working on a new setup with GETM of the northwestern European shelf at 6-7 km resolution. And at met.no, a triple nested system with ROMS in currently in use as the operational ocean weather forecast model. The smallest domain of the Norwegian Coastal area, which just incorporates de location of site 22/4b, is run at 4 km resolution.

Nowadays, 3D hydrodynamic models are built in such a way that it allows the user to choose between a suite of option with respect to the resolution, but also the advection scheme and turbulence closure scheme applied. With this modular approach it is also relatively easy to couple other modules to the 3D hydrodynamic model, such as particle tracking, tracer or even full biogeochemical models. As to the fate of methane; coupling a particle tracking model to a state-of-the-art 3D hydrodynamic model will already provide possible pathways for the methane. However, if the fate of methane is to be determined from gas seeps, a bubble dissolution module, which provides the amount of methane dissolved at any location in the water column should be coupled and additional a biogeochemical module should be written in which the bacterial oxidation of methane is well-represented and methane is one of the inorganic nutrients that is explicitly calculated as a source. Then, instead of making just one simple simulation under the most realistic forcing conditions (meteorology and boundary conditions), an ensemble of simulations should be performed under slightly different initial and forcing conditions. This is an approach that has already been used for many years in numerical weather prediction. The outcome of this ensemble forecasting will be a range of pathways and the most probable pathway of methane.

Contents

Introduction

(Part of) the gas phase methane released from different (bottom) sources in the North Sea will dissolve and will be transported with the currents. The fate of the dissolved methane thus ultimately relies on the hydrodynamics in the North Sea. The North Sea is a complex system, which is driven by tidal forcing, wind and heating/cooling at the sea surface. Moreover, rivers introduce significant amounts of fresh water into the North Sea basin. All in all, the North Sea displays tidally driven currents, wind driven setup, waves. Due to heating and freshwater influence (part of) the North Sea can become stratified introducing baroclinic (or depth dependent) currents that increase the complexity of the hydrodynamics even further.

The most obvious way to identify the fate of the dissolved methane is to apply a hydrodynamic model to the greater North Sea, which is coupled to a biogeochemical model that handles the dissolution and the role of methane in the marine carbon cycle. This report will give an overview of state-of-the-art modeling tools currently available to determine the hydrodynamics in the greater North Sea and will discuss differences between them. It is beyond the scope of this report to discuss all models of the North Sea, because many models only focus on a (small) specific part of the North Sea, or a certain phenomenon. Within these models assumptions are made to simplify the problem at hand, since the objectives of these models is not to describe the hydrodynamics of the North Sea as accurately as possible. For instance, to describe the tidal behavior within the North Sea it is not necessary to know the exact vertical (baroclinic) current profiles; knowing the depth averaged currents is already satisfactory. For this specific problem depth-averaged or 2-D hydrodynamic models have been constructed. For the scope of this report the vertical structure is essential for the fate of the (dissolved) methane in the North Sea, since the model must be able to reproduce a (seasonal) thermocline. Therefore, we will focus on 3D hydrodynamic models only.

Site 22/4b in the northern part of the North Sea is characterized by seasonal stratification during the summer period. The circulation in the upper and lower layer may be (and have shown to be) different due to baroclinic processes. 2-D hydrodynamic models are inherently unable to reproduce such layered structure and therefore will not be able to predict the fate of methane released from site 22/4b, at least not in summer.

In this report we wish to assess which models can be used to understand or predict the fate of methane released from site 22/4b. For this purpose, a literature review was conducted on 3D hydrodynamic models applied in the North Sea context. Focus will be on the ability of the models to establish the North Sea circulation realistically, as the current structure determines the transport path of parcels of water passing site 22/4b. First, a detailed overview is given on the current knowledge of the North Sea circulation, its variability and (variability in) its external forcing. Subsequently, the mathematical modeling of the hydrodynamic transport equation will be discussed and especially the inherently different approaches that can be taken in modeling. The resulting differences in hydrodynamic behavior are demonstrated in the various intercomparison studies performed. The fate of methane as it is released into the water column either from bubbles or directly from pore waters is then explained in the two cases: the winter well-mixed and the summer stratified case. The fate of the dissolved methane in the water column can then be described by coupling a 3D hydrodynamic model to a tracer model, leading to the different pathways for water parcels containing methane at site 22/4b.

Basic features

The North Sea is one of the best and most intensively investigated seas in the world. Since the review by Otto et al. (1990) a still increasing amount of in-situ and remotely sensed data are gathered mostly stored at BODC (British Oceanographic Data Centre), DOD (German Oceanographic Data Centre), NODC (National Oceanographic Data Committee of the Netherlands) and PANGAEA (Data Publisher for Earth & Environmental Science) . Moreover, modeling efforts have been substantial over the last decades. Here, we present an overview of the current knowledge of the hydrodynamics of the North Sea and the most important driving forces.

The North Sea is a shallow Sea with an average depth of 80 m. The maximum water depth is in the Norwegian Trench, here water depth reach 800 m. To the north there is a broad connection to the North Atlantic Ocean. At this open end tidal motions are forced into the basin. Continental influences are primarily from fresh water discharge of the major rivers, but also from the Baltic Sea. The atmosphere influence plays an important role in the momentum, heat and to a lesser extent freshwater exchange.

Forcing

Tides and (storm) surges in the North Sea

The North Sea has specific bottom topography, which roughly decreases from 200 m deep at the northern entrance to 50 m deep at the Doggers bank and further decreases to 20 m off the Dutch-German coast. Therefore it is susceptible to resonance from tidal forcing at the open boundary to the north and water level rise during storm surges (especially from the north).

The most dominant tidal components in the North Sea are the semi-diurnal lunar tide, M_2, and the semi-diurnal solar tide, S_2. These have a period of 12:25 hours and 12 hours, respectively. Figure 1 shows the tides in the North Sea (Tomczak (1996) and is slightly different from the one given in Otto (1990). The most northern amphidromic point is located over land, indicating that there is no location offshore of Norway where the tidal amplitude is zero. The tidal wave enters the North Sea from the North Atlantic and travels along the British coast and proceeds around the two amphidromic points along the Dutch, German and Danish coast, leaving the North Sea along the Norwegian coast again. Another wave enters from the south west, through the English Channel. In the Irish Sea the wave enters from the south. The influence of bottom friction is clearly visible by the decrease of tidal amplitude along its path.

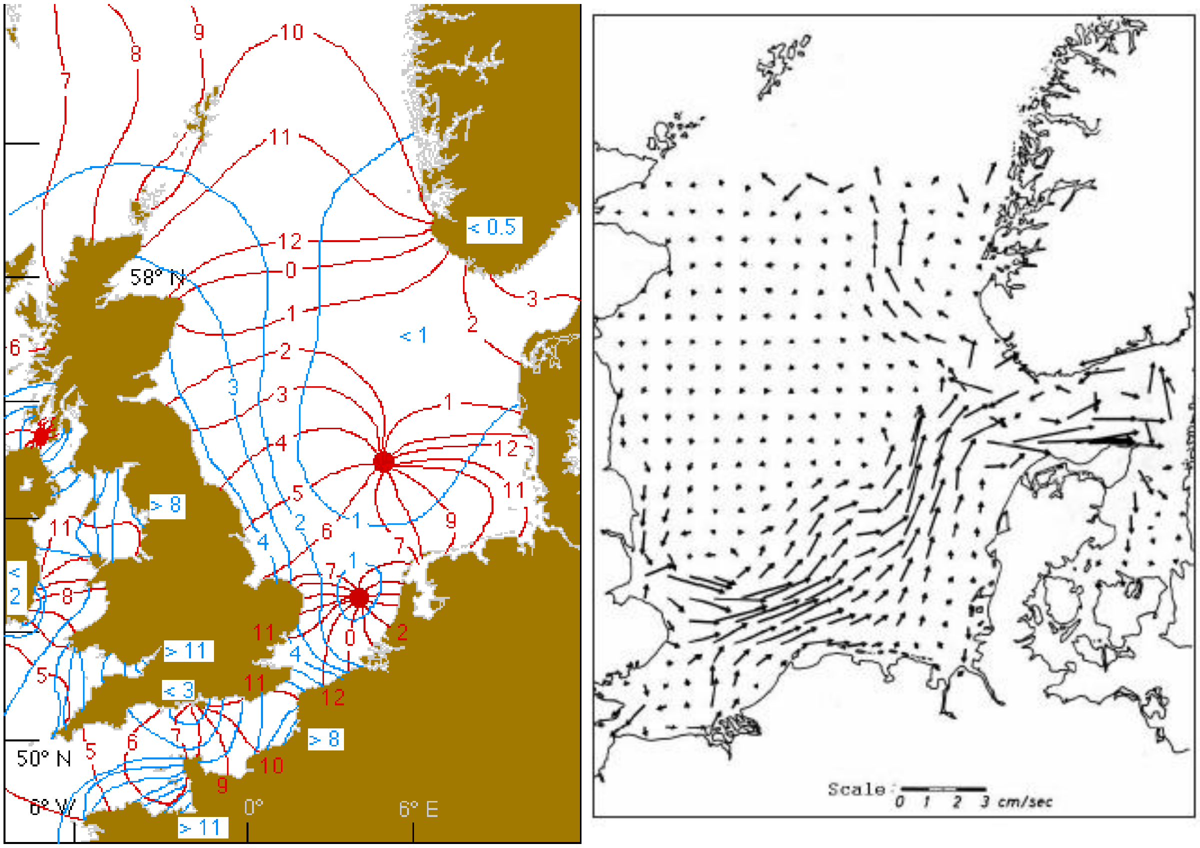

Figure 1: Left: tides in the North Sea as derived from observations. Red lines are co-phase lines of the M_2 tide, labeled in hours after the moon's transit through the meridian of Greenwich. (There are thus only 25 minutes between the co-phase lines labeled 12 and 0.) Blue lines give the mean tidal range at spring tide (co-range lines of the sum of M_2 and S_2). Taken from Tomczak (1996). Right: residual currents of the M_2-tide from Brettschneider (1967), figure reprinted from Figure 9 on page 672 of Sündermann and Pohlmann (2011).

Non-linear interaction between these two components generate the 14-day spring-neap tidal cycle. The other astronomical components can be found in Pugh (1987) and Hoitink et al. (2003). Non-linear interaction between tidal components due to advection and friction generate long-term averaged values or residuals (Figure 1, right) and compound tides. Of these the M_4 is perhaps the most important in the North Sea (Egbert et al. (2010).

Tidal and residual currents are strongly modified by local bathymetry. To first order, the tide follows bathymetry and in second place, tide-topography interaction can cause a residual current along the lines of equal water depth, is there is a small amount of dissipation (for instance due to bottom friction). Some 40 km to the southwest of site 22/4b, at the Forties field, the British Geological Survey have done detailed measurements on the local current conditions (Graham (1985). Tidal and residual currents at the latter location are orientated south to north, which is very much dominated by the local bathymetry (Figure 2). Bathymetry at site 22/4b is more oriented southwest to northeast, which will induce tidal and residual currents in that direction. These currents will transport the methane away from site 22/4b and will subsequently become influenced by larger scale currents such as the FIC and be transported more north-eastward.

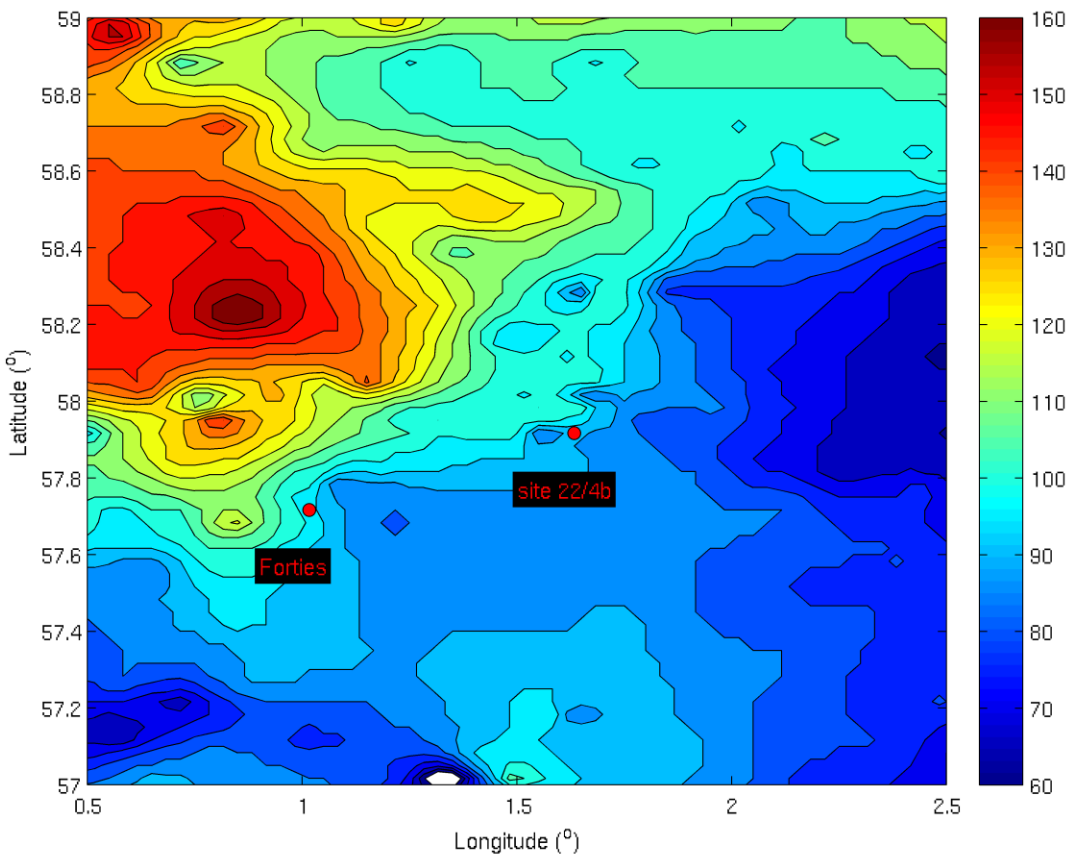

Figure 2: Bathymetry locally at sit 22/4b. Also indicated is the location of the Forties field, where BSG has done a detailed survey.

Besides the high-frequency variable tides, also the 18.6 year lunar cycle adds to the variability (only marginal). The frequency originates from the variation in lunar declination. The amplitude of the nodal cycle is about 2.2 cm in the coastal areas. In Baart et al. (2012) it is shown that failing to account for the nodal cycle results in an overestimation of Dutch sea-level rise.

Storm surges are of great importance for the inhabitants of the lower laying parts around the North Sea. Rossiter (1954) shows the evolution of the 1953 storm surge that led to a major flooding in the southwestern parts of the Netherlands. A combination of a high spring and a northwesterly storm led to a tidal surge exceeding 5.6 meters (18.4 ft = tidal +surge elevation). In Figure 3, it is clearly seen that the largest elevation occur in the southeastern. This is due to the shape of the basin and the decreasing bottom topography (Sündermann and Pohlmann (2011).

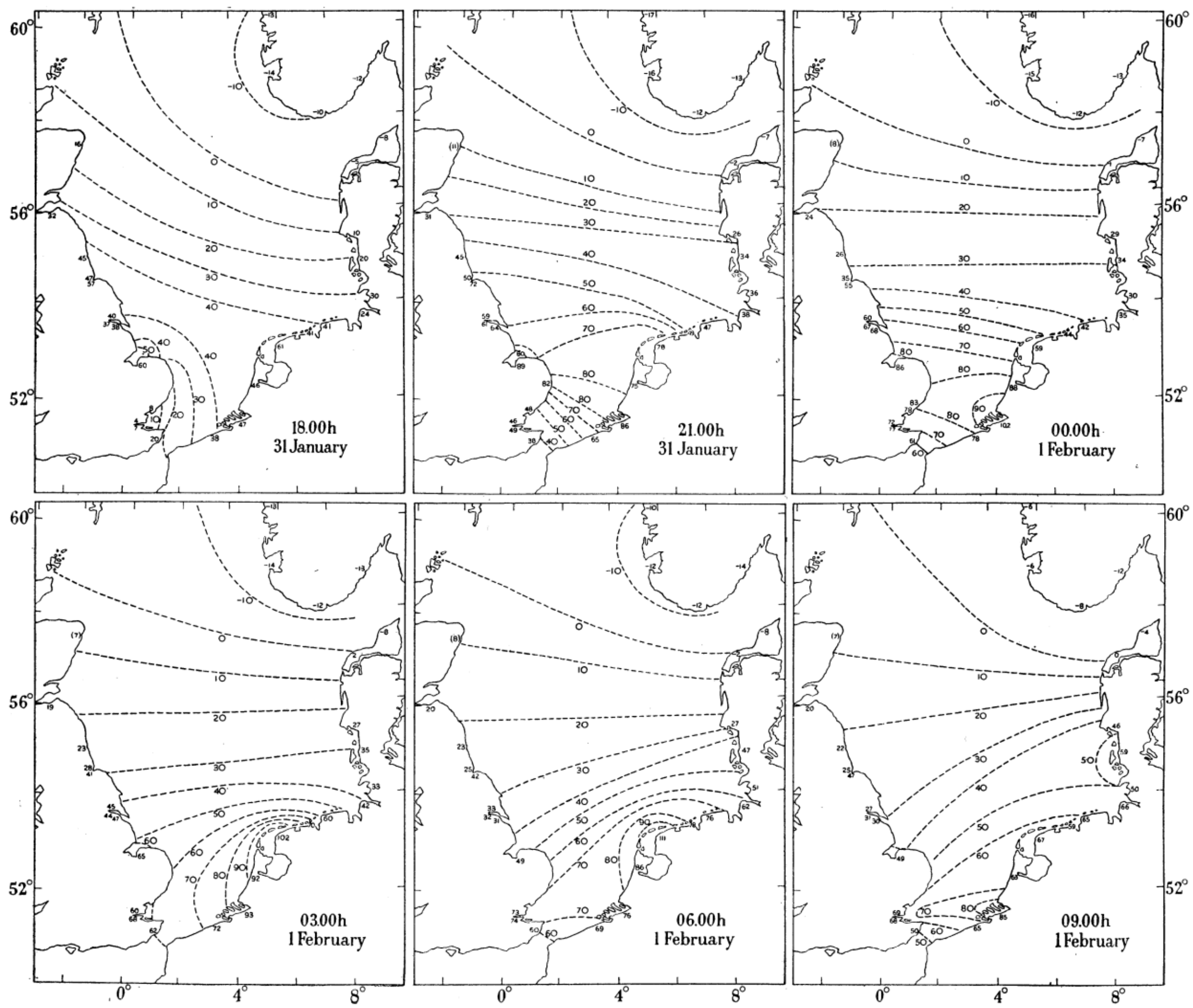

Figure 3: : Lines of equal disturbance, North Sea, 18.00h January to 9.00h 1 February. (unit, 1/10 ft.), reprinted from Figure 4 on pages 388 and 389 of Rossiter (1954).

Strom surges can be of the static or dynamic type (Hewer (1980).

The static type is defined as a low pressure track from Iceland into the North Sea. It is long-lasting and does not necessarily have extreme winds. The 1953 storm surge is a typical example. A dynamic type of storm surge is generated by a storm track over the Subtropical Atlantic, crossing Britain towards Denmark. It is small-scale, short lived and has strong rotating winds that move North Sea water like a centrifuge.

Climate (change) over the North Sea

Besides tidal forcing, meteorological forcing is an important factor in driving the hydrodynamics in the North Sea. The climate over the North Sea consists predominantly of westerly winds. Especially, during winters the average pressure system over the North Sea is controlled by a large scale system over the North Atlantic, consisting of a low pressure area over Iceland and a high pressure area over het Azores. The associated westerly winds blowing across the North Atlantic bring moist air into Europe and over the

North Sea. Variability in the wind speed and direction, however, is strong. The most prominent influence is from the North Atlantic Oscillation (NAO), which causes wind variations on a decadal frequency (Hurrell (1995). The NAO describes variations in the strength of the Icelandic low and Azores high pressure area. The winter (December through March) index of the North Atlantic oscillation (NAO) is defined as the normalized sea level pressure (SLP) difference between Lisbon (Portugal) and Reykjavik (Iceland). Figure 4 shows the NAO index for the period 1864 until 2010. The black line shows the five year moving average. Fluctuations between a positive and negative NAO index on the decadal frequency are apparent. A positive (negative) NAO is associated with stronger (weaker) than normal westerly winds. In years when westerlies are strong, summers are cool and winters are mild and rain is frequent. In periods with weak westerlies, temperatures over Europe are more extreme both in summer and in winter, heat waves and deep freezes occur more often and the weather is characterized by reduced rainfall.

The years 1950 to 1970 a negative NAO prevailed, whereas the NAO was strongly positive in the years 1980 to 2000. The sea-surface temperature (SST) response of the North Sea to negative and positive NAO conditions is examined by Pingree (2005). The response to a changing NAO is estimated to be about 5 months. This comprises the wind induced inflow, the shelf circulation and the local climate forcing. Under marked positive NAO conditions, associated with strong North Atlantic wind induced inflow, mean temperatures in the North Sea are about $1^{o}C$ warmer than under negative conditions. In 1996, the NAO was extremely negative, causing the North Sea wind-driven circulation to be halted. The conditions near Dogger Bank became continental influenced and the temperatures in March reached a minimum of $3.1^{o}C$, whereas in 1995, under positive NAO the minimum temperatures were only $6.4^{o}C$.

A significant correlation is found between the spring NAO value and the wind stress. The relation is not significant between spring NAO values and the spring air temperatures. Thus the NAO can directly influence the timing of stratification through changes in the spring wind stress. The weaker link between NAO and the spring air temperature is probably via changes in winter Atlantic surface water temperatures and their later warming of spring air masses as they move towards the North Sea (Sharples et al. (2006). This is also suggested in Reid et al. (2003), where high or positive NAO index conditions were associated with strong inflow and transport through the North Sea and weaker flows were associated with negative NAO anomalies. Changes in the NAO are correlated with changes in the strength of the North Atlantic Current (NAC). The correlation is maximal with a lag of about 6.5 months. Variations in NAO explain 67% of the total variance in the NAC (Pingree (2005).

Plag and Tsimplis (1999) show a coherent pattern in the annual and semi-annual constituents in sea level, air pressure, air temperature and the wind field. Based on the patterns of the climatological variables, North-western Europe can be clearly separated into a continental and maritime area. The intermediate zone is slightly different for each variable. The position and extend of this intermediate zone indicates changes in the late 20^{th} century. The decadal variability in sea level is closely correlated with the atmospheric forcing. Changes occurred in the last two decades of the 20^{th} century. The variation in air pressure may be linked to variations of the North Atlantic Oscillation on decadal time scales as well as a general warming trend.

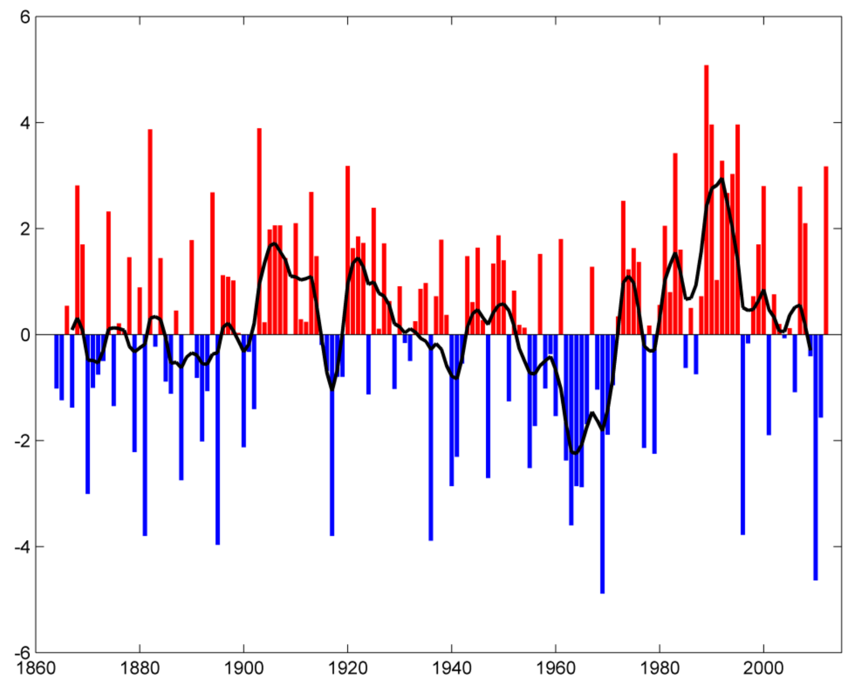

Figure 4: The winter (December to March) NAO index is defined as the normalized pressure difference between Lisbon (Portugal) and Reykjavik (Iceland). The black line shows a five year moving average. Constructed with station based December January February March (DJFM) North Atlantic Oscillation Index data obtained from http://climatedataguide.ucar.edu/guidance/hurrell-north-atlantic-oscillation-nao-index-station-based.

A warming trend has been observed in the North Sea. Becker (1996) investigated sea surface temperature changes in the North Sea and their causes. Based on a 25-year time-series of patterns of sea surface temperature (SST), Becker (1996) came up with the eight different regions in Figure 5a, which closely resembles the ICES boxes for North Sea water masses given in Figure 5b and also the distribution in hydrographical regions given in Otto et al. (1990). The approximate location of site 22/4b is indicated with a red dot and falls in box 7 in Figure 5a and in box 2 in Figure 5b. With regards to the sea surface temperatures it behaves as any point in the central North Sea, but in the ICES boxes distribution a clear relation is shown with the currents between the Faroe and Orkney islands.

The oceanic influence in the northwestern part and the continental influence in the northeastern part is clearly reflected in the different SST behavior. Positive SST anomalies usually start in the Southern Bight and move with a delay of several weeks into the central and northern North Sea. No temperature trend was observed in either of the boxes in the period between 1969 and 1993. High correlations between SST anomalies and the NAO index were expected in advection regions 1 and 5, but the contrary was found (Figure 6). Apparently, SST anomalies in the Southern Bight are independent of the North Atlantic Atmospheric Circulation. However, a distinct correlation was found between the NAO and the SST time series with highest correlations in the central northern part of the North Sea (region number 7). Site 22/4b is close to the location of the highest correlations and thus the SST at this site is strongly influenced by the NAO. This region is less dynamics and characterized by small advection and variable and weak current. Here, it is likely that the SST is dominated by air-sea exchange, which is obviously closely related to atmospheric forcing and weather patterns.

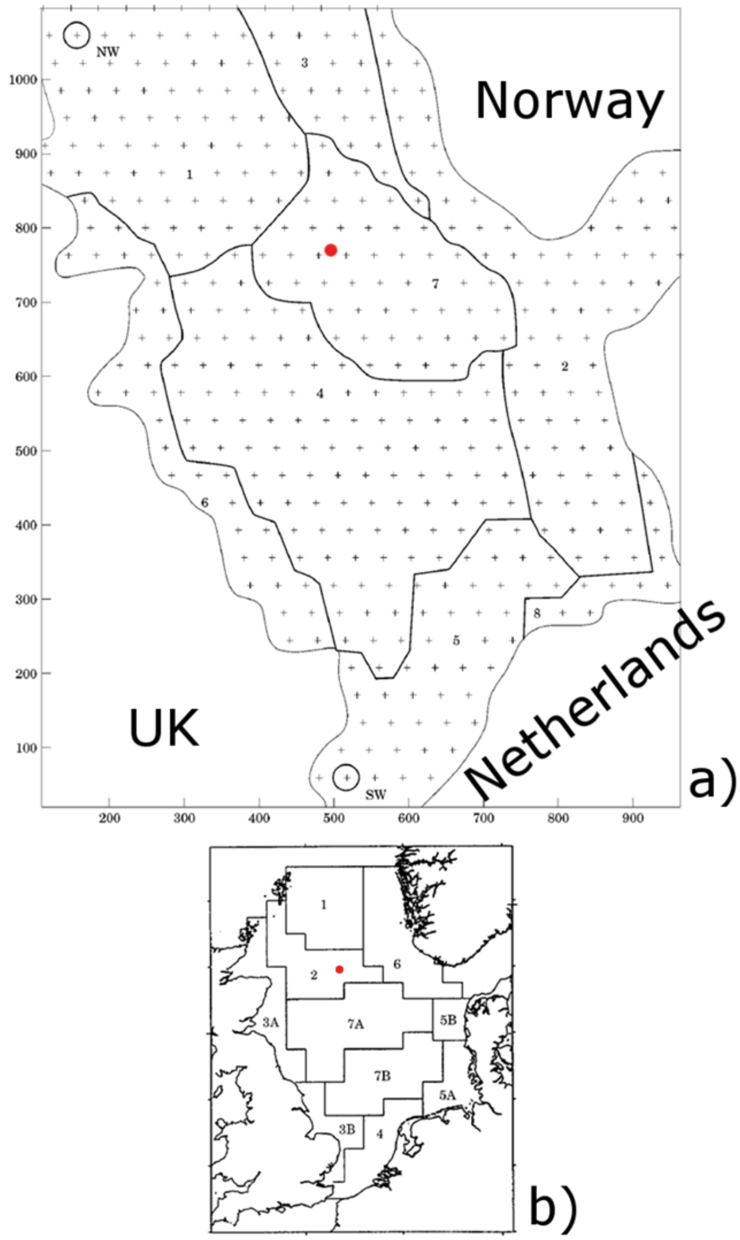

Figure 5: Subdivision of the North Sea in areas. Top panel: Based on SST patterns; position of 10 selected representative points is indicated. Lower panel: Based on hydrographic and biological information (ICES boxes). The red dots mark the approximate location of site 22/4b, reprinted from Figure 4 on page 891 of Becker (1996).

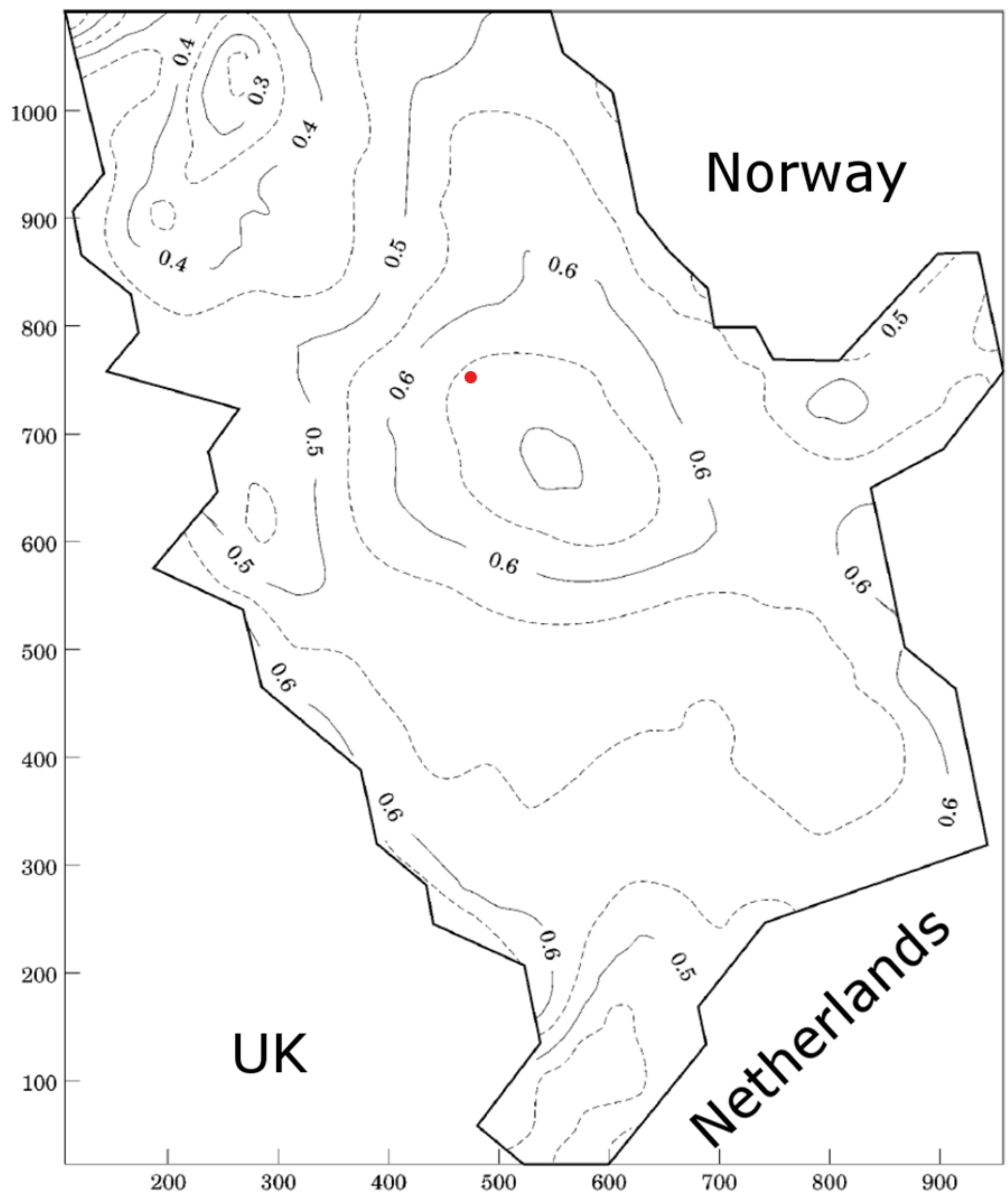

Figure 6: Correlation between NAO index and standardized annual SST anomalies, 1969-1993. The red dot marks the approximate location of site 22/4b, reprinted from Figure 8 on page 895 of Becker (1996).

Two relatively sudden climate changes have been observed in a wide-scale and rather sudden change in plankton, benthos and fish populations stand out as exceptional (e.g. Weijerman et al. (2005); Kirby and Beaugrand (2009). The first change occurred in the late 1970s, and was distinguished by a reduced inflow of Atlantic water and cold-boreal conditions (Reid and Edwards (2001). In the late 1980s, oceanic inflow increased markedly, as did sea surface temperature (Reid et al. (2001) Beaugrand (2004). This warm temperate period has continued to the present day. In the future, air temperatures over the North Sea are expected to increase by 2 °C to 3.5 °C by the 2080s, with high summer temperatures becoming more frequent and very cold winters becoming increasingly rare (e.g. Hulme et al. (2002); van den Hurk et al. (2006).

An example of the increasing seawater temperatures is given in Figure 7, which shows observations of the temperature at Arendal on the Norwegian Skagerrak coast (ICES 2007b (2007). The temperatures in the autumn of 2006 remained above average, sometimes even above the 2SD line.

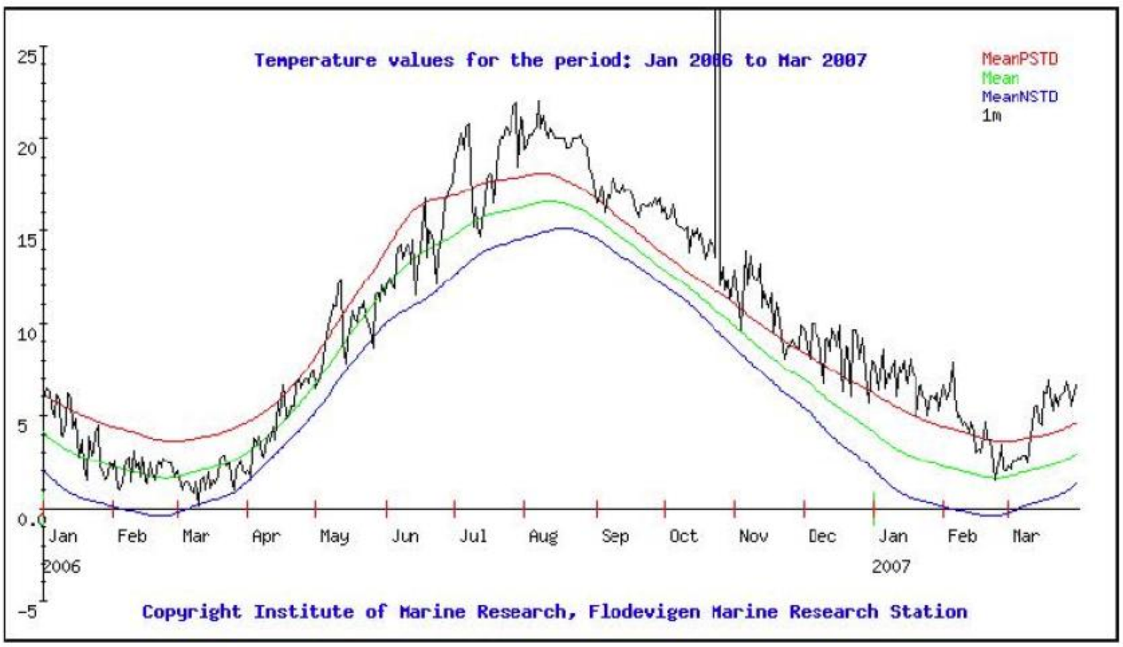

Figure 7: Daily sea surface temperature recordings at Arendal on the Norwegian Skaggerak coast from January 2005 to December 2006. Also shown is the long-term average temperature +/- 1 SD (standard deviation). The data is from the Norwegian Institute of Marine Research (IMR) and the figure is reprinted from Figure 15 on page 22 of ICES 2007b (2007).

The low NAO in the 1960s coincided with the “Great salinity anomaly”, which was a low salinity pattern propagating in the North Atlantic (Dickson et al. (1988) Mork and Blindheim (2000). The anomaly arrived in the North Sea in the late 1970s and induced pronounced minima in the salinity and temperature. It was first observed in the Rockall channel in 1976 and later in the northern and central North Sea, in 1977/1979 (Becker (1996). During the latter period, the SST anomaly in the North Sea was markedly negative. In 1989/1990 a high salinity anomaly was connected with a position temperature anomaly in the North Sea (Becker and Dooley (1995). Pohlmann (1996a) shows that the interaction between wind stress and thermal forcing is the main cause of the heat content variability. Temperature anomalies in 1988-1992 were high, suggesting a trend. However, these were in the end of his simulation and Becker (1996) suggests that the temperature increase might be a temporal anomaly similar as in the 1970s.

Wave height and wave period in the North Sea

In analysis of extreme wave conditions in the North Sea (Weisse and Günther (2007) a model was driven with NCEP/NCAR reanalysis data. The results show a reduction of severe wave conditions in the UK North Sea over much of the hindcast period from 1958 to 2002. The model results had a good agreement with a 3-month dataset observed at station K13 (53.22°N, 3.22°E) in terms of significant wave height, wave period and mean wave direction. The model consists of a low-resolution outer model extending over a large part of the North Atlantic and a high-resolution inner model of the North Sea. Focus of the study is on the North Sea south of 56°N. Along the northern edge between 1 and 2°E, not a lot of change is observed in the 99%-ile significant wave heights. These results may possibly be extrapolated further north. However, further north a stronger influence is expected from the open boundary between Scotland and Norway, which could alter the results significantly.

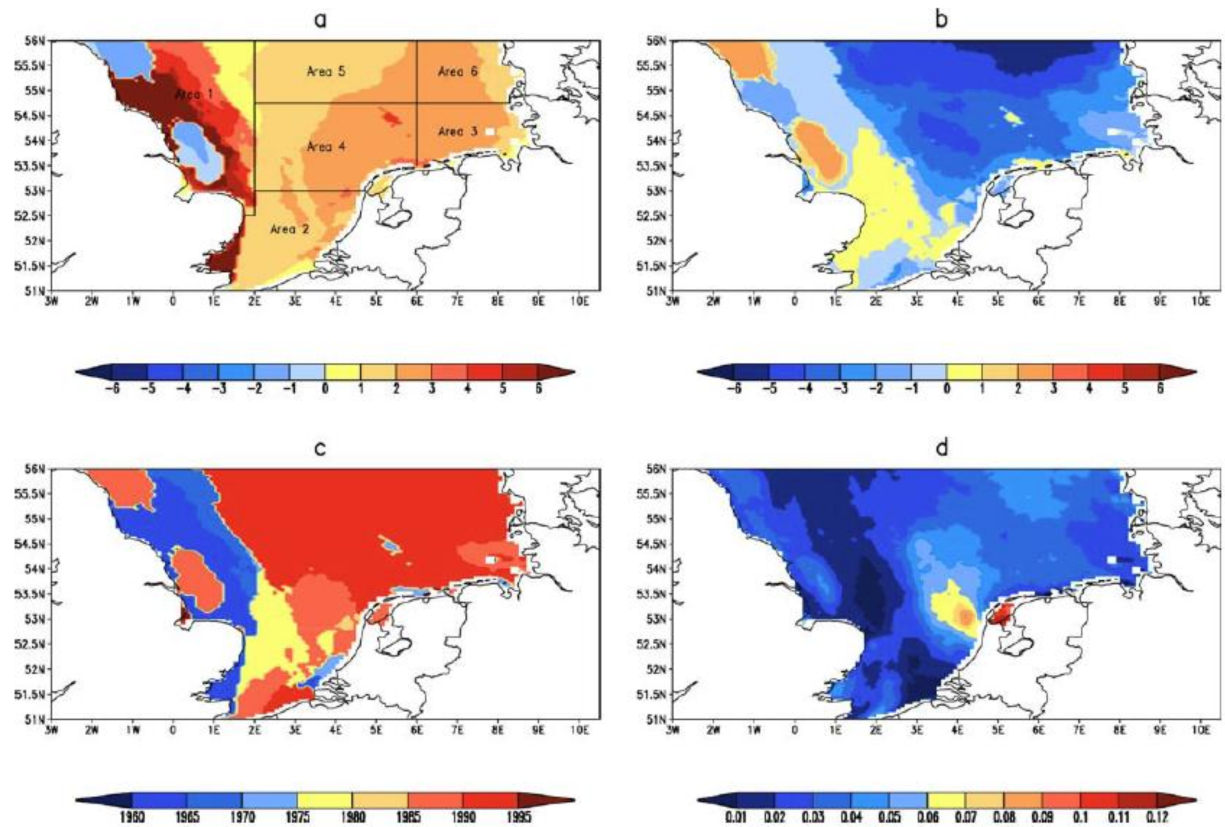

Figure 8: Piecewise linear trends of the annual 99%-ile significant wave heights. a) linear trend for the period 1958-T, b) linear trans for the period T-2001. Units in both cases are in cm year^{-1}. c) Year T at which a change in trends is indicated by the statistical model. d) Skill of the piecewise linear trend model relative to the simple linear trend model, reprinted of Figure 8 on page 169 of Weisse and Günther (2007).

In Gulev and Hasse (1999), the trends in wind sea and swell height were estimated between 1864 and 1993 for the entire North Atlantic based on the Comprehensive Ocean – Atmosphere Data Set (COADS). In general a positive trend is observed of about 20 to 22 cm/decade in both wind sea and swell height for the North Sea. They conclude that the swell changes are probably driven by the intensification of high frequency synoptic processes. The years 1972-1973 and 1986-1987 show significantly higher power in the 2 to 3 cycles per day band than the 1966-1970 and 1978-1980 period. The periods with higher power correspond to NAO+ or ‘zero’ conditions, whereas the lower power period are in the NAO- phase (previous section). The latter indeed corresponds to weaker winds and thus reduced swell.

Circulation pattern in(to) the North Sea

The classical presentation of the circulation in the North Sea is described by an anticyclonic gyre driven by windforcing and non-linear tidal interaction. However, Kauker and von Storch (2000) applied an atmospheric forcing by the ECMWF reanalysis from 1979 to 1993 to an ocean general circulation model. They found that the resulting circulation in the North Sea is dominated by two circulation patterns. One displays the great gyre circulation, which can be either clockwise (15% of the time) or anti-clockwise (30% of the time). The (anti)-clockwise circulation is excited by (southwesterly) northwesterly winds. The other circulation pattern has a bipolar structure with a counter rotating flow in the northern and southern part of the North Sea and occurs 45% of the time. Moreover, during 10% of the time, the circulation in the North Sea even stopped. A schematic representation is given in Figure 9 for four basic wind patterns. The state with intensified cyclonic circulation (lower left picture) is dominant due to the prevailing wind in north-west Europe. In case of easterly winds, the circulation reverses into an anti-cyclonic one. With north- or south-easterly wind state a stagnation of the circulation appears.

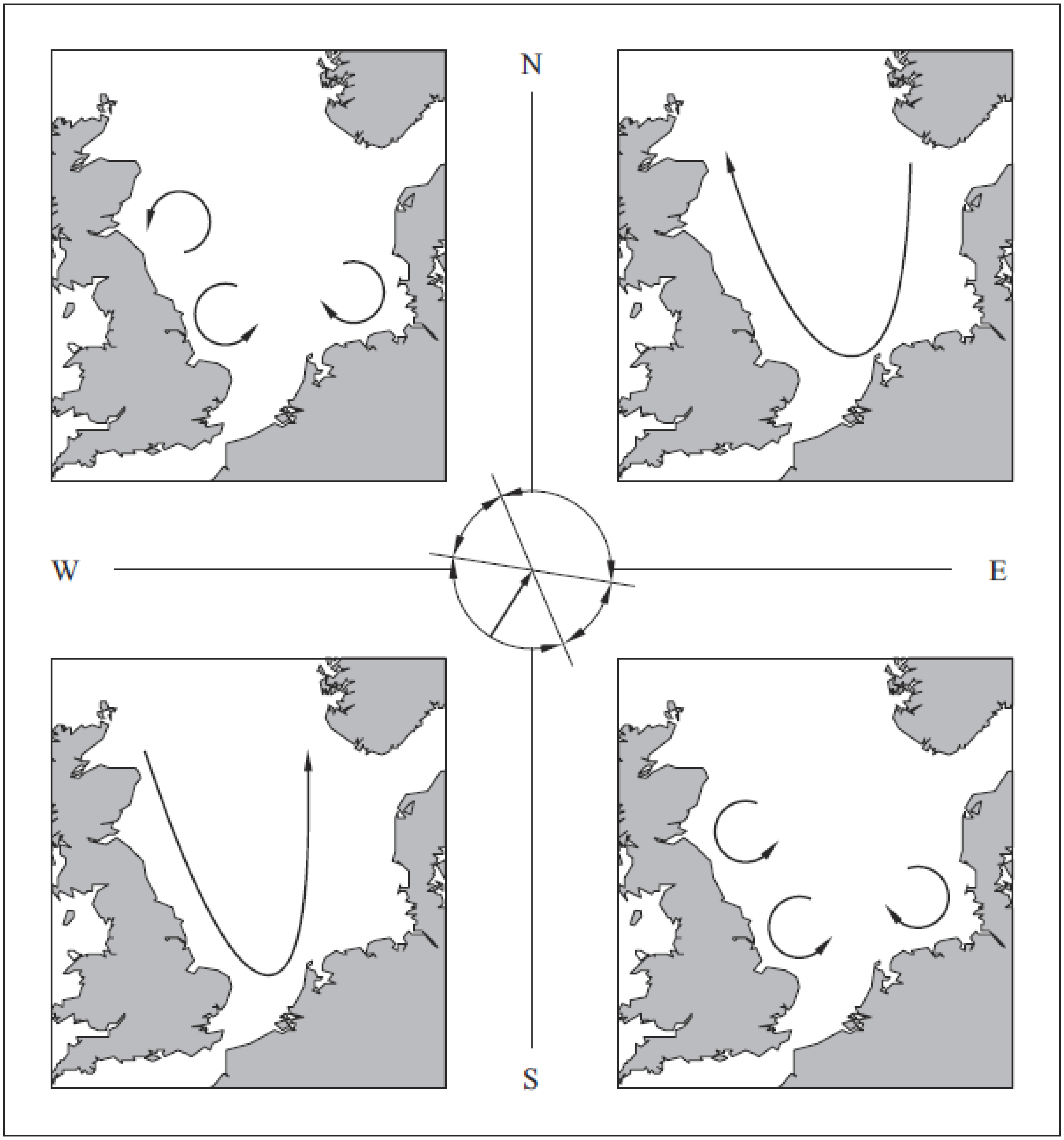

Figure 9: Wind-driven circulation in the North Sea. There are four basic states, corresponding to the sectors of the prevailing wind. Reprinted from Figure 3 on page 668 of Sündermann and Pohlmann (2011).

The hydrography and circulation in the North Sea is determined by the inflow of saline Atlantic water through the northern entrances and to a lesser extent through the English Channel. Oceanic water from the northern North Atlantic Ocean follows three paths of persistent inflows into the northern North Sea: the Fair Isle Current, the inflow along the western edge of the Norwegian Trench (Slope Current) and the East Shetland Atlantic Inflow, offshore of the Fair Isle Current (Turrell et al. (1996) and Figure 10). The East Shetland Atlantic Inflow is particularly persistent during the summer months. Substantial salinity changes have been observed in the northern North Sea, which could be related to a decadal variability of the two western North Sea inflows, being the Fair Island Current and the East Shetland Atlantic Inflow. Site 22/4b is located at (57°55'N, 1°38'E) within the Fair Isle Current on the 100 m isobath, slightly south of the East Shetland Atlantic Inflow. The Atlantic inflow displays a seasonal variation with maximum inflow during winter months. The minimum inflow during the summer correlates with a salinity maximum in the waters at the shelf edge.

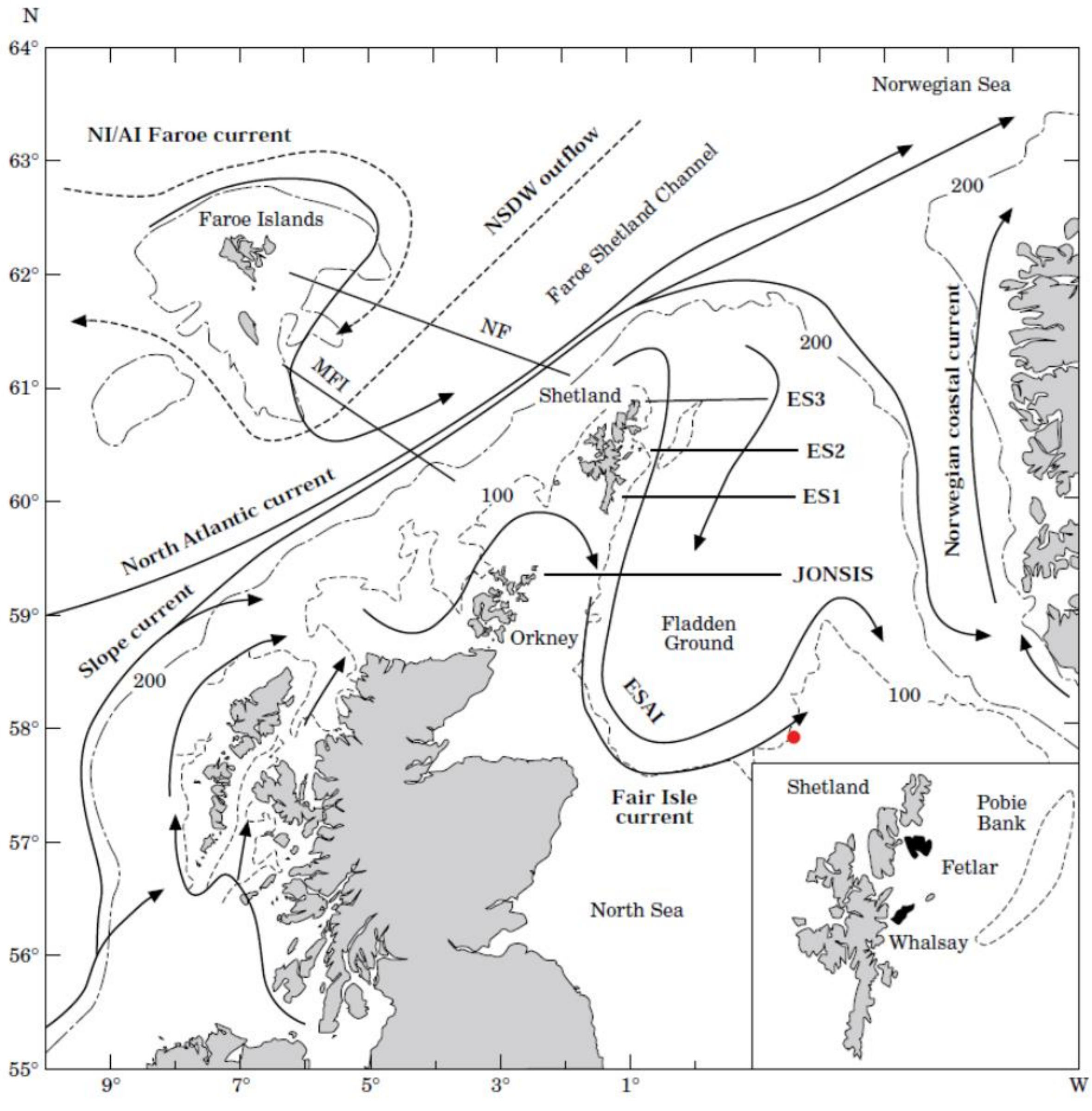

Figure 10: Map showing the key features of the topography of the North Sea and the adjacent oceanic areas in relation to the proposed circulation and the location of the standard hydrographic sections. Solid arrows represent surface circulation and broken arrows sub-surface. NF – Nolso-Flugga standard hydrographic section; MFI – Munken – Fair Isle section; ES1,2,3 – East Shetland sections; JONSIS – JOint North Sea Information Section; ESAI – East Scotland Atlantic Inflow; NI/AI – North of Iceland/Arctic intermediate water; NSDW – Norwegian Sea Deep Water. Insert shows details and local names of features east

of Scotland. The red dot marks the approximate location of site 22/4b, slightly modified from Figure 1 on page 900 of Turrell et al. (1996).

Figure 11 shows estimates of the inflow from the North Atlantic into the Northern North Sea between the Orkneys and Norway (ICES (2005) This flux is thus composed of the inflow due to the Fair Isle Current, the East Shetland Atlantic Inflow, the slope current and the Norwegian coastal current (introducing a negative contribution). These are based on the results from a numerical model. The time-series show significant annual variations with an average volume flux of 1.75 Sv (1 Sverdrup = $1.0 \cdot 10^6$ m^3/s) towards the south. Between 1988 and 1995 a significantly stronger inflow of nearly 2 Sv was estimated in the model.

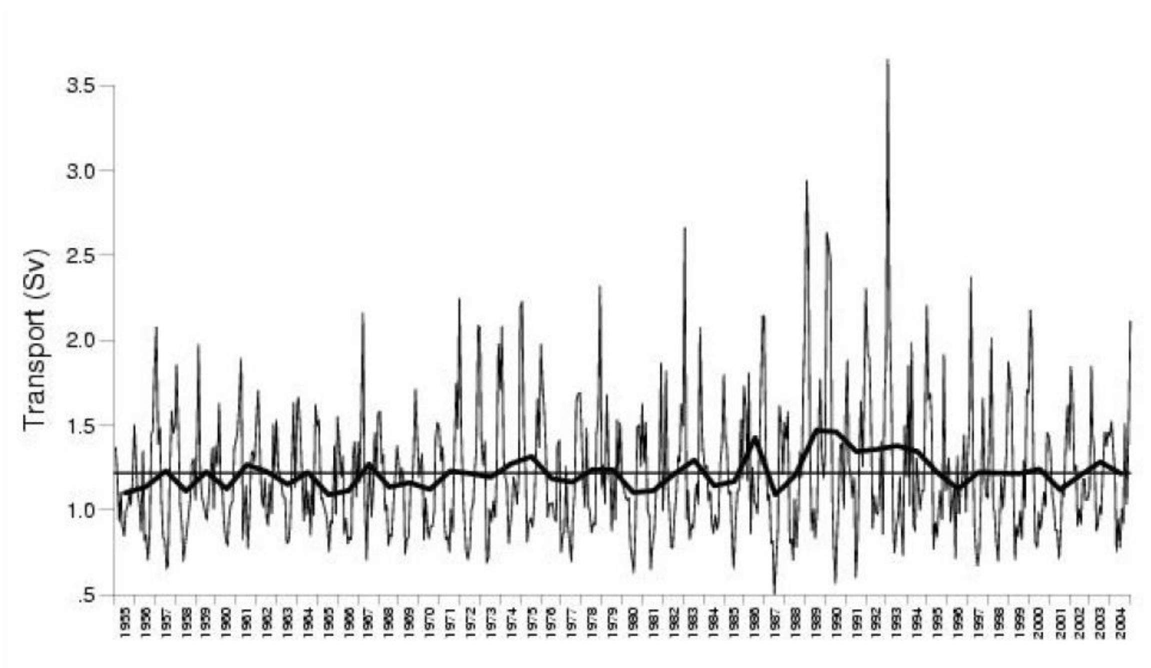

Figure 11: Time-series (1955-2004) of modeled annual mean (bold) and monthly mean volume transport of Atlantic water into the northern and central North Sea southward between the Orkney Islands and Utsira Norway. 1 Sv =10^6 m^3/s (anon, 2005), reprinted from Figure 34 on page 27 of ICES (2005).

In the south the North Sea is fed by oceanic transports from the English Channel. The estimated water flux through the channel is 1 to 2 Sv (du Bois et al. (1995). English Channel water predominantly follows the European continent and based on radioactive tracer measurements it is estimated that it takes about 170 – 250 days for this water to reach the Baltic.

In the Skagerrak, North Sea water leaves the domain along the Danish coast. Estimates are about 0.2 Sv Otto et al. (1990) and 0.05 Sv Rydberg et al. (1996). The flow of surface water from the Kattegat is estimated at 0.05 -0.06 Sv by Andersson and Rydberg (1993), which contains about 0.015 Sv freshwater, mainly from rivers in the Baltic. Geostrophic transport estimates varied from 0.26 to 0.4 Sv inflow and 0.64 to 0.0 Sv outflow based on the SKAGEX data set (Danielssen et al. (1997) Skogen et al. (1997). Figure 12 shows a schematic representation of the circulation in the Skagerrak from Danielssen et al. (1997).

Note that the maximum latitude in Figure 10 is 6°E and thus connects perfectly to the western part of Figure 12. Apparently, what is called the East Shetland Atlantic Inflow in Figure 10 is fed into the Atlantic Water Mass AW^d in Figure 12. Moreover, the Fair Isle Current in Figure 10 feeds the Atlantic Water Mass AW^u in Figure 12. Since, the former pass by site 22/4b it is likely that dissolved substances such as methane will be transported into the Skagerrak. Therefore special attention will be given to the skill of 3D hydrodynamic models in the latter area.

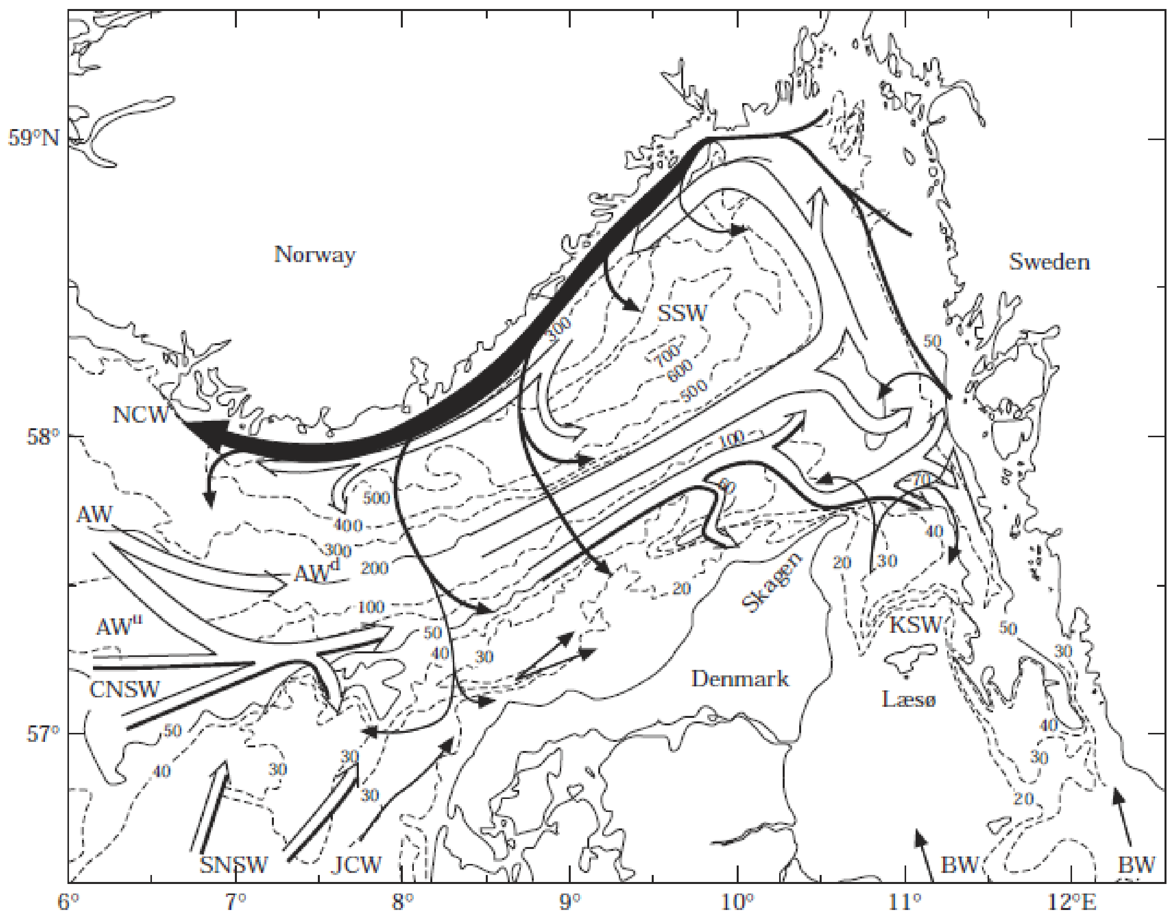

Figure 12: Schematics of the general circulation of the relevant water masses in the Skagerrak and adjacent areas. Open and filled arrows indicate subsurface and surface water, respectively. AW= Atlantic Water, AW^u= Atlantic water upper (shallow), AW^d=Atlantic water deep (deep), BW=Baltic Water CNSW=Central North Sea Water, JCW=Jutland Coastal Water, KSW=Kattegat Surface Water, NCW=Norwegian Coastal Water, SNSW=Southern North Sea Water, SSW=Skagerrak Surface Water, reprinted from Figure 1 on page 655 of Danielssen et al. (1997).

The wind-driven and thermohaline and tidal residual circulation in North Sea is significantly influenced by the NAO. This can be seen in Figure 13, which shows the result from a model calculation in which it becomes clear that the currents under a NAO+ situation are much stronger than during a negative one. Moreover, currents in the central northern part of the basin, where site 22/4b is located, are directed eastward under NAO+ conditions and northwestward under NAO- conditions, which obviously influences the spreading of (passive) tracers, such as methane.

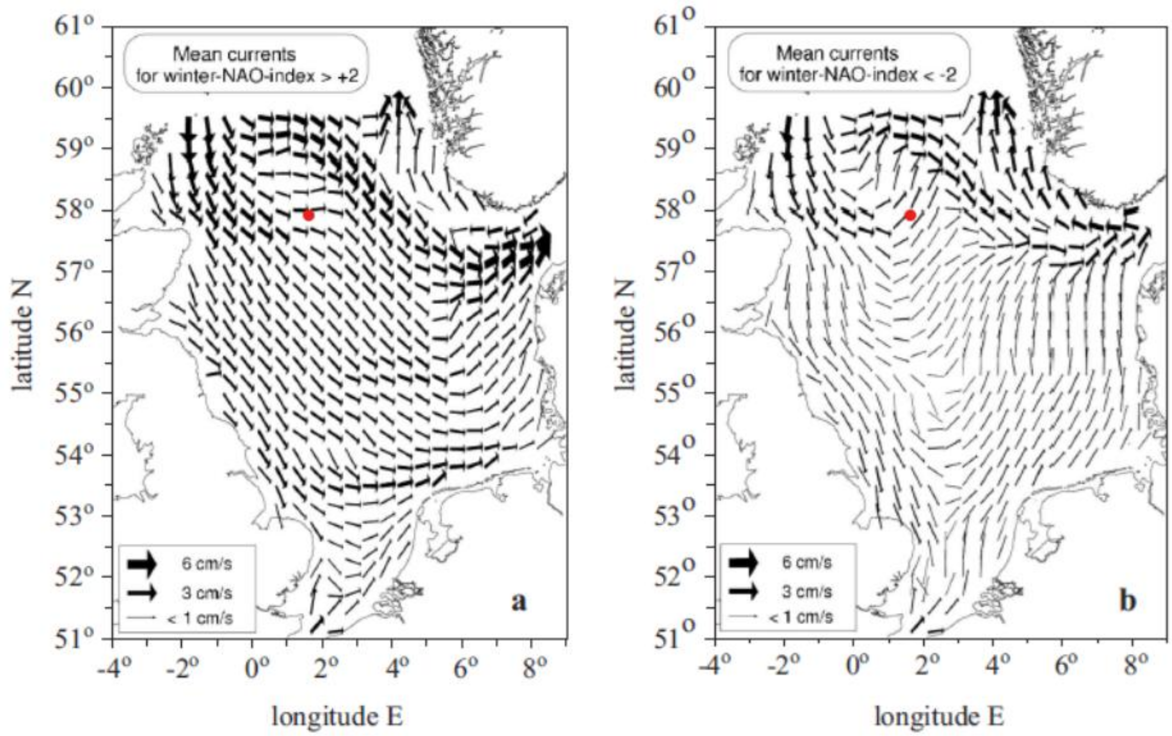

Figure 13: Circulation of the North Sea for different values of the winter NAO index. (a) index > 2. (b) index <-2. The direction of the arrows points in the direction of the flow. The thickness of the arrow indicates the strength of the current. The red dot marks the approximate location of site 22/4b, slightly modified from Figure 7 on page 670 of Sündermann and Pohlmann (2011).

Hydrography of the North Sea

The temperature of the North Sea is mainly controlled by local solar heating and heat exchange with the atmosphere. The salinity and the temperature generally reflect the influence of the NAO on the movement of Atlantic water into the North Sea and the ocean-atmosphere heat exchange. A balance between tidal mixing and local heating introduce the development of a seasonal stratification from April/May to September in the northern parts of the North Sea. The annual cycle of Sea Surface Temperature (SST) in the North Sea (Figure 14) show highest temperatures in late summer (August) and lowest temperatures in February. Also significant interannual variations can be observed with highest summer temperatures in 2003 and 2004. These positive SST anomalies started in June 2001 and ended in March 2005 (ICES (2005), a period with somewhat higher than normal NAO (Figure 4). The temperature of the upper layer of most of the North Sea was between 0.5 and 1.5^{o}C warmer than normal, with the exception of the western Norwegian coastal water which was close to normal during the first half year.

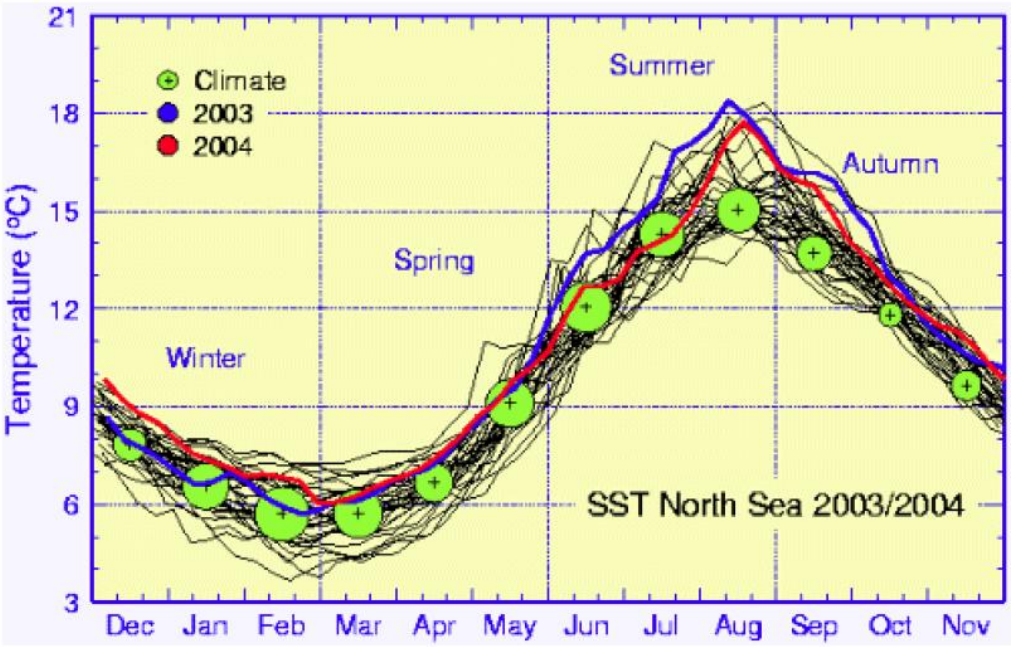

Figure 14: North Sea area averaged SST annual cycle, monthly means based on operational weekly North Sea SST maps. Climatology 1971-1993 green dots; blue line 2003, red line 2004; black lines individual years, reprinted from Figure 35 on page 28 from ICES (2005).

The annual mean temperature and the salinity anomalies of the FIC (Figure 15) also show strong variability. The time-series of the anomalies appear to be correlated, higher than normal temperatures appear to be correlated with higher than normal salinity anomalies and vice versa. Moreover, both time-series appear to display decadal variability.

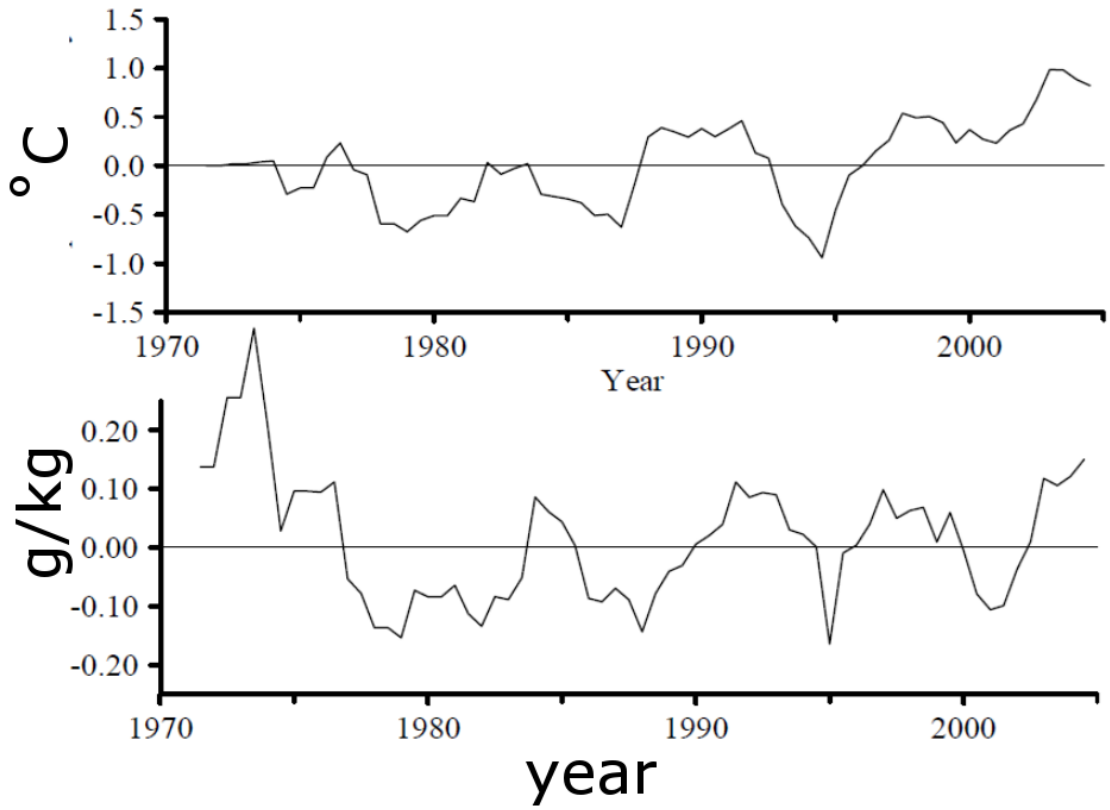

Figure 15: Temperature (top) and Salinity (bottom) anomalies in the Fair Isle Current (FIC) entering the North Sea from the North Atlantic reprinted from Figure 36 on page 28 of ICES (2005).

A new improved climatology of temperature and salinity on the European Shelf is given in Berx and Hughes (2009) on near bottom and surface values. It is an improvement to the Janssen et al. (1999) climatology. Overall a minor increase is observed between the Janssen et al. (1999) and the Berx and Hughes (2009) climatology, which is due to the fact that the period 1997-2000 was much warmer than average. Figure 16 shows the annual cycle of temperature for the near-surface and near-bed levels. The temperature decreases with latitude and the influence of the North Atlantic Ocean is clearly visible in the northern part of the North Sea. The largest seasonal variations occur in the southern part of the North Sea and the German Bight, where the shallower regions are located. In the near-bed layer the amplitude of the seasonal variation of temperature is only small in the northern part of the North Sea, indicating the separation of the lower layer from the upper layer during the summer stratification in this area. In this area tidal mixing is relatively weak is not able to mix the input of buoyancy from solar heating down (Bowers and Simpson (1987). At the transition between fully mixed waters and stratified waters, mixing fronts occur. The stratification is also visible in the month where maximum temperatures are observed. This is August in most of the North Sea at the surface, but moves later in the year towards the north in the near-bed levels. In areas of seasonal stratification the maximum temperatures are achieved when the thermocline breaks down and warmer surface water mixes downwards. Site 22/b in the northern part of the North Sea has an average SST of about 9°C and varies between about 5 and 13°C and the maximum sea surface temperatures are observed in August. The near bed temperature is about 7°C and varies less than 2^{o}C per year. The maximum near bed temperature is observed in November, when warmer surface waters are mixed downward.

The thermohaline circulation driven by density differences during the summer stratification generates a cyclonic current pattern (Sündermann and Pohlmann (2011), similar to the residual tidal transport.

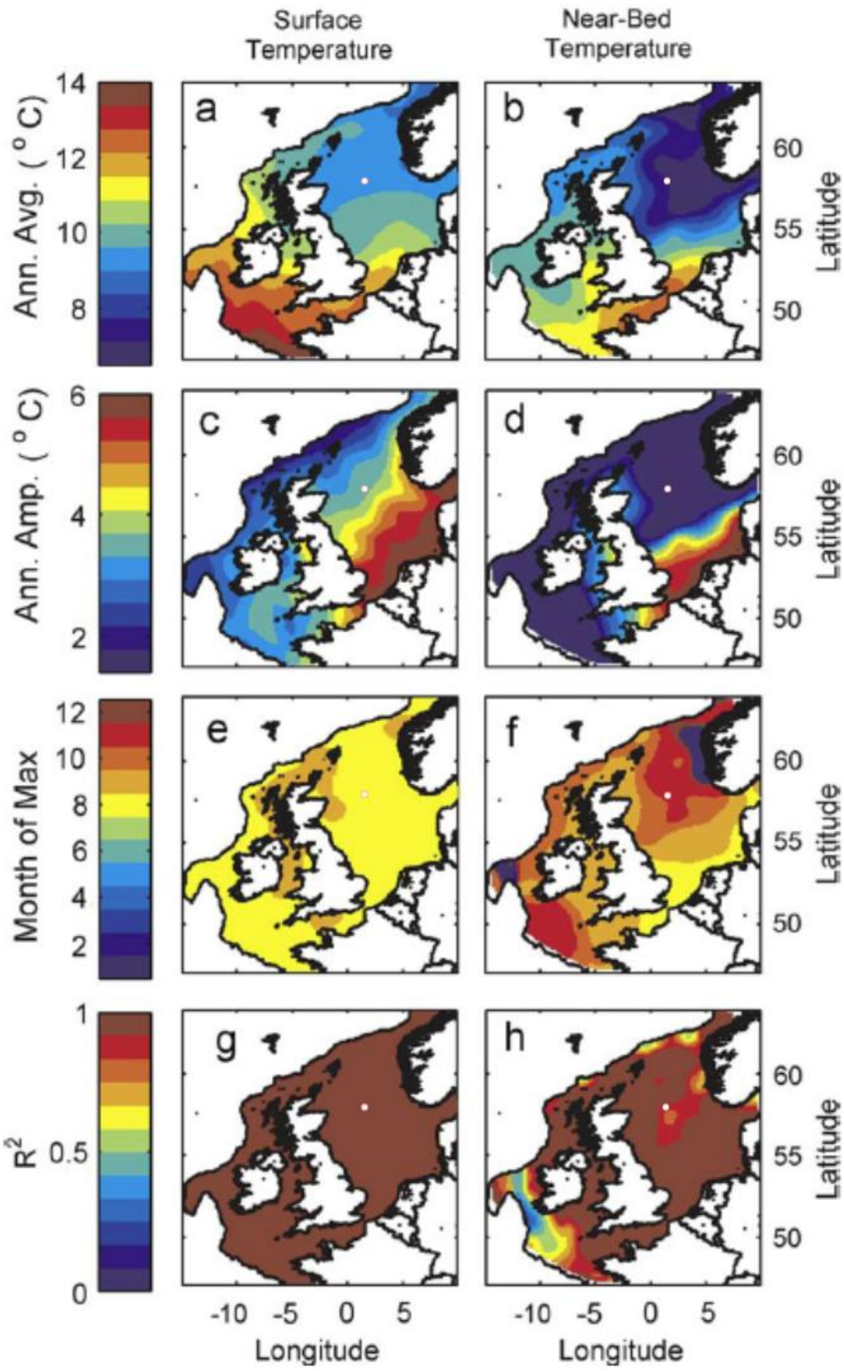

Figure 16: Left- surface layer, right near bed layer: (a,b) annual mean temperature (°C), (c,d) annual seasonal cycle amplitude (°C), (e.f) phase (expressed as month of maximum), and (g,h) R^2 of the HAMELS analysis for the period 1971-2000. The white dot marks the approximate location of site 22/4b, slightly modified from Figure 2 on page of 2289 of Berx and Hughes (2009).

The salinity distributions (Figure 17) shows that waters close to the North Atlantic are more saline. Moreover, the highest amplitudes in the surface salinities are observed in the regions of fresh water inflow (ROFIs), especially in the Baltic outflow region. The seasonal cycle in the salinity is caused by a changing balance in precipitation minus evaporation and variations in land and river runoff. Besides a seasonal cycle, there is still ample of irregularity in these parameters, which makes it difficult to identify the seasonal cycle in the salinity distributions and is represented by the low R^2. Only a clear seasonal cycle can be identified in the Baltic outflow, where maximum surface salinities are observed in January-March, when the presence of ice in the Baltic Sea blocks the outflow of freshwater. The Sea Surface Salinity (SSS) near site 22/4b is determined by the inflow from the north and is about 35 PSU, the annual amplitude is only small: less than 0.4 PSU. The maximum salinity occurs in the middle of winter. Near the bed the salinity is also about 35 PSU and the annual variability equally small as near the surface. There, the salinity also attains its maximum in the middle of the winter.

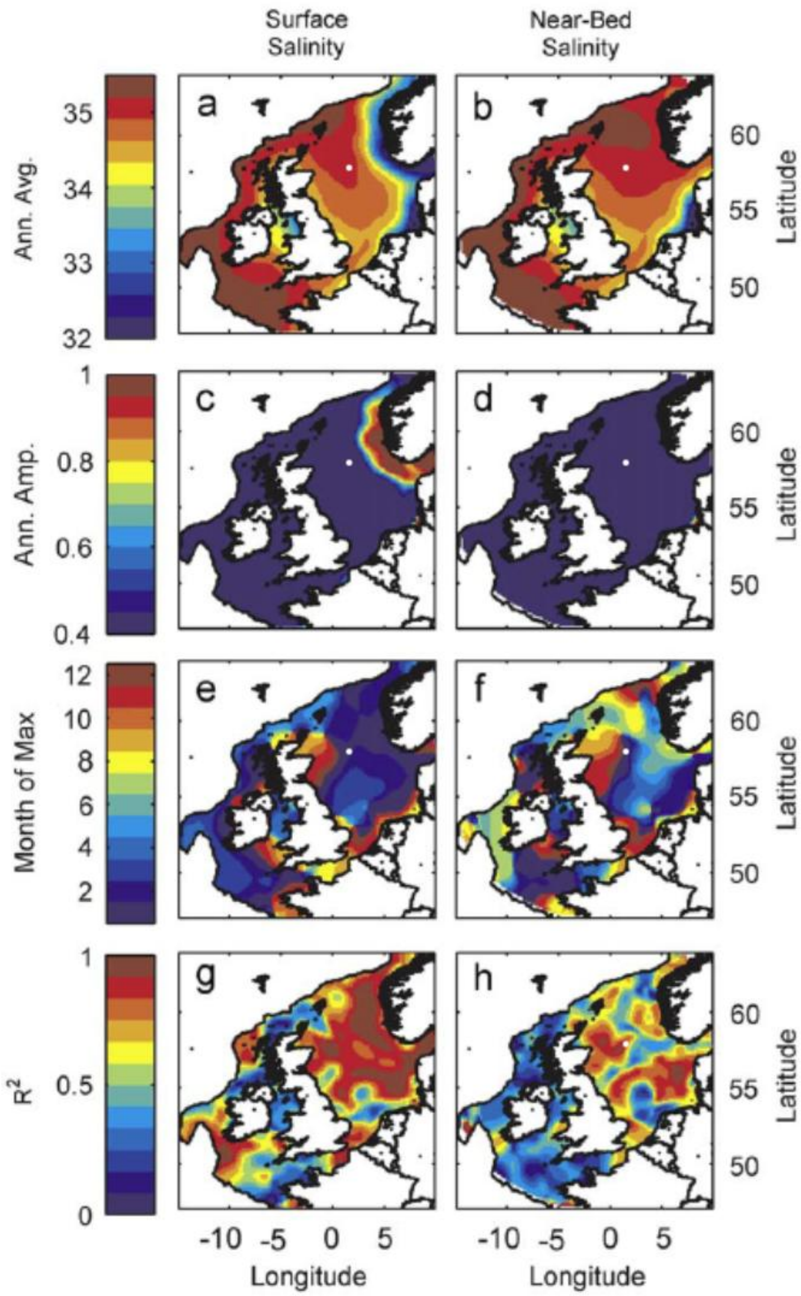

Figure 17: Left- surface layer, right near bed layer: (a,b) annual mean salinity, (c,d) annual seasonal cycle amplitude, (e.f) phase (expressed as month of maximum), and (g,h) R^2 of the HAMELS analysis for the period 1971-2000. The white dot marks the approximate location of site 22/4b, slightly modified from Figure 3 on page of 2289 of Berx and Hughes (2009).

Hydrodynamic models

Three-dimensional hydrodynamic models that have been applied in the (northern part) of the North Sea will be listed here. Focus will be on 3D models only, because the ability of the model to reproduce the seasonal stratification is crucial. The main characteristics will be given, for example the way the hydrodynamic equations are solved numerically and what kind of meteorological forcing is applied and its origin. In available in literature, the quality of the model is assessed for the North Sea area in general and if possible for the location of site 22/4b specifically. The most appropriate models will be discussed further in terms of applicability in the cases proposed below.

General model description

The purpose of hydrodynamic models of the North Sea is to estimate the current structure under (realistic) forcing conditions. Some models are used in an operational sense and are used to predict storm surges and tidal elevation. Other models are tools for decision making in terms of construction activities. Already a coupling is made between 3D-hydrodynamic models and ecosystem models as detailed information is needed about the stratification for the dispersion of nutrients and particles.

Figure 18 shows the interaction diagram between the different physical processes inherent to a 3D hydrodynamic model. The internal dynamics of the system are indicated within the dashed square. The only two processes that interact with a substance concentration, such as methane, are the turbulent diffusion and advection. All other processes outside of the square box are defined as “external forcing”.

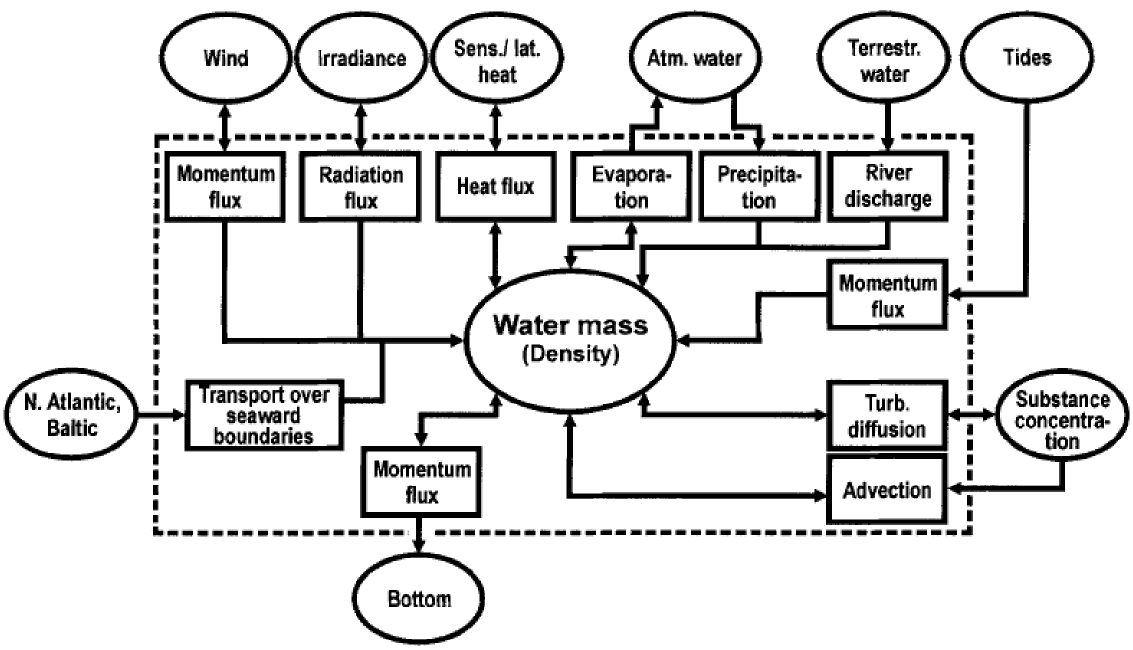

Figure 18: Interaction diagram of the physical subsystem of a 3D hydrodynamic model, reprinted from Figure 1 on page 66 of Lenhart and Pohlmann (2004).

In general, any 3D-hydrodynamic model could be applied to the North Sea area, but here an overview will be given on those models that have actually already been used in a North Sea context (Table 1). Focus will be on those models that have been part of one or more comparison studies in order to determine their relative skill.

Table 1: Acronyms of models applied in the North Sea context and part of one or more comparison studies. The top 9 were involved in the NOMADS 1 and 2 study and the bottom 3 in the CONMAN study.

Acronym	Developed at	Citation
DE/DELFT3D	WL|Delft Hydraulics now Deltares, the Netherlands	Gerritsen et al. (2007)
DA/SYSTEM3	Danish Hydraulic Institute, Denmark	
ZM/HAMSOM	Institute for Meereskunde - Hamburg, Germany	Pohlmann (1996b)
IF/IFREMER	Ifremer, France	Lazure and Jegou (1998)
IM/NORWECOM	Institute for Marine Research – Bergen, Norway	Skogen et al. (2004), Skogen et al. (1995)
MU/COHERENS	Management Unit of the North Sea Mathematical Models, Belgium	Luyten et al. (1999)
PO/POLCOMS	Proudman Oceanography Laboratory, Great Britain	Proctor and James (1996)
RI/SIMONA, TRIWAQ, WAQUA	RIKZ, the Netherlands	Heemink et al. (2002), van Velzen (2010)
UL/GHER NWECS	GeoHydrodyncamics and Environment Research Universite de Liege, Belgium	Delhez and Martin (1992)
OPYC	Deutsches Klimarechenzentrum (DKRZ), Hamburg, Germany	Kauker and Oberhuber (1997), Kauker and von Storch (2000)
ISPRAMIX	Joint Research Centre Of the European Commission	Eifler and Schrimpf (1992), Ouberdous et al. (2002)
GETM	Leibnitz Institute for Baltic Sea Reseach, Warnemünde Bolding & Burchard Hydrodynamics, Rostock Germany and Asperup Denmark	Burchard and Bolding (2002), Stips et al. (2004)
NEMO	European Consortium	Madec (2008), O'dea et al. (2012)
MIPOM	Princeton University	Blumberg and Mellor (1987)
HYCOM	Multi-institutional	Bleck (2002), Chassignet et al. (2003)
ROMS	Rutgers University and UCLA	Shchepetkin and McWilliams (2005)

The goal of these models is to understand and predict the numerous influences of (external) forcing on the coastal seas. These are wind stress, heat, precipitation minus evaporation at the surface, together with river run-off and the influence of the large-scale circulation. Nowadays, state of the art shelf sea models used on supercomputers are able to simulate realistic circulation for periods of at least a decade, fully solving the tidal behavior.

Discretization

All of these models are based on the Reynolds-averaged Navier-Stokes equations together with a divergence-free continuity equation. The eddy viscosity term is solved by applying a turbulence closure scheme. The resulting partial differential equations need to be discretized in order to be solved numerically. Two methods are applied, which are the finite difference method (Rasmussen (1993) and the finite element method (Ciarlet (1978).The former uses a regular grid, whereas in the latter triangular or other shapes are used in order to increase resolution in areas where this is specifically needed. The numerical solution of the partial differential equations using the finite differencing methods is often complicated by numerical dispersion, the presence of wiggles at fronts, and mass falsification. A variety of numerical schemes have been developed with the purpose of overcoming these obstacles (Vested et al. (1992).

In the horizontal, various grid types have been applied: rectangular Cartesian, curvilinear, or spherical. Most of the models adopt a horizontal staggering of variables that follows the Arakawa C grid (Arakawa and Lamb (1977). In the vertical, the traditional method is the geopotential (or z) coordinate system (constant horizontal levels), but also sigma or terrain following coordinates have been used. Lately, a hybrid s-coordinate system becomes more in use, which combines both advantages of z and sigma coordinates. With this system enough layers are located near the surface and bottom to solve the boundary layer dynamics, while the bottom topography is nicely followed. Nowadays, models are constructing meshes with adaptive grids, such that grid resolution automatically locally increases, when strong gradients appear, for example near fronts (Hofmeister et al. (2010).

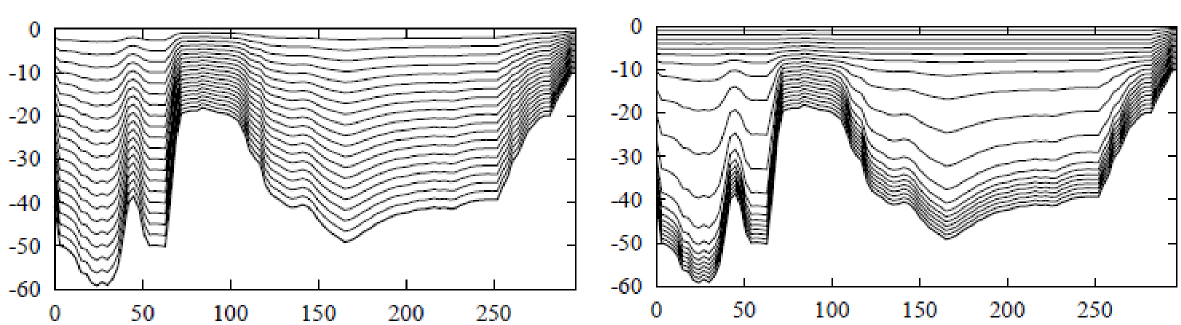

Figure 19: Left: σ-coordinates and right: hybrid coordinates, reprinted from Figure 1 on page 13 of Burchard et al. (2006).

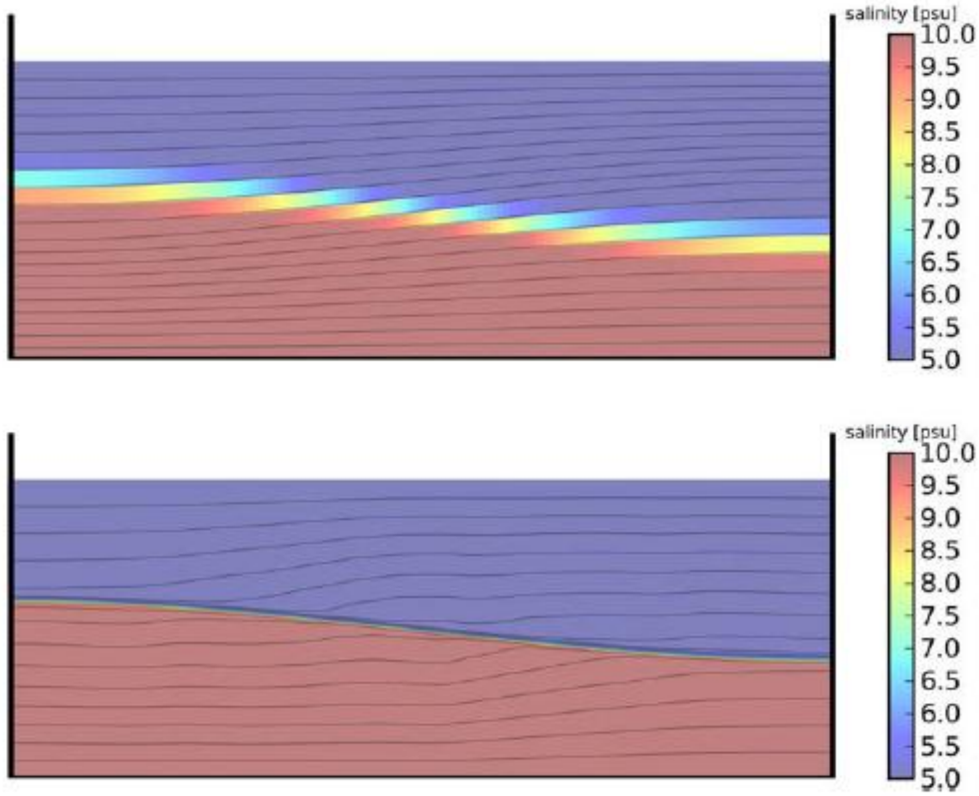

Figure 20: The salinity distribution for the fixed grid (upper panel) and the adaptive grid (lower panel). The black lines denote the positions of the layer interfaces, reprinted from Figure 2 on page 77 of Hofmeister et al. (2010).

The next step is to set a certain set of initial conditions to start out from and a set of boundary conditions and forcing to drive the model.

In shallow seas gravity waves should be represented. But this gives severe constrains on the time step. In explicit models usually time-splitting is applied in which the depth-averaged equations, which contain the gravity waves, are solved on a much smaller time step than the depth varying part of the solution. A complex alternative is to use an implicit method of time stepping, which is much more time consuming.

Sub grid scale processes such as turbulence may display strong spatial and temporal variations. Therefore, these processes should be incorporated in the model somehow. This is done via parameterizations.

Model Forcing

Models are usually driven by surface fluxes of momentum, heat and freshwater from observations or re-analysis products such as the ECMWF-reanalysis data set. Boundary conditions at the open boundary are mostly taken from coarser models over a larger model domain. Temperature, salinity, sea level elevation or vertical averaged velocity are taken from the coarser model, interpolated on the points located at the boundary to force the simulation within the smaller domain. Tidal elevations are sometimes also taken from tidal models describing the global sea surface as a function of time (Egbert and Erofeeva (2002). In this case, temperature and salinity are commonly obtained from climatology such as Janssen et al. (1999) or Berx and Hughes (2009).

Advection

Baroclinic processes, i.e. depth-dependent processes, influence the flow in the North Sea significantly. The performance of numerical schemes for solving advection and dispersion of salt, temperature and (passive) tracers, such as methane is of fundamental importance. However, the advection equation can be discretized in many ways. Many numerical methods have been developed and applied. The most common problems are excessive numerical dissipation with upwind discretizations and spurious oscillations from higher order methods.

Turbulence Closure

In numerical ocean modeling it is not possible to calculate all scales of variability. The variability on scales smaller than the grid-size or the ones that take less time than the (minimum) time-step are not solved. Therefore, not the original hydrodynamic transport equations, the Navier-Stokes (NS) equations, are solved, but the Reynolds averaged NS equations (RANS). In the RANS equation, the variables, such as the velocity components in east-, north- and upward direction and the temperature and salinity, are replaced by a superposition of a slow-varying and a fast varying part (on time-scales smaller than the time-step), which is called Reynolds averaging. These are substituted in the original NS equations and then averaged over time. These resulting Reynolds Averaged Navier-Stokes (RANS) equations contain terms due to the non-linear interaction between fast varying variables, called the Reynolds stresses and turbulent fluxes, adding 14 additional unknowns. As they are based on the fast-varying variables they cannot be solved numerically at that resolution and some sort of parameterization needs to be applied.

The simplest parameterizations relate the turbulent Reynolds stresses to characteristics of the low-varying flow itself, such as the horizontal of vertical shear. This introduces a frictional term similar to the kinematic viscosity and is called eddy viscosity. Such models are called eddy viscosity models. If the eddy viscosity parameter is not a constant, but also a function of the local flow, it is called a zeroth-order turbulence or algebraic closure model. As a consequence, zero equation models may not be able to properly account for history effects on the turbulence, such as convection and diffusion of turbulent energy.

In one equation turbulence models, one equation describing the evolution of a turbulent variable is solved. Usually, an equation is solved for the turbulent kinetic energy, k, which is based on the three components of the fast-varying velocity in east-, north- and upward direction.

Two equation turbulence models are one of the most common types of turbulence closure models, such as the k-ε, k-ω and the k-L model. For these models, besides an equation for the turbulent kinetic energy, k, a second transported variable is prescribed by an equation for the turbulent dissipation, ε, the specific dissipation, ω, or the turbulence macro-scale, L.

Two-equation models are much more sophisticated than the zero equation models as both the velocity and the length scale are solved used separate transport equations. However, the higher order turbulence closure model are less computational efficient.

The above models are called first order models. In second order models, direct use is made of the governing equation for the second order moments (Reynolds stresses and turbulent fluxes) instead of the Boussinesq hypothesis, which assumes that there exists an analogy between laminar and turbulent flow. In second order models, a large number of equations are involved for Reynolds stresses and turbulent fluxes (the correlations between the fast-varying variables). The most famous are the Algebraic Stress Model (ASM) and the Reynolds Stress Model (ASM).

Comparison studies

NOMADS 1 and 2 by Proctor et al. (1997), Tartinville et al. (1998), Proctor (2000), Delhez et al. (2004)

One of the most promising comparison studies on modeling the North Sea circulation was the NOrth Sea Model Advection-Dispersion Study 1 and 2 (NOMADS 1 and 2, Proctor et al. (1997) Tartinville et al. (1998) Proctor (2000) Delhez et al. (2004). Nine three-dimensional hydrodynamic models took part in this study and are listed as the top 9 models in Table 1. In this table, the acronyms of the models are shown, the institute at which it was developed and a general citation to this model. If a citation isn't provided, it was not found on the internet, which suggests that either the model is no longer in operation, or has evolved and given another name. In any case, this makes the model in question, SYSTEM3, no longer interesting for this review.

In Lenhart and Pohlmann (2004) a summary is given of the first NOMADS study by Proctor et al. (1997), which is summarized below. The two main objectives of NOMADS were:

1) To compare the spatial and temporal coherence of realistic simulations of the North Sea hydrodynamics
2) To compare characteristics of the models using a schematic idealized test case.

We will describe the results of the former; most interesting objective, for this review, the latter is described in Tartinville et al. (1998), but is outside the scope of this review. The evaluation of the hydrodynamics models was performed by means of different tracer studies. The model common area was chosen to be the North Sea south of 55°40' (Figure 21), so unfortunately slightly south of the location of site 22/4b. However, it is safe to assume that a hydrodynamic model, that can simulate this part of the North Sea, can also simulate the North Sea a bit further to the North. A choice for three different simulations was given to the modelers: a 2D simulation from 1988/11/01 to 1989/10/31, a 3D simulation for the period from 1989/3/1 to 1989/8/31 or two 3D simulations of March and August 1989, separately.

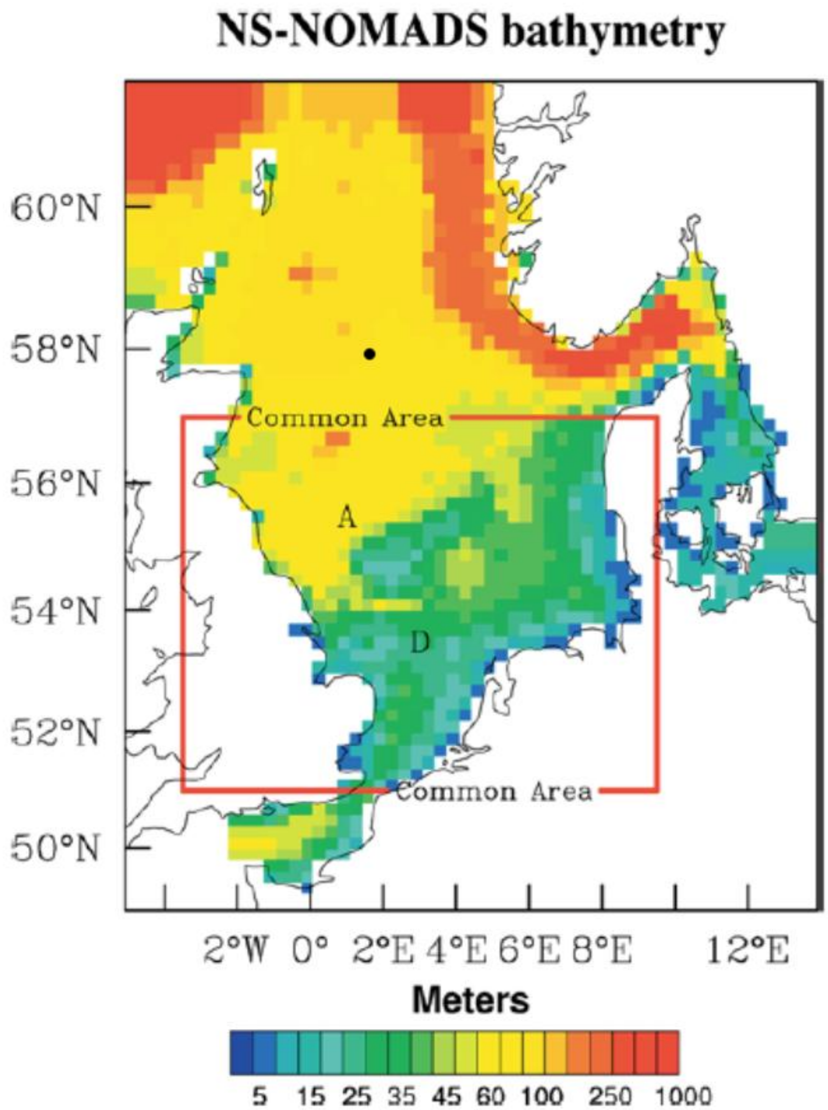

Figure 21: Model bathymetry (depth in m) for the HAMSOM and GETM model. The specified common area is indicated by the red box. The selected stations from the North Sea Project are denoted by A (stratified) and B (well-mixed).The black dot marks the approximate location of site 22/4, reprinted from Figure 1 on page 271 of Stips et al. (2004).

The models were forced with meteorological data, freshwater runoff and boundary conditions for temperature, salinity and tidal forcing. Moreover, a model bathymetry was used as well as initial conditions for salinity and residual flows. Tracers were released every 3 months at 6 specified locations. The characteristics of the models were examined using the age distribution for 180 days of continuous discharge in the 2D case; establishing advection characteristics of trajectories of single particles (both 2D and 3D) and determining spatial advection/dispersion characteristics (2D and 3D). Besides this, the hydrodynamics were investigated by comparing transports of mass and salinity through certain sections.

The main conclusions from the NOMADS study were that:

1) All models reproduced the generally acceptable features of the circulation, advection and dispersion within the southern North Sea. But significant differences have been found between the models.
2) It has proved to be extremely difficult to quantify these differences.
3) It proved impossible to characterize all variability in terms of a limited set of parameters and/or forcing functions.
4) Variability in the hydrodynamics is the largest factor in establishing the variation between the simulations.
5) The major variation in the hydrodynamics was caused by different forcing data sets applied in the different models.
6) The methodology for this study was not able to separate the causes of the differences between the models simulations, probably because the methodology was chosen on the expectation that the variability within the models was small. Differences between the underlying hydrodynamics should be eliminated and common forcing data sets need to be applied.

From the first NOMADS study, a follow-up study was proposed in which all inputs would be identical in order to identify what the causes are for the different model results. Then this could lead to suggestions for model improvement. The two main objectives of the NOMADS2 study were:

1) To provide a scientific methodology to be able to evaluate, compare and classify 3D hydrodynamic models and advection-dispersion models.
2) To demonstrate the degree of correspondence between the model results and in-situ observations of considered processes. This led to the introduction of so called "benchmark methods", such as the cost function.

Within NOMADS2 the focus of the model comparison was on the variability as observed in nature with that in the model simulations. The following steps were applied:

1) A statistical tool (cost function) was established to provide a measure for the variability.
2) Sensitivity studies were run under controlled variations of the input (forcing) functions.
3) An assessment of the natural spatial and temporal variability of the marine system is given.
4) The model spatial and temporal variability is assessed against the natural variability.
5) Model variability is assessed in detail by direct comparison with in-situ observations.

The quantitative comparison between model results and in-situ observations appeared to be an important aspect, although suitable in-situ measurements proved to be the most crucial problem. But also, a comparison of model results should always contain a comparison between the different models under study. However, it was demonstrated that an extensive effort is needed to do so. And that it remains to be difficult to assess the difference quantitatively. The major conclusion is that such a comprehensive model validation study is still missing.

Delhez et al. (2004) also states that the assessment of the error bounds was usually defined by the uncertainty levels and RMS errors of the tidal and storm surge predictions. But if a model is able to predict the tides and storm surges well, does not necessarily mean that it does well in the hydrodynamics too, as tidal and storm surge levels are an integrated quantity. An assessment of the long-term advective and dispersive properties of a model is much more difficult. Delhez et al. (2004) therefore aims at monthly mean volume fluxes and salinity and temperature variations.

An overview of the model characteristics is given in Table 2. It indicates the models domain extension, grid size and the turbulence closure scheme and discretization (z or σ coordinates). These characteristics are intrinsic to the model and the very foundation of it. The models were run using the same bathymetry, meteorological forcing, surface stress and heat flux formulation, river inflows, initial conditions and consistent open boundary conditions for the free surface elevation, velocity, temperature and salinity to avoid additional variability not inherent to the model. Before running realistic simulation, first some sensitivity tests were performed under different wind stress, heat flux and bottom drag. Qualitatively similar results were obtained, but quantitatively in terms of volume flux across a section at 54.5^{o}N substantial differences are found.

Table 2: Overview of model characteristics overview.

Acronym	Horizontal resolution	vertical resolution	Model domain	Turbulence model
DE/DELFT3D	1-30 km	10 σ	up to 57^{o}N	k-ε
DA/SYSTEM3	9 nm ~17 km	40 z (5, 2 m)	51^{o} to 59^{o}N	k-ε
ZM/HAMSOM	1/3^{o} long. by 1/5^{o} lat. (spherical)	10 z (5 m)	up to 61.5^{o}N	2nd order Algebraic
IF/IFREMER	3 km	10 σ	up to 59^{o}N	Munk-Anderson
IM/NORWECOM	20 km	11 σ	Extended continental shelf	MY2.5 (k-kL)
MU/COHERENS	1/10^{o} long. by 1/15^{o} lat.	20 σ	Up to 57^{o}N	k-L
PO/POLCOMS	1/30^{o} long. by 1/45^{o} lat.	18 σ	Up to 59^{o}N	MY2.5 (k-kL)
RI/SIMONA, TRIWAQ, WAQUA	1/8^{o} long. by 1/12^{o} lat.	11 σ	Up to 57^{o}N	k-ε
UL/GHER NWECS	1/6^{o} long. by 1/6^{o} lat.	10 σ	Continental shelf	k-L

In a realistic simulation of a year a model-model and a model-data comparison is performed. The models were forced with three hourly meteorological data from the U.K. MetOffice and monthly mean river discharges from climatology were imposed scaled with a factor 0.8 to reflect that the simulated year of 1989 was a relatively dry year.

The models agree within 1.5°C of each other in terms of the time series of the average temperature in the top 20 m (Figure 22). The difference in temperature between the bottom and the surface, however, indicates quite some disagreement between the models even though the onset of stratification occurs approximately on the same day (Figure 23). The annual mean heat flux of IM and DA is negative, related to the fact that a sharp temperature gradient is maintained between the first thin layer of about ~1m and the second layer. This hardly affects the mean temperature, but prevents heat transport downwards. Something similar occurs with IG and MU, which developed a strong thermocline that hinders the vertical redistribution of heat. The differences observed between the models are essentially dictated by the vertical diffusion, which sets up the stratification and is thus indirectly related to the turbulence closure scheme used.

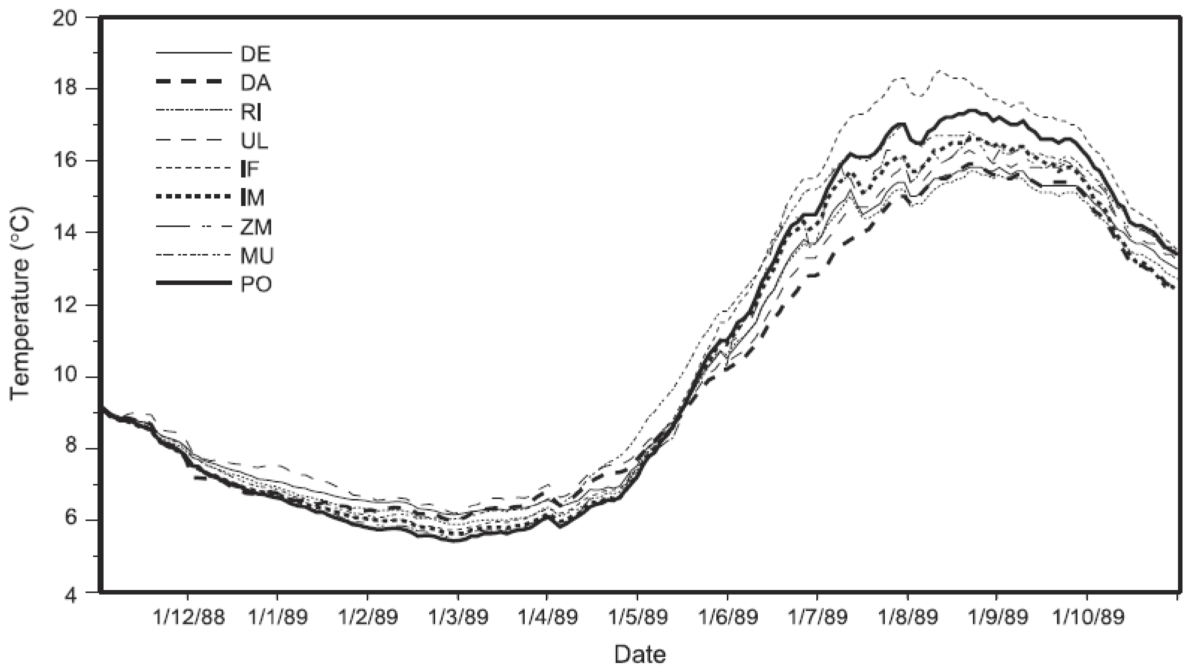

Figure 22: Evolution of the mean temperature (°C) in the top 20 m. A list of acronyms is given in Table 1, reprinted from Figure 4 on page 47 of Delhez et al. (2004).

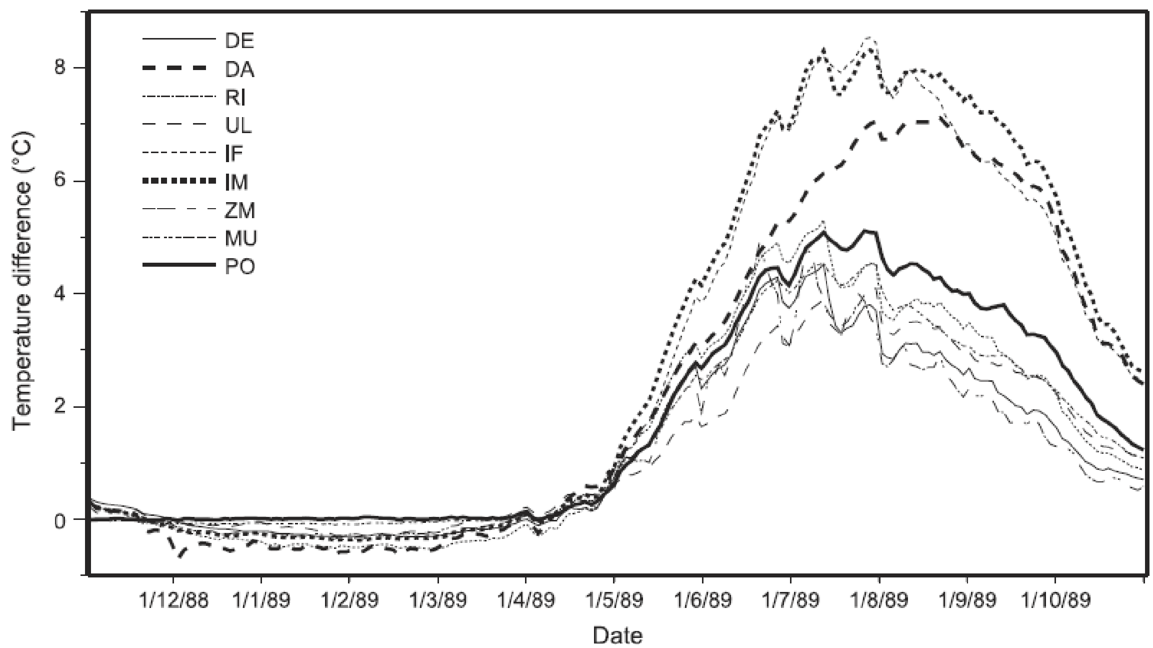

Figure 23: Evolution of the difference between the mean temperature (°C) in the top 20 m and the mean temperature in the rest of the water column. A list of acronyms is given in Table 1, reprinted from Figure 5 on page 47 of Delhez et al. (2004).

A cost function was defined (Søiland and Skogen (2000), which describes the mean error between the model results and the climatological ICES data (1998) of the natural variability.

Table 3 shows the results for the cost function for each model and for different periods of the year and for the near surface and bottom temperature values. Winter is defined as January-February; spring is May-June-July and summer July-August-September. The mean error is 0.57 to 0.97, meaning 57% to 59% of the natural variability. Bold indicate the values that are less than or equal to the mean error. In the surface layer the spreading of the error is larger in winter than in summer, probably due to initialization. A significant jump in the error is observed in late summer, when stratification is at its maximum and starts to collapse. Table 4 shows the results of the same analysis for salinity. The mean error varies between 0.71 and 1.43, so significantly larger than for temperature. A jump of about 0.3 is observed at the onset of the stratification. A large part of the error appears to be related to the initial conditions and the forcing, as the model results are closer to each other than to the measurements. A detailed analysis shows that the higher resolution models (PO, MU and DE) do a slightly better job than the coarser ones (DA, IM, ZM and UL).

Table 3: Cost function for the sea surface (top 20 m) and bottom (below 20 m) temperature. Taken from Delhez et al. (2004)

	Surface			Bottom		
	winter	Early summer	Late summer	winter	Early summer	Late summer
DA	0.62	0.54	0.83	0.56	0.90	1.67
PO	0.92	0.51	0.88	0.97	0.73	0.93
IM	0.83	0.58	1.07	0.85	0.99	1.37
ZM	0.81	0.53	0.64	0.87	0.52	0.85
MU	0.63	0.67	0.55	0.64	0.75	0.62
RI	0.53	0.56	1.02	0.51	0.54	0.99
DE	0.44	0.50	0.75	0.45	0.48	0.74
UL	0.25	0.52	0.78	0.27	0.45	0.70
IF	0.74	0.74	1.75	0.75	0.61	0.89
mean	0.64	0.57	0.92	0.65	0.66	0.97

Table 4: Cost function for the sea surface (upper 20 m) and bottom (below 20 m) salinity. Taken from Delhez et al. (2004).

	Surface			Bottom		
	winter	Early summer	Late summer	winter	Early summer	Late summer
DA	0.97	0.67	1.21	0.86	0.94	1.61
PO	0.72	0.55	0.79	0.76	0.79	1.37
IM	0.66	0.65	0.96	0.62	0.79	1.18
ZM	0.74	0.83	0.98	0.80	0.97	1.67
MU	0.77	0.62	0.83	0.83	0.87	1.25
RI	1.10	0.82	1.01	1.04	1.13	1.41
DE	0.74	0.83	1.12	0.57	0.69	1.19
UL	0.95	0.73	1.19	0.92	0.93	1.87
IF	0.83	0.68	0.98	0.73	0.96	1.37
mean	0.83	0.71	1.01	0.79	0.89	1.43

Figure 24 shows the transport (Sv = $1.0 \cdot 10^6$ m^3/s) though a section across 54.5°N. Unfortunately, there are no in-situ measurements to compare with. There is qualitative agreement between the models displaying maximum northward transport in March. However, the spread between the models is relatively large, about 0.08 Sv. UL has the lowest transport estimate in the first four months with an extreme outlier in December. ZM shows the lowest transports in most of the rest of the year. The highest transports are obtained with the MU model. The location of the open boundary (which is different for the models) doesn't seem to influence the transport much.

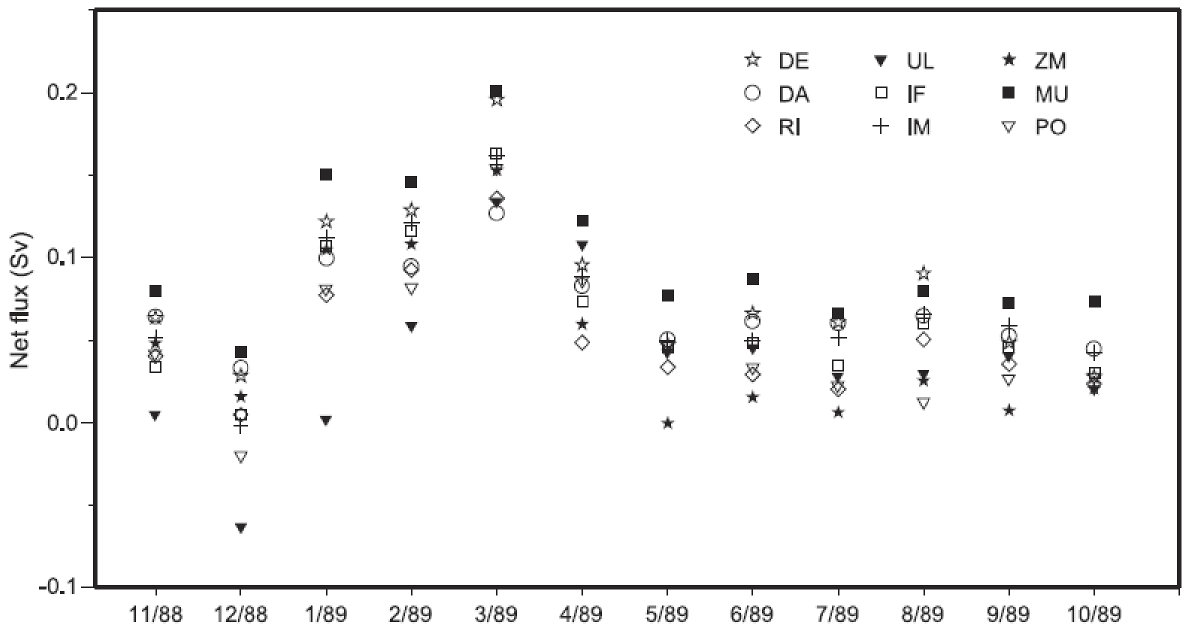

Figure 24: Monthly mean net water fluxes (Sv) across a section at 54.5°N (northward transport are positive), reprinted from Figure 6 on page 51 of Delhez et al. (2004).

The main conclusions from the NOMADS2 study are that the model responses are qualitatively similar, but that large quantitative differences have been observed. For instance, the range of estimates for the volume flux across 54.5°N is 0.1 Sv for each individual month, which is the same order of magnitude as the volume flux itself. Using the cost function showed that the error in the temperature and salinity reaches 70% and 90% of the parameter's natural variability. And above all, the differences cannot be explained by one single model parameter (spatial resolution, turbulence closure scheme, model domain).

North Sea area with OPYC by Kauker and von Storch (2000), ISPRAMIX by Ouberdous et al. (2002) and GETM by Stips et al. (2004) and HAMSOM

The HAMSOM model participated in NOMADS2 and was ranked among the models which gave good and realistic results for the 1-year North Sea run, (ZM in the previous section). Therefore, it was probably selected in (at least) three comparison studies with other (newer) models.

In Kauker and von Storch (2000), the Ocean isOPYcnal Model (OPYC) was run in a regional version of the North Sea and results were compared with the HAMburg Shelf Ocean Model (HAMSOM, ZM in the previous section). In this comparison study the HAMSOM model was reduced to a 2D version a with prescribed 'frozen' density structure from climatological monthly mean distributions for this evaluation of the sea level variations. This disqualifies a thorough description of the comparison for this review, as this review focusses on models that can accurately describe the 3D circulation, of which stratification is an important aspect.

In Ouberdous et al. (2002) a comparison is described between ISPRAMIX and HAMSOM.

HAMSOM is developed for application in the North Sea (Pohlmann (1996a). The circulation model is a modified version of the shelf sea model developed by Backhaus (1985) added to the equation of state for sea water (Fofonoff and Millard (1983). A Cartesian coordinate system is used and the hydrostatic approximation is applied. The turbulence closure scheme uses the Kochergin approach (Kochergin (1987) is described in Pohlmann (1996a). The equations are solved on an Arakawa-C grid in a semi-implicit form. The Coriolis term is stable up to second order. Advective terms are threated explicitly. A selective vector-upstream algorithm is used for the horizontal components. At the closed boundaries a semi-slip and zero flux condition is applied. And the sea surface elevation is prescribed at the open boundaries and a zero gradient condition for the transports is used. Furthermore, inflow conditions of temperature and salinity are prescribed at the open boundaries. At closed boundaries river inflow is simulated by changing temperature and salinity at the respective grid points. At the sea bottom a quadratic stress law is assumed and fluxes of momentum, heat and fresh water are adopted at the sea surface.

The ISPRA ocean general circulation model (ISPRAMIX) is developed at the Joint Research Centre of the European Commission for combine shelf and deep waters (Eifler and Schrimpf (1992). ISPRAMIX was developed as a stand-alone model, which would also permit data assimilation of satellite data. The hydrostatic primitive equations are used and the Boussinesq and shallow water approximations are made. The model uses spherical coordinates. The equation of state for sea water is as defined by UNESCO1981. Turbulent processes are prescribed in terms of Laplacian mixing. Turbulent viscosity and diffusivity are parameterized in terms of a k-l turbulence model. A specific parameterization of the vertical transport due to processes in the near-interface layer is applied (Eifler and Schrimpf (1992). The equations are solved by applying a finite volume method on a C-staggered grid. The model solution for the horizontal velocities is divided into two parts: depth independent external (barotropic) mode and depth dependent internal (baroclinic) mode. The fast gravity waves appear in the external mode; variations in the internal mode occur on a much larger time-scale. The external mode equations are solved explicitly leading to a small time step that has to satisfy the CFL criterion (Courant et al. (1928). A time-splitting approach analogous to those used by Killworth et al. (1991).

Both models runs covered the years 1982 to 1997. The initial fields for salinity and temperature are from the January climatology, the tidal forcing is derived from the output of a 3D hydrodynamic model simulation of the northwest European shelf and also the same atmospheric data set from the German Weather Service (DWD) is used for both model setups. The horizontal grid resolution is 12’ in the North-South and 20’ in the East-West direction (~20x20 km). The vertical grid contains 19 layers. The top 50 meters, in which a thermocline can occur, contains 10 layers of 5 m thickness each. Below this, the layer thickness increase from 10 to 400 m. The time step was 20 minutes.

Observed sea surface temperatures (SST) and salinities (SSS) are prescribed at the surface as opposed to prescribing heat and fresh water fluxes from bulk formulae. At the open boundaries climatological temperature and salinity values are prescribed. Mass and freshwater inputs are monthly mean climatological run-off values at 21 different river locations.

The two models reproduce the same circulation in the North Sea for the year 1989. In the winter time the models are in full agreement with each other on the 'daily' mean (averaged over two tidal cycles, thus 24 and 50 minutes) temperature and salinity fields at the surface as well as in the deeper layers. A well-mixed water column is reproduced. Lateral distributions are also markedly similar: e.g. the intrusion of saline and relatively warm northeastern Atlantic water is well reproduced as well as the strong front at the location where these waters meet the fresh and cold waters originating from the Baltic (Figure 25 and Figure 26). A slight discrepancy can be seen along the Norwegian coast, where in the ISPRAMIX simulation, the salinity gradients are more pronounced. In the spring, the model simulations are still comparable and show a transition towards a temperature stratification. The ISPRAMIX simulation shows more pronounced stratification. In the summer, well-defined summer stratification has developed in both simulations. In the surface mixed layer, the same salinity and temperature fields have developed. This may probably be due to the boundary conditions which force the temperature and salinity towards the same values. Great differences are found below the thermocline, due to the different turbulence modules used in both models.

The North Sea displays high variability due to its location which is under influence of a maritime climate from the North Atlantic and a continental climate from Europe. This variability is well reproduced by the models, which is mainly contributed to the high quality atmospheric and tidal forcing leading to the distribution of temperature and salinity. The variability in the haline stratification is mainly contributed from changes in the freshwater runoff and the input from the North Atlantic. Thermal stratification, however, is more pronounced especially in summer, when heat forcing is strongest.

The simulation of the North Sea circulation by ISPRAMIX agrees reasonable well with the one by HAMSOM. Both models reproduce the general cyclonic basin wide circulation in the North Sea, but also smaller-scale features like the anti-cyclonic circulation near Scotland. The main areas of inflow and outflow in the North Sea are very well reproduced. The Fair Isle Current and the East Shetland Atlantic Inflow are the main inflow regions and the Norwegian Coastal Current the main current generating outflow from the North Sea. The velocity fields and the magnitude of the simulations are very similar. The variability in the mean circulation shows the three patterns dominated by the wind driven circulation: the enhanced cyclonic circulation, the halted circulation and the anti-cyclonic circulation (Figure 27, Figure 28, Figure 29 and Figure 30).

On 15 January, temperatures at 2.5 and 7.5 meter depth at site 22/4b are 7.6^{o}C and slightly warmer at 32.5 and 52.5, being 8.0^{o}C in the HAMSOM model output. Temperatures in the ISPRAMIX model are a little warmer for this particular day, being 8.1^{o}C in the same top three levels and 8.0^{o}C at 52.5 meter depth. The current structure on this day displays strong eastward currents at the surface and northward currents near the bottom in the ISPRAMIX model (Figure 27). On 15 June, a stagnant current structure is found throughout the North Sea and currents near site 22/4b are weak and do not have a distinct direction, both near the bottom as well as at the surface (Figure 28). In Figure 29 a typical reversed circulation is observed in which the surface circulation is westward in the near surface area at sit 22/4b. The circulation near the bottom is rather 'normal' having a northeastward direction. The normal circulation is depicted in Figure 30, where the surface circulation is eastward at site 22/4b. In this particular case no significant bottom currents are observed, which would mean that any substance released at site 22/4b would be transported in all directions by diffusion.

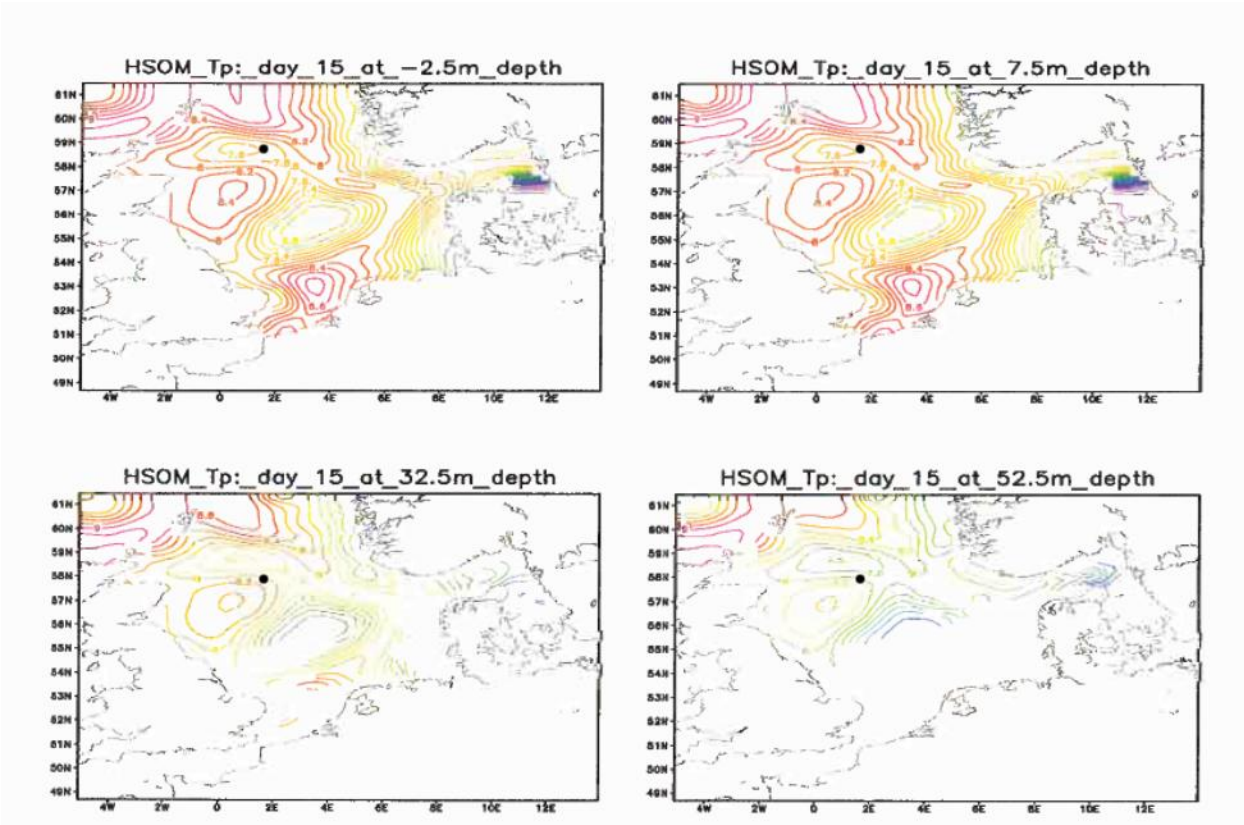

Figure 25: HAMSOM simulated temperature on 15 January, 1989. The contour interval is 0.2°C. Note that the color scale differs between the panels. The black dot marks the approximate location of site 22/4b, slightly modified from Figure 1 on page 16 of Ouberdous et al. (2002).

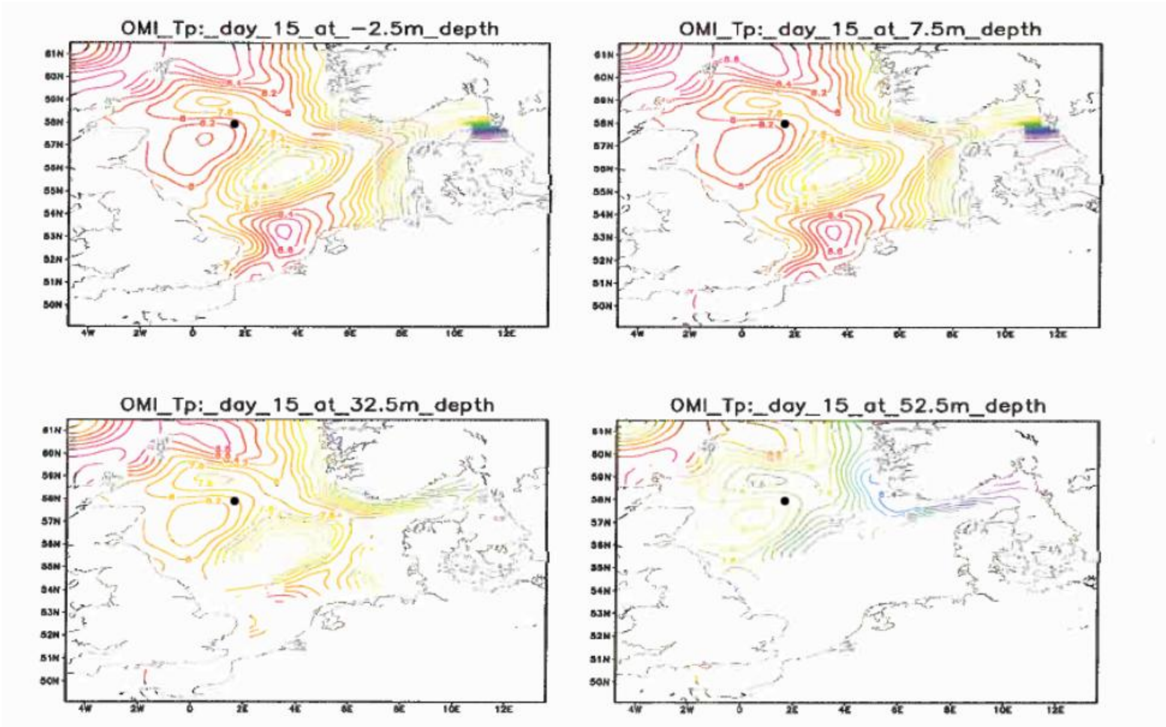

Figure 26: ISPRAMIX simulated temperature on 15 January 1989. The contour interval is 0.2°C. Note that the color scale differs between the panels. The black dot marks the approximate location of site 22/4b, slightly modified from Figure 2 on page 16 of Ouberdous et al. (2002).

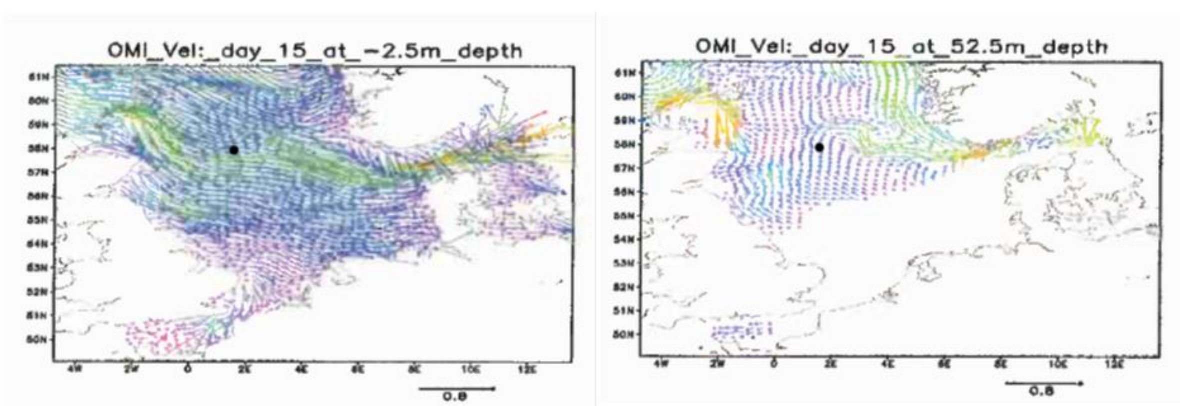

Figure 27: Typical enhanced circulation in simulation by ISPRAMIX daily mean currents on 15 January 1989; left: surface, right: bottom. The color scale indicates the strength of the currents with magentas being the weakest and yellows the strongest currents. The black dot marks the approximate location of site 22/4b, slightly modified from Figure 50 on page 42 of Ouberdous et al. (2002).

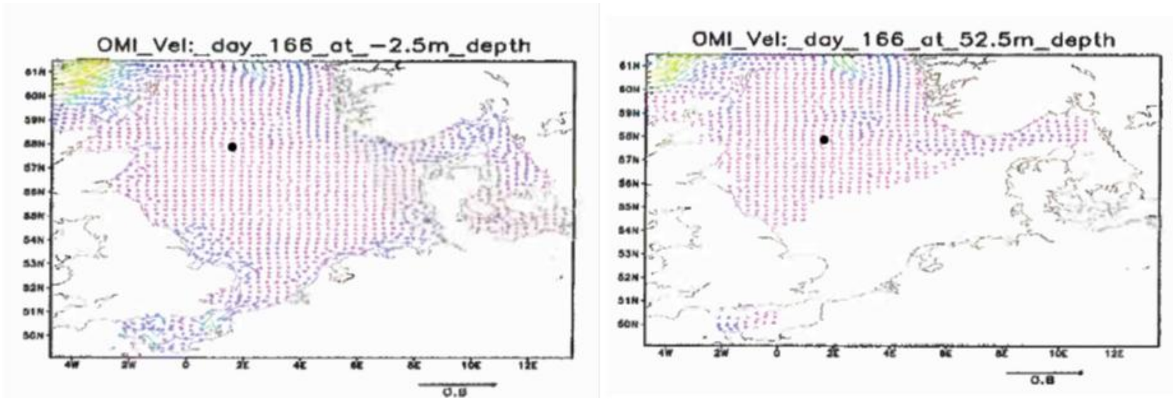

Figure 28: Typical halted circulation in simulation by ISPRAMIX daily mean currents on 15 June 1989; left: surface, right: bottom. The color scale indicates the strength of the currents with magentas being the weakest and yellows the strongest currents. The black dot marks the approximate location of site 22/4b, slightly modified form Figure 60 on page 47 of Ouberdous et al. (2002).

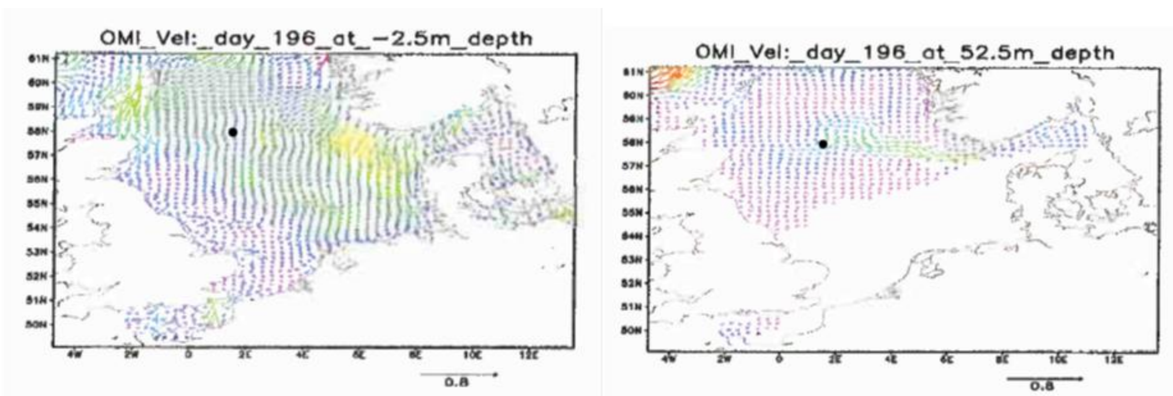

Figure 29: Typical reversed circulation in simulation by ISPRAMIX daily mean currents on 15 July 1989; left: surface, right: bottom. The color scale indicates the strength of the currents with magentas being the weakest and yellows the strongest currents. The black dot marks the approximate location of site 22/4b, slightly modified from Figure 62 on page 48 of Ouberdous et al. (2002).

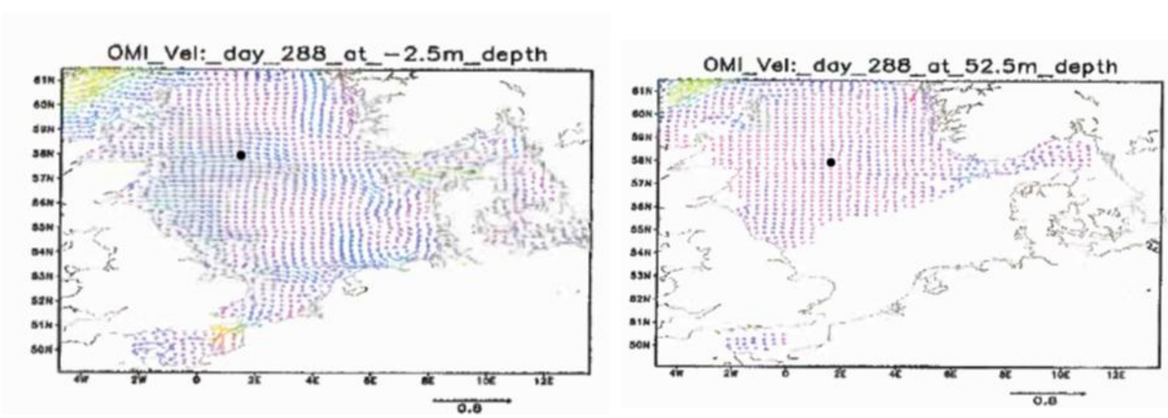

Figure 30: Typical normal circulation in simulation by ISPRAMIX daily mean currents on 15 October 1989; left: surface, right: bottom. The color scale indicates the strength of the currents with magentas being the weakest and yellows the strongest

currents. The black dot marks the approximate location of site 22/4b, slightly modified from Figure 68 on page 51 of Ouberdous et al. (2002).

Stips et al. (2004) describes a comparison between HAMSOM (Backhaus (1985) and a relatively new model GETM (General Estuarine Transport Model) and investigates the details of the stratification and destratification in the North Sea. Details on the model can be found in Burchard and Bolding (2002) and Stanev et al. (2003). Model simulations of HAMSOM for the period November 1988 to October 1989 are compared against measured data from the North Sea Project and against satellite sea-surface temperature measurements. The model has evolved under a minimum of constraints: temperature and salinity are provided at the open boundary. The simulated period coincides with that of Holt and James (1999) and Holt and James (2001). In this study the same integral parameters are selected that were used for the NOMADS2 study by Proctor (2000). The HAMSOM model was chosen because it was ranked amongst the models that gave realistic results for the 1-year North Sea run.

The comparison between HAMSOM and GETM was performed as optimally as possible by choosing the same horizontal grid, initial, boundary and forcing conditions for GETM as were used for HAMSON in the NOMADS2 run. Also a first-order upstream scheme for tracer advection was chosen in GETM as a basic test even though higher-order advection schemes usually perform better (Schrum (1997). Then the models still differ in the applied turbulence scheme (algebraic in HAMSOM and two-equation turbulence closure model in GETM), the chosen vertical discretization (geopotential z-coordinates in HAMSOM and general vertical coordinates in GETM) and to some extent the temporal discretization.

GETM uses the 3D hydrostatic equations of motion in flux form and applies the Boussinesq approximation and the eddy viscosity assumption together with a continuity equation for non-compressible fluids. The equation of state for seawater is used to calculate density as a function of temperature, salinity and pressure (Fofonoff and Millard (1983). At the surface and at the bottom a kinetic boundary condition is applied (no water is allowed to pass through these surfaces) and a no-slip boundary condition is applied at the bottom boundary (all velocity components are zero at the bottom). At the surface a dynamic boundary condition is applied in which surface stresses due to the wind speed, wind direction, surface roughness, etc. are incorporated. At the closed boundaries the flow must be parallel and across an open boundary velocity gradients must vanish. Sea level elevation is forced at the open boundaries. Tracer equations are applied for temperature and salinity. The bulk formulae prescribed by the NOMADS2 consortium have been used for prescribing the momentum and heat-surface fluxes due to air-sea interaction. The GOTM (General Ocean Turbulence Model, Burchard et al. (1999) is implemented in GETM to provide the turbulent closure. GOTM contains a suite of turbulent closure modules ranging from simple algebraic expressions to two-equation models. In general, two-equation models are used and extensively tested against observations in Burchard and Bolding (2002), but the best experience is with two-equation models such as the k-ε model and the Mellor-Yamada model.

For GETM, a staggered C-grid was used in the horizontal. A selection of different advection schemes can be chosen from, e.g. UPSTREAM (UP), SUPERBEE (SU) and ULTIMATE QUICKEST (QU). They were used for comparison and were used to transport temperature/salinity and momentum separately. The k-ε turbulence closure model is used. The micro and macro time steps are 60s and 1800 s, respectively, applied to the barotropic and the baroclinic part of the model. No background horizontal diffusion is used, which is usually done to described sub-gridscale mixing, but will mask the differences between the performed simulations.

The potential energy, the stratified area, the mean kinetic energy and the average temperature are computed throughout the 1-year simulation. The potential energy shows that GETM belongs to the group of models (in NOMADS2) with the lowest potential energy during the peak stratification (and thus strongest stratification), similar as HAMSOM. Moreover, the potential energy is strongly dependent on the advection scheme used. Also the stratified area is comparable to the one of HAMSOM, with the onset of the stratification and start of the mixing occurring at approximately the same time. The mean kinetic energy displays the spring-neap tidal cycle and is similar for both models, although MKE maxima of HAMSOM are about 20% larger than the GETM ones. The mean MKE is still similar, suggesting that GETM has MKE in the middle range of the NOMADS2 models similar as HAMSOM. The average temperature in Figure 31 also shows similar behavior for both models throughout the year. The difference between the models was less than 0.5K. The model averaged temperature was raised by 4K in one year, but that magnitude was also seen in the observations. The temperature difference between the upper layer and the lower layer in summer is strongly dependent on the advection scheme used. Higher-order advection schemes, such as SUPERBEE, result in a much more pronounced stratification Figure 31).

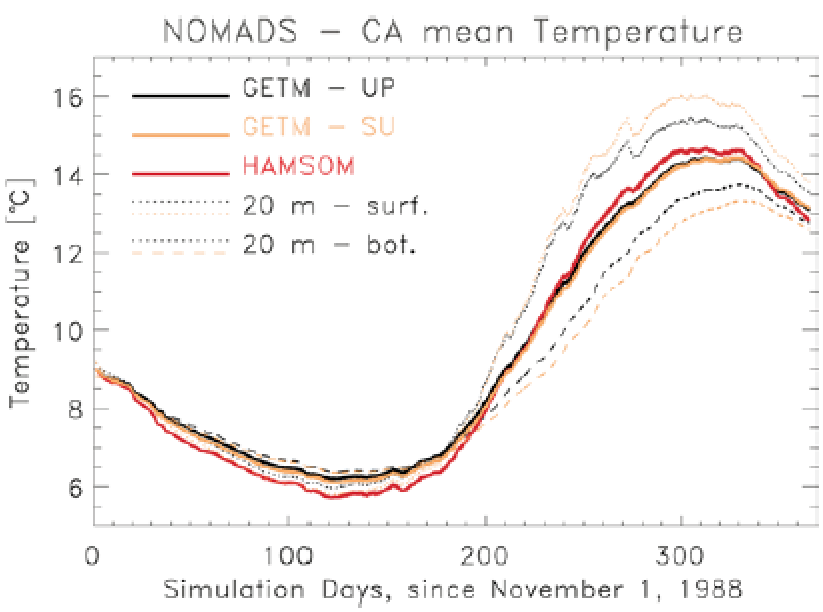

Figure 31: Heat content of the NOMADS common area, expressed as mean temperature. The *bold lines* show the mean temperatures of the total water column, the *dotted lines* represent the upper 20 m, whereas the *dashed lines* represent the part from 20 m down to the bottom, reprinted from Figure 5 on page 273 from Stips et al. (2004).

Figure 32 shows the temporal evolution of the temperature at station A (Figure 21) at (55.5°N, 0.9°E), which is well-mixed during winter and becomes stratified in summer. The summer stratification is more pronounced with higher order advection schemes (third panel), leading to a sharper thermocline, which is better in agreement with the observations (fourth panel). The modeled surface temperatures are in good agreement with the observations, but the lower layer temperatures heat up too early and too fast. The model probably overestimates the vertical diffusion, which will smear out the thermocline and transports too much heat downward.

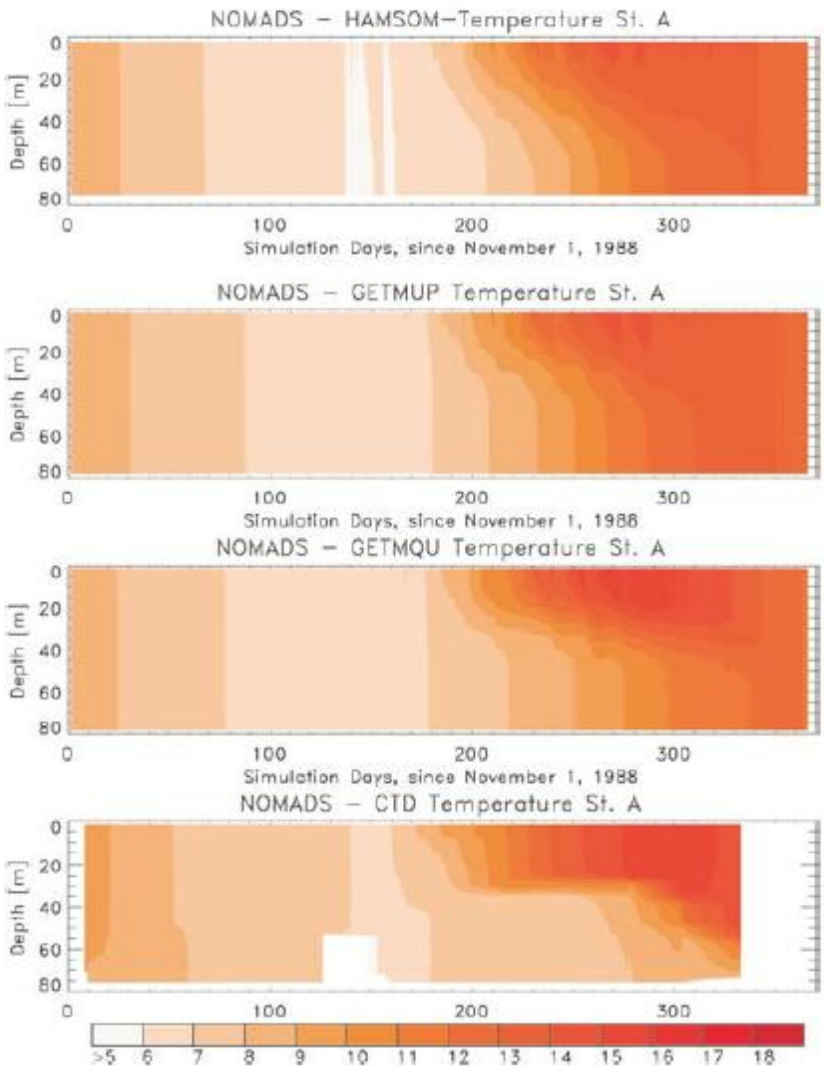

Figure 32: Temporal evolution of the temperature fields at the NOMADS station A (stratified) for different advection schemes. The lower most panel shows the measurements from the North Sea Project, reprinted from Figure 6 on page 274 of Stips et al. (2004).

Seasonal salinity variability is small at this station, e.g. less than 1 PSU. It turned out to be a challenging task to simulate the salinity distribution well. The measurements show that the salinity stratification is either stable or neutral throughout the year, whereas the models display instable salinity stratification. For this parameter, HAMSOM performs best. The salinity in the North Sea is influenced by freshwater from several large rivers as well as brackish water from the Baltic Seas and evaporation minus precipitation. As in the NOMADS2 study the freshwater forcing (being from monthly mean values) is not sufficient to achieve a realistic simulation. Likely, at least daily fresh water fluxes are needed. Moreover, a point measurement is compared with the mean value within a selected grid box.

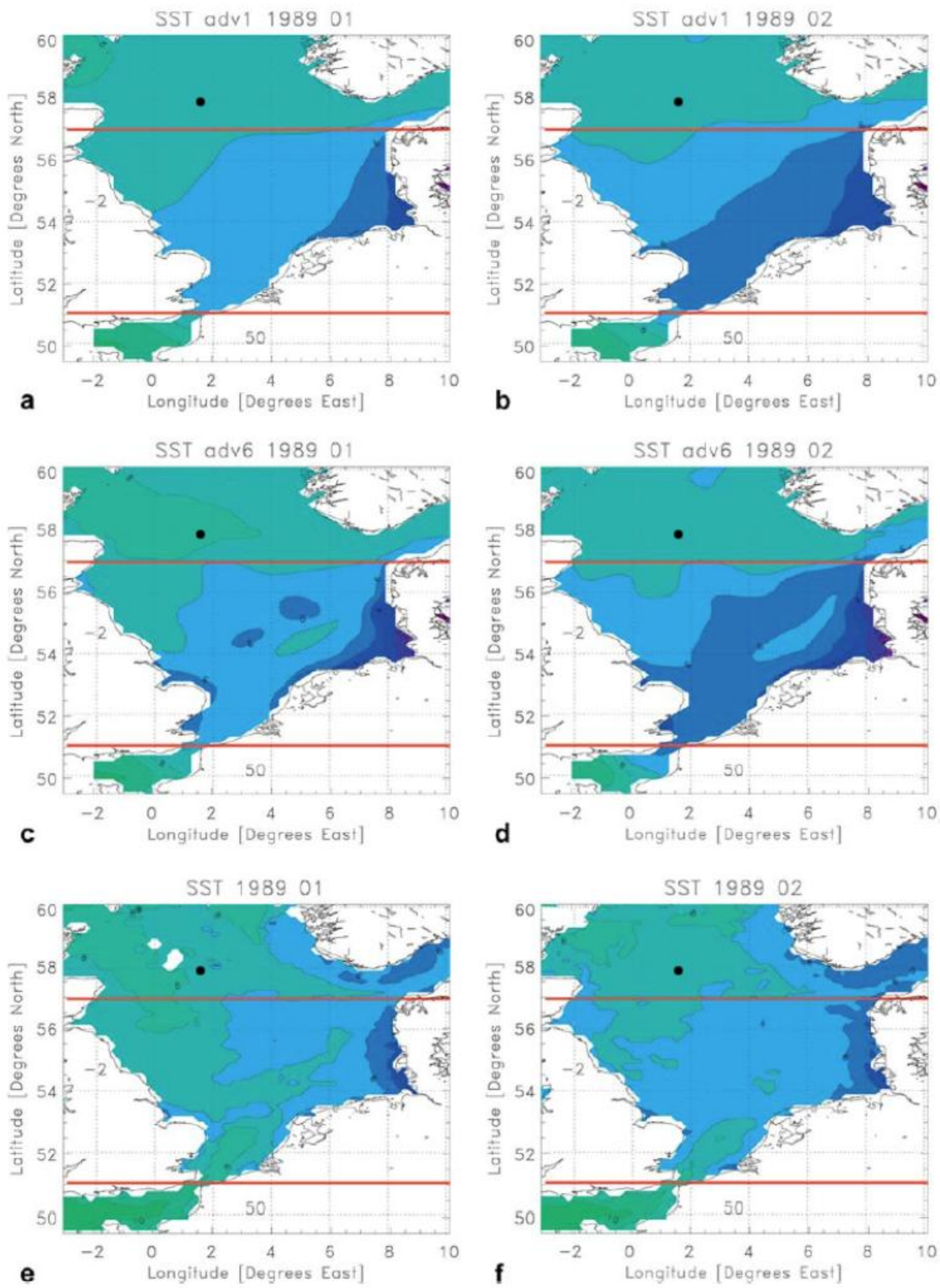

Figure 33: Monthly mean SST from GETM-UP (upper panel), GETM-QU (middle panel) and NOAA pathfinder satellite (lower panel) for the months January and February 1989. The temperature interval is 2°C, varying from blue (4°C) to green (8°C). The black dot marks the approximate location of site 22/4b, slightly modified from Figure 15 on page 278 of Stips et al. (2004).

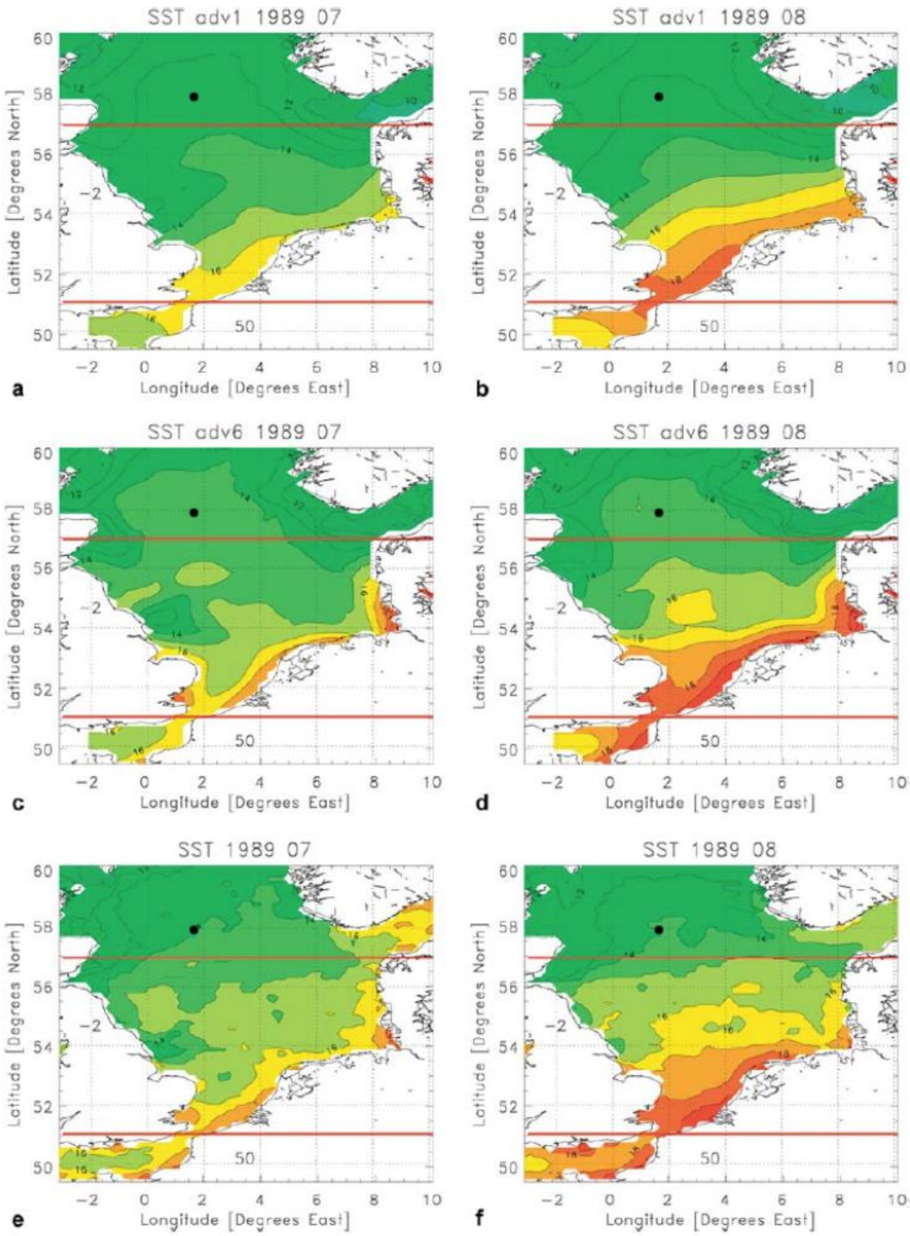

Figure 34: Monthly mean SST from GETM-UP (upper panel), GETM-QU (middle panel) and NOAA pathfinder satellite (lower panel) for the months July and August 1989. The temperature interval is 2°C, varying from green (14°C) to red (20°C). The black dot marks the approximate location of site 22/4b, slightly modified from Figure 16 on page 279 of Stips et al. (2004).

The monthly mean SST for the winter and summer months from satellite measurements and from model simulations are shown in Figure 33 and Figure 34. Large scale features are well reproduced by the model simulations, but the satellite images clearly show much more small-scale variations. The GETM-UP simulations show much smoother (less realistic) results compared with the GETM-QU simulations, indicating again that higher-order advection schemes reproduce small-scale frontal behavior much better. Moreover, the seasonal dynamics in the Norwegian trench is not underestimated with GETM, whereas Holt and James (2001) indicate that the underestimation in their model (POLCOMS) is due to the use of σ-coordinates. Apparently, this problem is not an issue in GETM, which uses general vertical coordinates and a quasi-constant uppermost layer thickness of about 2 m. The SST near site 22/4b is much better reproduced with the higher order advection scheme, both in summer and in winter. The lower order advection scheme underestimates the SST near site 22/4b both in winter and in summer. In winter the higher order advection scheme works fine, but in summer SSTs are somewhat overestimated at site 22/4b.

Stips et al. (2004) further states that the model results are very dependent on the boundary conditions used, which are far from being optimal for a realistic study, but chosen such that they are equal for all partners in the NOMADS2 study.

In summary, GETM agrees with most of the investigated parameters with HAMSOM, which confirms that is reproduces the basic North Sea dynamics well. The annual cycle of the heat content in the common area gave realistic results and the temperature difference between summer and winter agrees well with the observations of the North Sea Project (Holt and James (1999). Model comparison studies like NOMADS 1 and 2 demonstrate that comparisons should be done under the same conditions, e.g. bathymetry, initial and boundary conditions and meteorological forcing. Models can then be evaluated by comparing different integral parameters. Results are that large deviations exist between the models, due to specific model details such as the turbulence closure model used, the advection scheme, the boundary conditions and slightly different domains. The study by Stips et al. (2004) shows that if an almost identical setup is chosen, the simulations from different models agree well. Moreover, it has also shown that GETM can produce an improved simulation compared to HAMSOM if the advanced features incorporated in the former are used. The main conclusion is that GETM is able to reproduce the temperature and salinity observations of the North Sea at least as well, if not better than HAMSOM, which was ranked amongst the best models for the North Sea in the NOMADS2 study.

Thus, higher-order advection schemes improve the simulation of the North Sea as they lead to stronger horizontal gradients that in turn lead to more pronounced vertical stratification. Moreover, the use of the k-ε turbulence closure model lead to a shallower and sharper thermocline and is thus essential for establishing realistic summer stratification. The freshwater fluxes should be prescribed daily to be able to reproduce the observed salinity distributions. The use of general vertical coordinates with a quasi-fixed surface layer depth improves the simulation of the deeper parts of the North Sea, such as the Norwegian trench.

North Sea area with FOAM-AMM (NEMO) by O'dea et al. (2012) with POLCOMS

A new operational ocean forecast system, the Atlantic Margin Model (AMM) implementation of the Forecast Ocean Assimilation Model (FOAM-AMM) is developed for the North West European Continental Shelf (NWECS). The physics are based on the Nucleus for European Modeling of the Ocean (NEMO) and a Sea Surface Temperature (SST) assimilation scheme is included. The use of NEMO allows short-term operational ocean forecasting systems to employ the same ocean model code as the global and basin scale seasonal and climate prediction systems at the Met Office. Assimilation of SST makes FOAM more suitable for the application in the shelf sea, whilst NEMO is also coupled with the European Regional Seas Ecosystem Model (ERSEM). Here, we focus only on the details of the physics and the assimilation.

The previous operational model of the NWECS at Met Office was the Proudman Oceanography Laboratory Coastal-Ocean Model System (POLCOMS), which was also used in the NOMADS study. NEMO was developed as an open ocean model, so significant modifications to NEMO had to be applied to make is suitable for application in the NWECS. POLCOMS is a well-established and validated system (NOMADS; Holt and James (1999) Holt et al. (2001) Holt and James (2001) and thus provides a reliable reference.

The model covers the North-West European continental shelf and a part of the North-East Atlantic (Figure 35). The main focus is on the dynamics on the NWECS, but off-shelf dynamics and the shelf slope current are also important as they impact the cross-slope transport. Furthermore, accurate representation of tidal dynamics, turbulence production and dissipation, and the air-sea flux of momentum and heat are critical for modeling the regional dynamics. The winds both induce turbulence production and drive currents, which provide residual circulation. Wind forcing in combination with atmosphere pressure gradients induce storm surges in the North Sea, which interact with the tides. Sources of freshwater are specified for 320 European rivers and the low saline water from the Baltic is derived from the Danish Hydrographic Institutes' Dynamics of Connected Seas (DYNOCS) experiment.

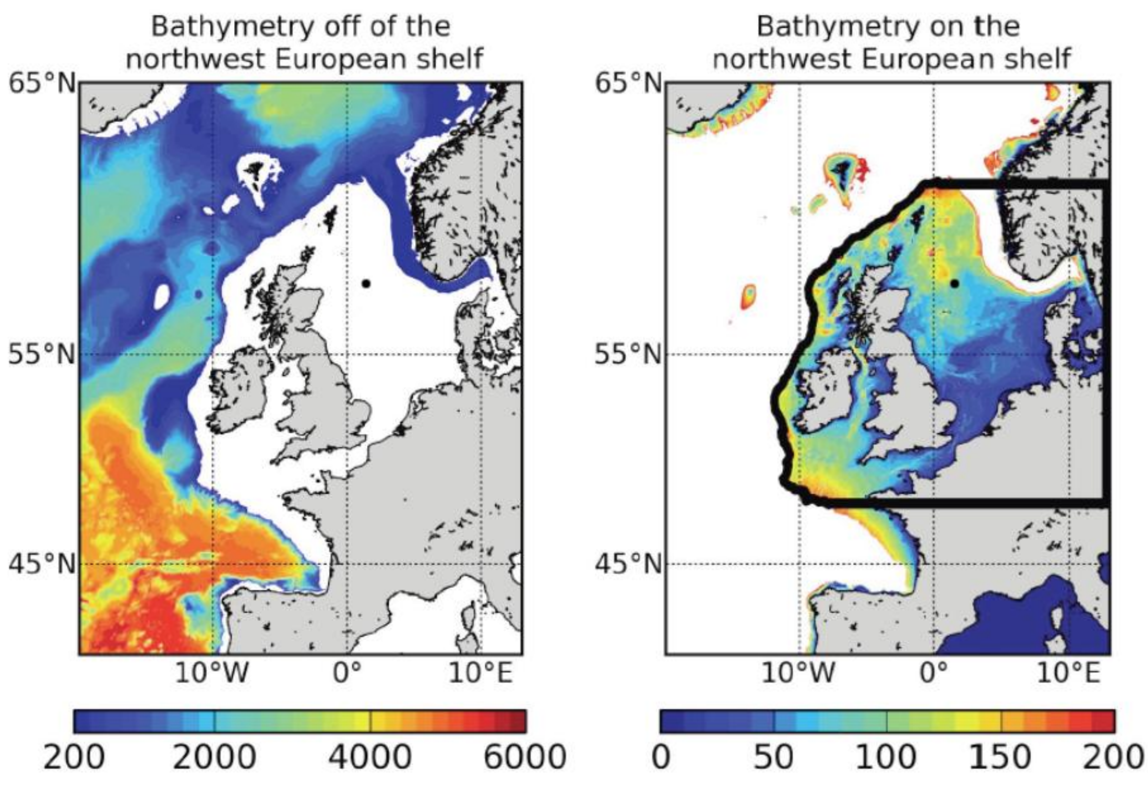

Figure 35: Atlantic Margin Model Domain. Left Panel: Off Shelf bathymetry > 200 m. Right panel: On shelf bathymetry < 200 m. The Medium Range Continental Shelf domain boundary is indicated by a thick black line. The black dot marks the approximate location of site 22/4b, reproduced from Figure 1 of O'dea et al. (2012) with permission of the IMarEST Journal of Operational Oceanography.

The existing coupled POLCOMS-ERSEM Medium Resolution Continental Shelf (MRCS) system (having 7 km resolution) is nested into a physics only POLCOMS-AMM model (having 12 km resolution). In the new FOAM-AMM system the coupling with ERSEM extends over the entire AMM region at a resolution of $1/15^o$ latitude by $1/9^o$ longitude, which is about ~7 km. This is sufficient to resolve the external Rossby Radius (~200km), but for the internal Rossby Radius a resolution of <2 km is needed, which is impractical for a coupled hydrodynamic-ecosystem operational forecast model. A hybrid s-σ terrain following coordinate system is used in the vertical with 32 levels to retain vertical resolution on the shelf, while allowing a reasonable representation of deep water processes. Focused resolution in deep water at the surface is important for air sea fluxes of heat, freshwater and momentum, and the bottom in relation to the bottom boundary layer. The bathymetry is smoothed such that the relative difference between adjacent grid points is less than 30%.

Time-splitting is used with a baroclinic time step of 150 seconds and a barotropic time step of 5 second. Momentum advection is energy and enstrophy conserving. Enstrophy is the integral of the square of the vorticity over the field. Vorticity is a measure of the rotation of the flow. The lateral boundary condition on momentum is free-slip. The total variation diminishing scheme (TVD) is used for tracer advection.

Fifteen tidal constituents are imposed at the open boundary from a tidal model of the North-East Atlantic. In addition to the tidal boundaries, FOAM-AMM is one-way nested in the Met Office operational FOAM $1/12^o$ deep ocean model for the North Atlantic (for temperature and salinity, surge level and barotropic currents). Vertical turbulent viscosities/diffusivities are calculated using the Generic Length Scale (GLS) turbulence model, allowing for a range of closure schemes. In FOAM-AMM the second-moment algebraic (k-ε) closure model of Canuto et al. (2001) is used. The model is forced at the surface by fluxes from the global Met Office Numerical Weather Prediction (NWP) model, which has a 25 km horizontal resolution and incorporates 4-Dimensional Variational Data Assimilation (4DVAR).

Data assimilation within FOAM-AMM is performed in three steps for each day. In-situ and level 2 satellite derived Sea Surface Temperatures (SST) are assimilated into the model simulation to bring the simulation closer to the observations, while taking into account that both simulated as well as modeled SST values are subjected to errors and/or biases.

A systematic validation is performed of the new FOAM-AMM model with the existing POLCOMS-AMM system using a 2-year hindcast period of 2007-2008. The FOAM-AMM shows greater skill in terms of the root mean square error of the Sea Surface Height (SSH) amplitude and phase versus tidal gauge data than POLCOMS-AMM (about 10% better). Also the co-tidal chart (Figure 36) shows a great improvement in the position of the M2 amphidromic point south of Norway for the FOAM-AMM system.

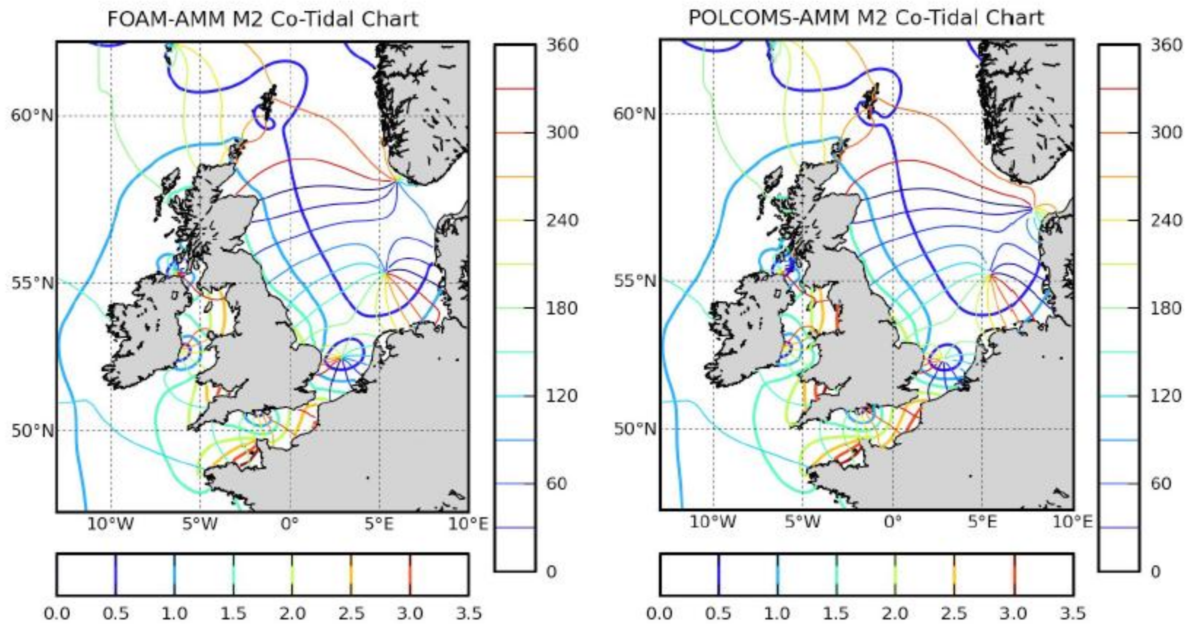

Figure 36: M2 Co_tidal chart for FOAM-AMM (left) and POLCOMS (right). Co-range lines are thick and values are given on the horizontal colorbars. Co-phase lines are thin and values are given on the vertical colorbars, reproduced from Figure 5 of O'dea et al. (2012) with permission of the IMarEST Journal of Operational Oceanography.

Free and SST assimilating hindcast were performed with FOAM-AMM for the two-year period of 2007-2008. These and the POLCOMS-AMM run are compared with the Operational Sea Surface Temperature and Sea Ice Analysis (OSTIA) SST fields for the same period. However, OSTIA is not an independent data source, both because the NWP derived fluxes use OSTIA data and the data assimilation uses data common to OSTIA. The free run of FOAM-AMM has an annual warm bias relative to OSTIA of 0.47^{o}C. This bias is most marked in winter, in contrast with the warm summer bias of POLCOMS-AMM. The latter is a result of the POLCOMS-AMM model over stratifying. The bias in FOAM-AMM is due to a combination of the turbulence scheme, the simple light attenuation scheme and the prescribed fluxes. The assimilated FOAM-AMM run has a mean discrepancy of only 0.11^{o}C with OSTIA. Also the RMS difference dropped from 0.78^{o}C to 0.37^{o}C using SST assimilation. Thus the SST assimilation improves the simulation of the SST throughout the year.

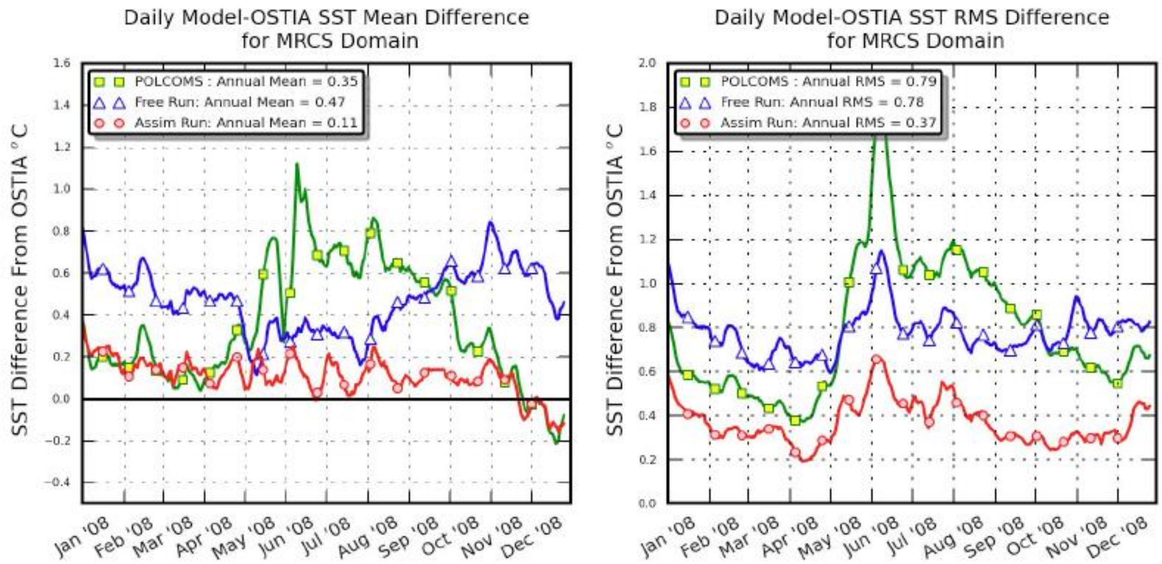

Figure 37: 10 day running mean of mean (left) and RMS (right) differences from OSTIA SST over the MRCS domain for POLCOMS-AMM (green), FOAM-AMM free run (blue) and FOAM-AMM assimilative run (red), reproduced from Figure 8 of O'dea et al. (2012) with permission of the IMarEST Journal of Operational Oceanography.

The locations of the seasonal tidal mixing fronts and the summer stratification are compared against ICES data. Figure 38 shows the summer surface – bed temperature differences for the ICES climatology and the models. The location of the front is indicated by the 0.5^{o}C contour. The location of the front in the FOAM-AMM is more close to the one of the ICES data set than POLCOMS-AMM. The difference in stratification between the models and the ICES data are shown in the bottom panels. POLCOMS-AMM (right) has much more stratification than either ICES or FOAM-AMM. This is due to the turbulence model used in POLCOMS-AMM. The locations of the tidal mixing fronts for the assimilative and the free run of FOAM-AMM do not differ significantly. However, the level of stratification, particularly in the Norwegian trench is different with the free run closer to the ICES data than the assimilative run. In the assimilative run, the SST is significantly corrected there. However, the bottom water temperature in the trench is also cooler in the assimilative run. The assimilation cools the water before it enters the domain, leading to a cooling of deeper waters. A comparison between the FOAM-AMM free and assimilative runs with temperature and salinity profiles not used in the assimilation shows an improvement of the assimilated temperatures and no significant change in the salinity profiles.

To conclude the new operational forecast system, FOAM-AMM, for the North-West European Shelf performs better than the well-established and validated POLCOMS-AMM model. The performance regarding representing the tides has improved. The RMS errors for SST are similar in POLCOMS-AMM and FOAM-AMM without assimilation. Addition of SST assimilation significantly reduces the RMS error, while the seasonal stratification is not altered much. Moreover, the locations of the fronts are closer to those observed in the ICES data. The system continues to evolve and adjustments are expected to improve the simulation further.

The location of site 22/4b is close to the area where the POLCOMS-AMM run displays an unrealistically strong surface-bed temperature difference in summer (June, July, August, JJA) of nearly 10^{o}C, where it is closer to 5^{o}C in the ICES data. The FOAM-AMM free run does the best job in reproducing the summer surface – bed temperature difference at that location.

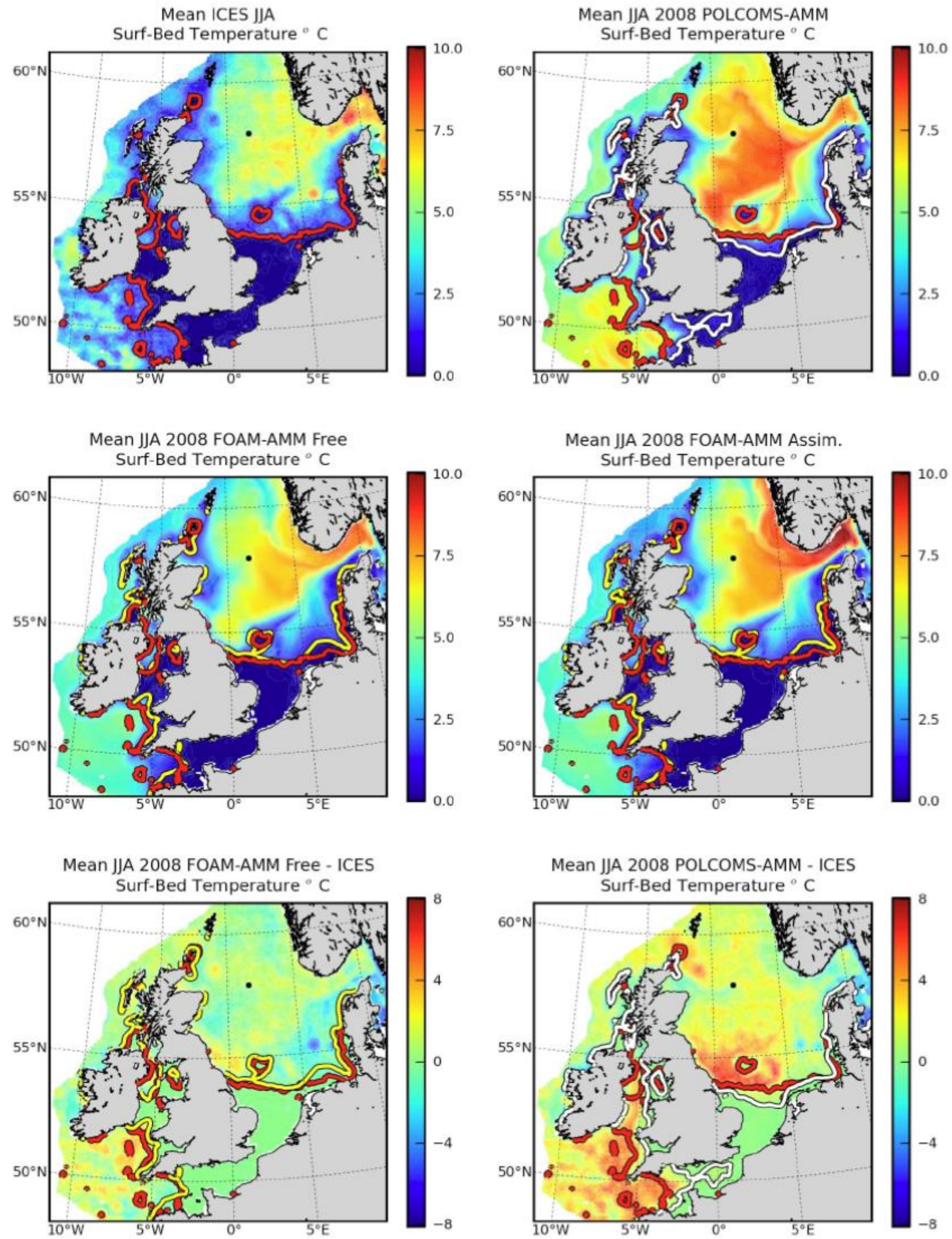

Figure 38: Top left panel is the mean ICES surface-bed temperature for summer (June, July, August - JJA). Top right panel is the mean POLCOMS-AMM surface-bed temperature for JJA 2008. Centre left is the mean FOAM-AMM free run surface-bed temperature for JJA 2008. Centre right is the same for FOAM-AMM assimilative. Bottom left is the JJA mean difference of the surface-bed temperature between ICES and free FOAM-AMM. Bottom right is the JJA mean difference between ICES and POLCOMS-AMM. Thick contours indicate mean frontal locations using the 0.5°C surface-bed temperature contour for the ICES data (red), POLCOMS-AMM data (white) and the FOAM-AMM data (yellow). The black dot marks the approximate location of site 22/4b, reproduced from Figure 10 of O'dea et al. (2012) with permission of the IMarEST Journal of Operational Oceanography.

CONMAN project: North Sea/Skagerrak area with ROMS and HYCOM compared with MIPOM by LaCasce et al. (2007), Albretsen and Røed (2010)

In LaCasce et al. (2007), a three year simulation from three eddy-permitting numerical models was compared. These are the Regional Ocean Modeling System (ROMS), the local version of the Hybrid Coordinate Ocean Model (HYCOM) and the local version of the Princeton Ocean Model (MIPOM). The latter is the former model used for ocean prediction at the Norwegian Meteorological Institute (met.no) and is a rather old model constructed in the 1970s. This is done in the Comparison of Numerical Ocean Models Applied to Norwegian waters project (CONMAN), in order to assess whether ROMS or HYCOM can replace MIPOM for numerical ocean "weather" prediction at met.no. Ocean weather is connected to eddies, jets and meanders, with a typical length scale of order 10 km in Norwegian waters (thus small-scale). In Albretsen and Røed (2010), ROMS and MIPOM are compared using a 27-year-long simulation, as ROMS is now used as the operational model at met.no (L.P. Røed, personal communication).

The models are run for a three year period starting October 1, 2003. The domain of the outer model covers the area of the Northeastern North Atlantic of Atlantic Margin. The grid size is 4 km (eddy-permitting) for all models and the forcing is taken to be as similar as possible (atmospheric input, river discharges, topography, initial conditions, lateral open boundary forcing). Some difference still exist: ROMS and HYCOM had different lateral boundary conditions. To make a direct comparison possible, MIPOM was run with both of them. Simulations from January 1, 2004 to September 30, 2006 were analyzed. Velocities are compared with in situ measurements for a specific area. The mean flows and the standard deviations of the models are comparable with ROMS being the most energetic, followed by MIPOM and subsequently by HYCOM. MIPOM and HYCOM display an equatorward mean flow at depth in the North Atlantic, which is absent in ROMS. Furthermore, ROMS inflow bifurcates at the shelf into a part that follows the shelf further and a part entering the North Sea. HYCOM displays something similar, with a stronger inflow into the North Sea. Almost the entire mean flow in MIPOM enters the North Sea, mixing with the Norwegian Coastal current, thereby altering the water mass characteristics, which doesn't seem to occur in reality, leading to the conclusion that the bifurcation displayed in ROMS is the most realistic one. This is probably due to the use of a third order horizontal advection scheme in ROMS, a higher vertical resolution and a more sophisticated numerical handling of the vertical turbulent processes. In Winther et al. (2007) it was found that a fourth order scheme at 4 km resolution gives results close to a second order scheme at 2 km resolution. LaCasce et al. (2007) advised to do the same study with identical setups for the models (same amount of vertical layers and exactly the same forcing). This is apparently done by Albretsen and Røed (2010) for ROMS and MIPOM only.

The computational domains for ROMS/MIPOM are slightly different from the domain of HYCOM. The mean mesh size is 4 km for all models, but the maximum and minimum grid size differs slightly due to the different projections. Atmospheric variables to derive momentum, heat and freshwater fluxes are extracted from the operational analysis of ECMWF. Climatological monthly values are used for the river discharges. Two sets of lateral boundary conditions are applied to the open boundaries, because they are different between ROMS/MIPOM and HYCOM. The first set are daily mean values of water level without tides, currents and hydrography from a coarser resolution wide version of HYCOM that covers all of the northern hemisphere Atlantic Ocean (TOPAZ). The second set is climatological monthly mean values extracted from the EKASC archive. Besides that, tidal elevation and tidal current are specified separately.

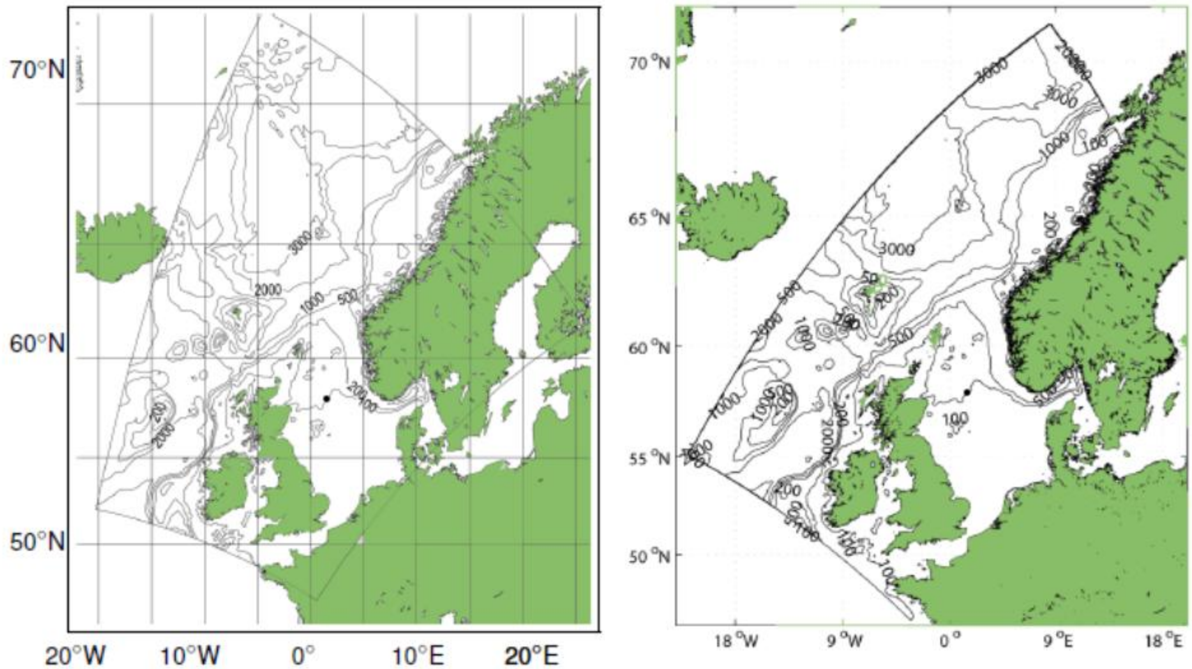

Figure 39: Computational domain and topography of MIPOM and ROMS (left) and HYCOm (right). Contours are at 100, 200, 500, 1000, 2000 and 3000 meters. Note the difference in map projection which gives rise to difference in the computational domain covered by ROMS/MIPOM compared to HYCOM. The black dot marks the approximate location of site 22/4b, reprinted from Figure 3 on page 5 of LaCasce et al. (2007).

MIPOM and ROMS use terrain-following vertical coordinates, whereas HYCOM uses a hybrid coordinate system. One consequence of this difference is that HYCOM has less vertical resolution (fewer layers) in shallower areas than the terrain-following models, but that the surface and bottom mixed layers are well resolved in deeper parts of the domain. The number of layers is 26, 32 and 22 for MIPOM, ROMS and HYCOM, respectively. In MIPOM, the Mellor-Yamada 2.5 level turbulence model is used to handle the vertical mixing; in ROMS, the Generic-Length-Scale second order turbulent closure scheme is used and in HYCOM the KPP mixing scheme. MIPOM and HYCOM use a second order advection scheme, whereas ROMS applies a third order upwind scheme. Besides that MIPOM assimilates Sea Surface Temperature for the last two years. Moreover, it is run with both the TOPAZ and the EKASC data at the lateral open boundaries. ROMS is only forced with the latter, while HYCOM is only forced with the former. No assimilation is applied in ROMS, whereas a weak relaxation to climatological temperatures and salinities is applied in HYCOM.

Mean surface currents in the Rio05 (Rio et al. (2005) product are derived from a combination of hydrographic data, surface drifter velocities and altimetry referenced to the geoid. Geostrophic velocities are then estimated by differencing surface height. Thus the Rio05 fields are solely based on in situ and satellite measurements and no numerical model is involved. Resulting surface currents and speeds (Figure 40) have some unrealistic features (such a south of Sweden and west of Scotland), but displays the general features such as the strong inflow from the North Atlantic through the Fair Isle Current, the East Atlantic Inflow, and the Slope Current and exiting via the Norwegian Coastal Current. The maximum speeds are only 25 cm/s, whereas in situ estimates from current meters provide speeds in the order of 40 cm/s, due to the coarse resolution of the observations (50 km). Near site 22/4b climatological surface currents are weak and so is the variability (less than 5 cm/s).

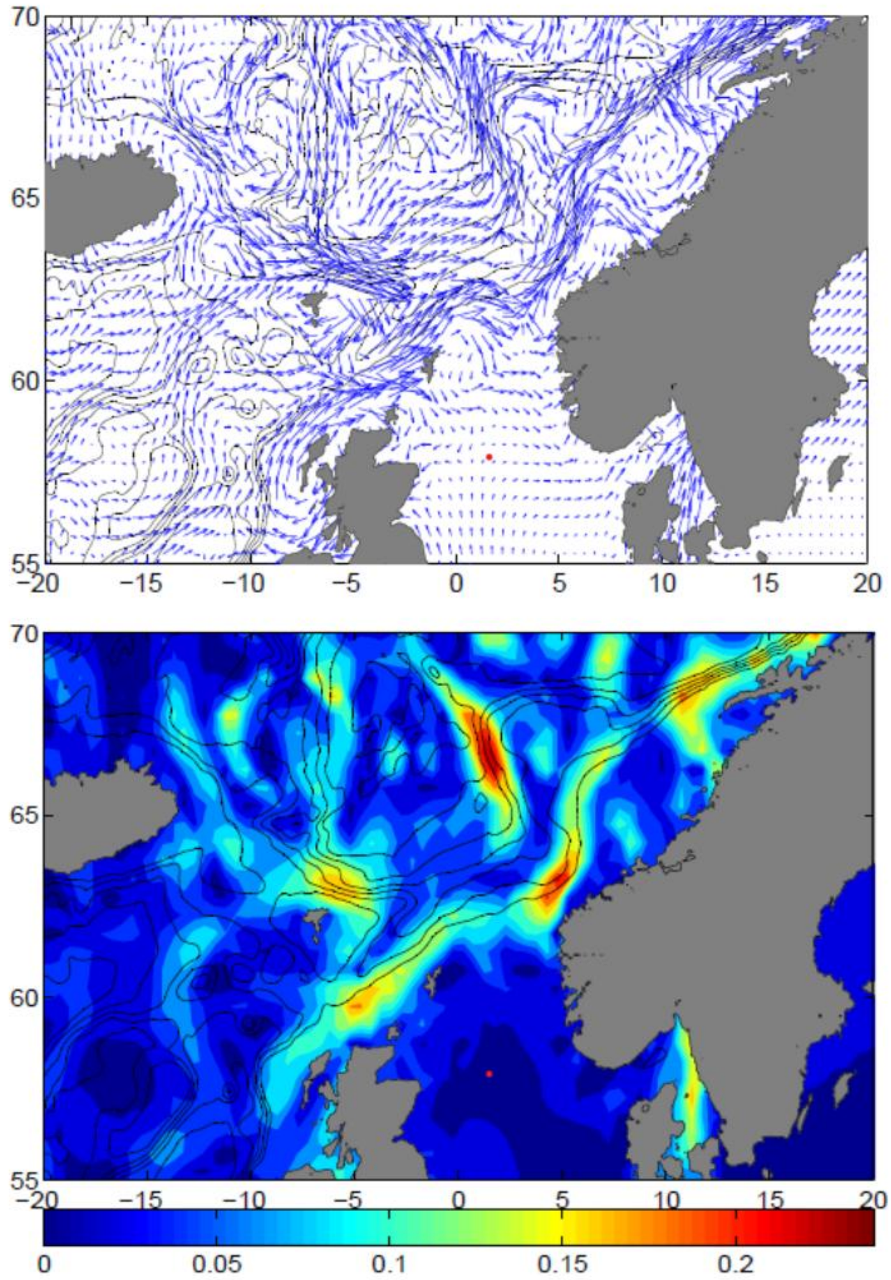

Figure 40: Surface velocities (upper panel) and speeds (lower) panel from the Rio et al. (2005) product. The velocities correspond to means from the period 1993-1999. The color scale shows speed in m/s. The red dot marks the approximate location of site 22/4b, reprinted from Figure 5 on page 13 of LaCasce et al. (2007).

The MIPOM speeds forced with the two boundary conditions (upper panels in Figure 41) are very similar and give maximum velocities in the order of 50 m/s. The FIC is stronger for the MIPOM/EKASC simulation and the SC is stronger for the MIPOM/TOPAZ simulation. The HYCOM run shows significantly weaker speeds (by a factor of 2) than the MIPOM runs. The ROMS speeds, however, are comparable to the MIPOM speeds. The primary difference between MIPOM and ROMS is where the Slope Current bifurcates at 62°N and 2°E. In ROMS a fraction peels of and enters the North Sea and the rest continues northeastward, whereas in MIPOM, the major part of the SC enters the North Sea and only a small portion continues. In MIPOM/EKASC the FIC is somewhat too strong, which may influence the dispersion of substances released at site 22/4b. In HYCOM, overall the currents are too weak, which will reduce the transport of dissolved material at any place in the domain and also at site 22/4b. Both MIPOM/TOPAZ and ROMS perform similarly in the central North Sea and especially in the area around site 22/4b.

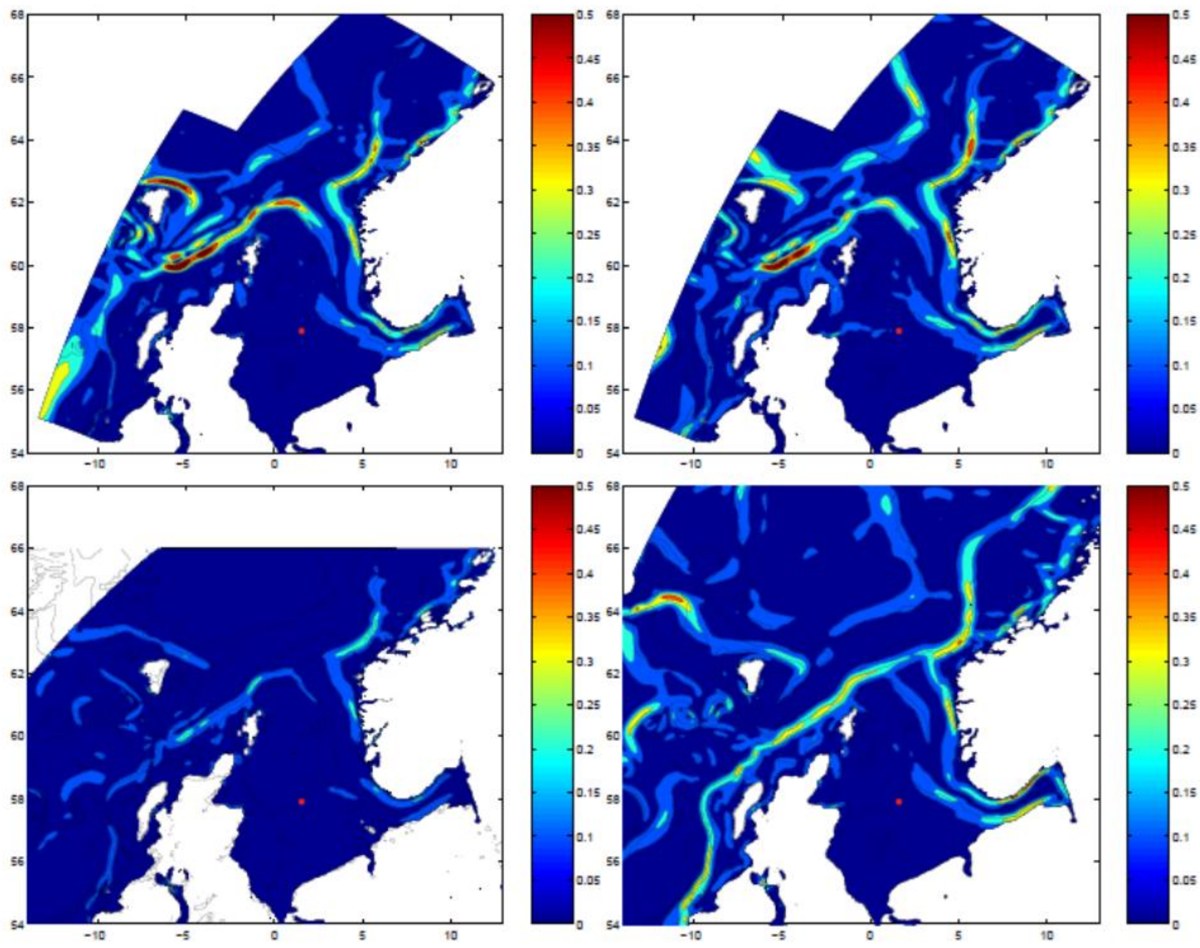

Figure 41: Mean speed contours at 50 m depth from the MIPOM/TOPAZ (upper left), the MIPOM/EKASC (upper right), HYCOM (lower left) and the ROMS (lower right) simulation. The color scale is in m/s. The red dot marks the approximate location of site 22/4b, reprinted from Figure 7 on page 16 of LaCasce et al. (2007).

The highest standard deviations are found near the major currents (Figure 42), which are the dominant sources of variability as instabilities are generated by the horizontal shear. Again the MIPOM/TOPAZ and

MIPOM/EKASC are alike with MIPOM/TOPAZ slightly more active in the southwestern part of the domain. Standard deviations in the HYCOM run are 10 cm/s, which are significantly smaller than in the MIPOM runs, where they can easily exceed 20 cm/s, but values of 40 cm/s are also found in the domain. The distribution of the standard deviation in the ROMS simulation is fairly similar to that of the MIPOM runs, but variability exceeding 20 cm/s extends over a larger region. Similarly, at depth, the HYCOM model seems to give less variability than the other three setups (not shown). Variability close to site 22/4b is only small and thus differences between the models are hard to distinguish from this figure.

In all models the standard deviation is less than the maximum mean velocities. This is not very realistic as eddies spawned from the mean flow should have similar speeds as the current itself. This suggests that a resolution of 4 km is still too dissipative to capture the full variability.

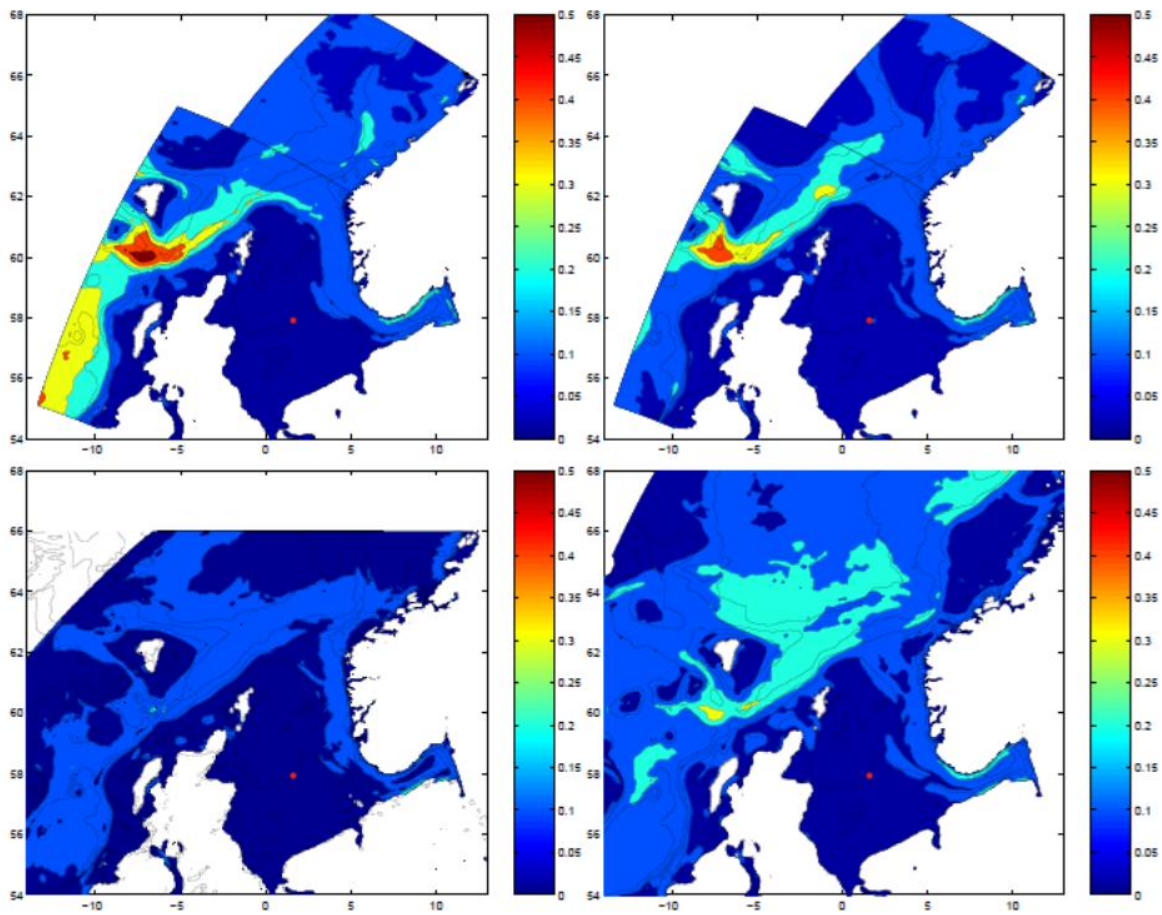

Figure 42: The standard deviation of the speed at 50 m depth from the MIPOM/TOPAZ (upper left), the MIPOM/EKASC (upper right), HYCOM (lower left) and the ROMS (lower right) simulation. The color scale is in m/s. The red dot marks the approximate location of site 22/4b, reprinted from Figure 10 of page 19 of LaCasce et al. (2007).

The model simulations have also been compared to long-term in-situ observations in the northern North Atlantic off the coast of Norway and led to more-or-less the same recommendation that if the older MIPOM model should be replaced with a newer model, it should be replaced with ROMS.

In a more recent study, Albretsen and Røed (2010) compared ROMS with MIPOM in which they investigate whether one truly needs an eddy-resolving model to capture the mesoscale statistics correctly. At front separating two water masses, usually a host of mesoscale structures are observed such as eddies, current jets and filaments. Pathways of particles, such a fish eggs or larvae, but also the water parcels themselves (and for water parcels coming past site 22/4b possible containing high concentrations of methane) are therefore heavily influenced by such features. The scale of these features is in the order of the Rossby radius of deformation, which is 10-15 km in this area. In order to resolve these structures a meshsize of 1.5 km or less is needed. Within in the model domain that was described above, a smaller domain is nested in the Skagerrak area (a depicted in Figure 43) in which the resolution was increased to 1.5 km.

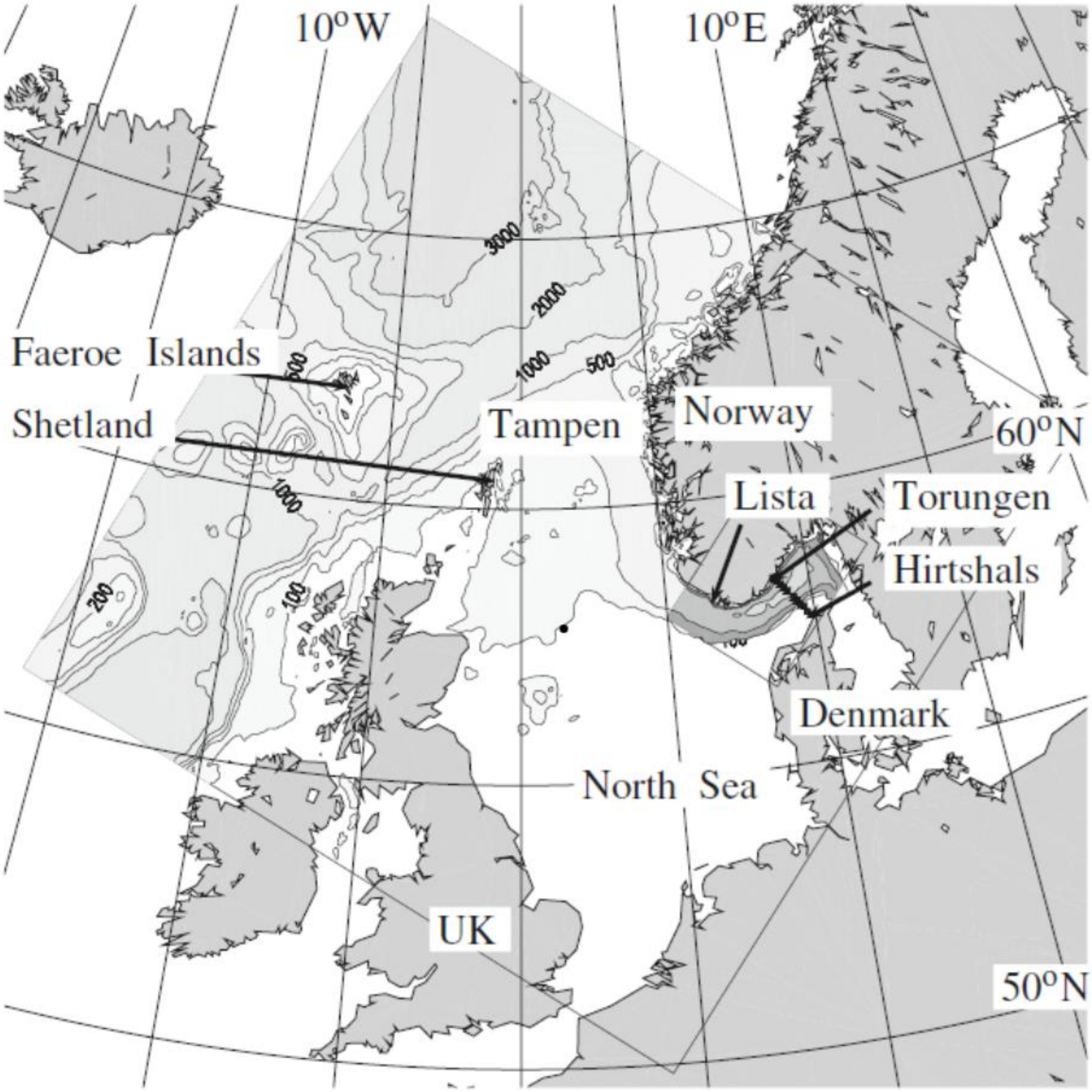

Figure 43: The regional model domains with bathymetry. The large domain shows the area for the 4 km models, and the small domain covering Skagerrak shows the area for the 1.5 km models (darker grey colors). The Skagerrak section from where IMR hydrographic data are provided is indicated with a black thin line. The black dot marks the approximate location of site 22/4b, slightly modified from Figure 1 on page 935 of Albretsen and Røed (2010).

The simulations with the two models are kept as similar as possible. Besides the domain, also the Simple Ocean Data Assimilation (SODA; Carton et al. (2000a) Carton et al. (2000b) is used for the conditions at the open boundaries. Eight dominant tidal constituents are included, 4 semi-diurnal and 4 diurnal ones. The atmospheric input was from the ERA-40 re-analysis (1.125x1.125 degrees resolution) data base developed by the European Centre for Medium-Range Weather Forecasts (ECMWF) with forcing fields every 6 hours and from the operational ECMWF model for the period 2002-2007. Monthly climatological values for the riverine freshwater fluxes are from all the major rivers in the area.

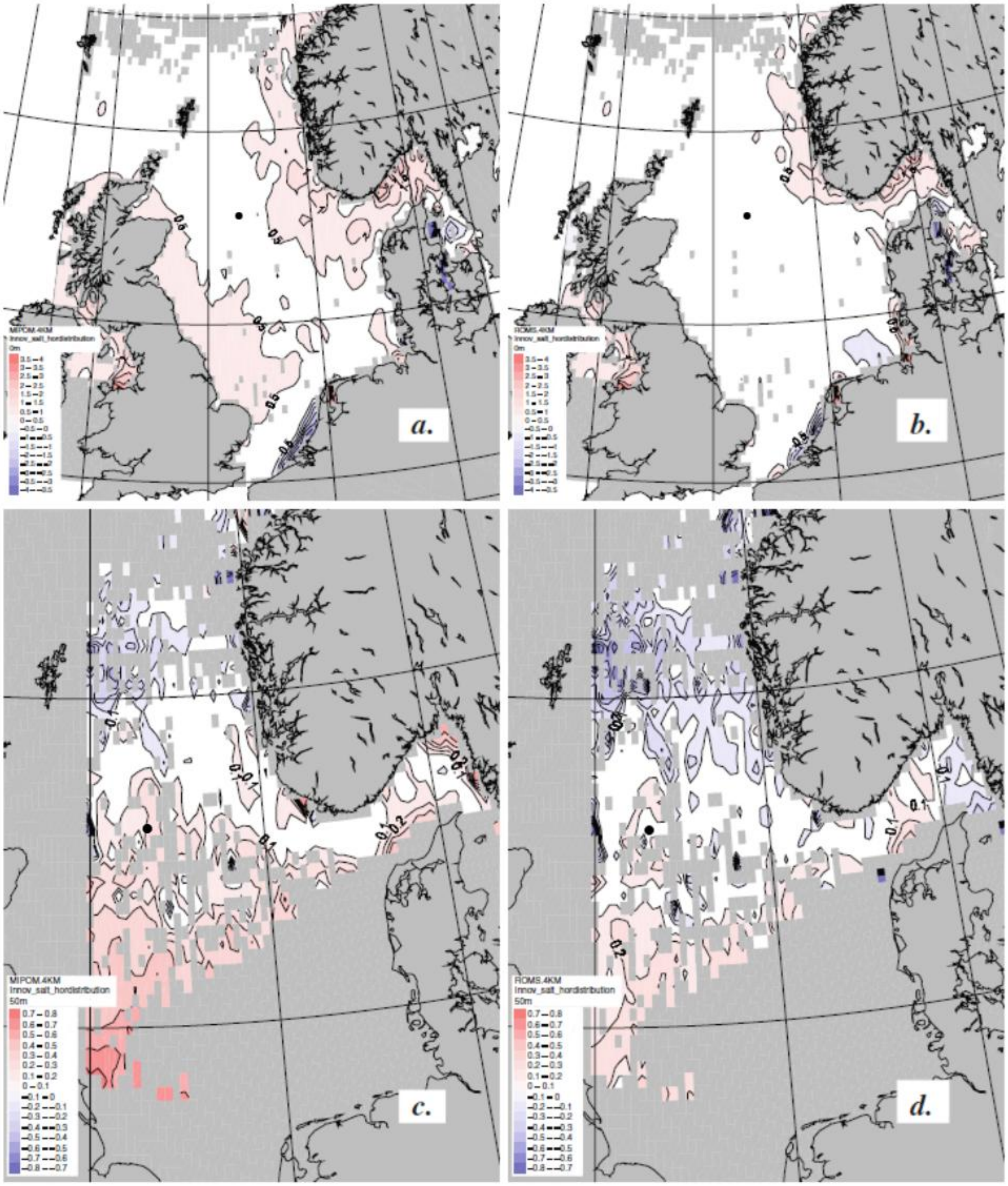

Figure 44: The salinity bias between ICES data and model results (from the 4-km models) for all depths above 20-m depth (upper panels) and below 50-m depth (lower panels) averaged over the years 1981 to 2007. Biases from MIPOM are shown in a and c and form ROMS in b and d. The contour interval is 0.5 psu for the surface salinity and 0.1 psu for the bottom salinity. Red colors indicate that the model has a positive salinity bias, i.e. too saline. The grey areas indicate that fewer than 20 observations where available. The black dot marks the approximate location of site 22/4b, slightly modified from Figure 2 on page 940 of Albretsen and Røed (2010).

The surface salinity averaged over the period 1981-2007 for the MIPOM simulations has a positive bias along the British and Norwegian coast of 0.5 – 1 psu compared with the ICES data (Figure 44a). The salinity bias in the mixed layer for ROMS is less positive (Figure 44b) and is primarily located near the Norwegian coast. As both MIPOM and ROMS display problems in the Norwegian Coastal Current area, this suggests that they are related to the discharge of brackish water from the Baltic or fresh water from the rivers. At depth both models display a positive bias in the central North Sea and a negative bias in the northern North Sea (Figure 44c, d). At site 22/4b, the salinity is generally well reproduced, except in MIPOM near the bottom. There a positive bias is observed with MIPOM overestimating the salinity by 0.2 PSU.

Comparison with hydrographic measurements along the section in the Skagerrak displayed in Figure 43 shows that the salinity in the near surface region close to Norway is too saline, but that the ROMS model performs better near the Danish coast. Since the positive bias in both models is similar, this suggests that it is caused by an erroneous external forcing.

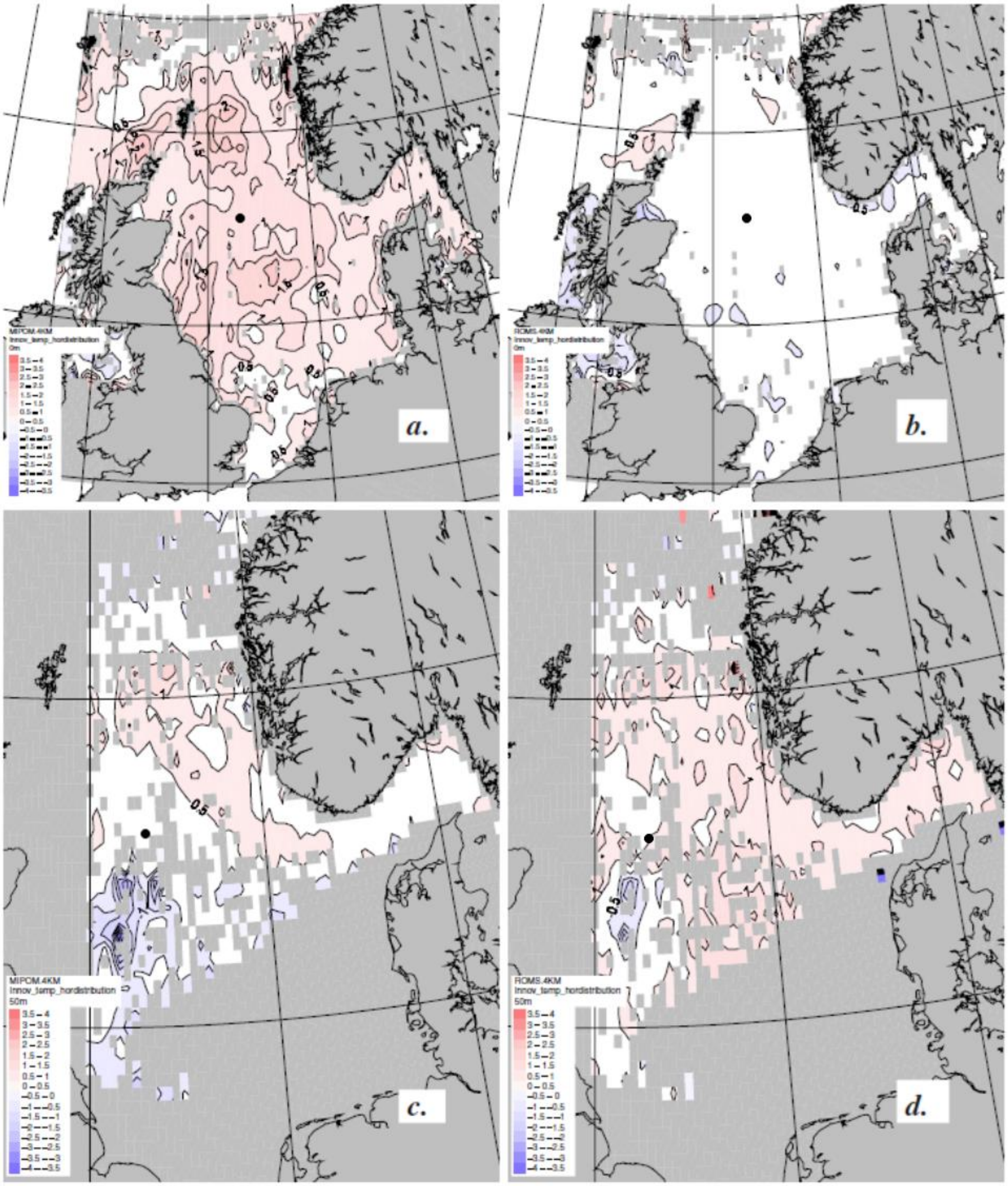

Figure 45: The temperature bias between ICES data and model results (from the 4-km models) for all depths above 20-m depth (upper panels) and below 50-m depth (lower panels) averaged over the years 1981 to 2007. Biases from MIPOM are shown in a and c and form ROMS in b and d. The contour interval is 0.5°C in all panels. Red colors indicate that the model has a positive temperature bias, i.e. too warm. The grey areas indicate that fewer than 20 observations where available. The black dot marks the approximate location of site 22/4b, slightly modified from Figure 6 on page 943 of Albretsen and Røed (2010).

The temperature bias in the model simulation in the mixed layer and below 50-m depth compared with ICES data for the period 1981-2007 is displayed in Figure 45. Obviously, the MIPOM simulation is too warm in the upper 20 m, with values exceeding 1°C at the location of site 22/4b, while ROMS shows no large biases at all in the upper 20 m. However, below 50 m ROMS has a larger warm bias than MIPOM. At site 22/4b the bias is about 0.5°C. The main contribution to the warm bias in MIPOM is the summer heating, as temperatures in winter are well reproduced. For a location 10 km offshore of Norway in the Skagerrak, the ROMS model shows a cold bias in the SST during summer. The average temperature increase between 1981 and 2007 is about 1°C per decade. This is reproduced by both models, with MIPOM having a warm bias of 0.5°C and ROMS a cold bias of 0.3°C.

The 27-year averaged currents at 50 m depth in both models essentially give the same results as in the study by LaCasce et al. (2007), who analyzed simulations for a much shorter period and under different forcing. The average current speed between the Faeroe Islands and Shetland is about 0.7 and 0.5 m/s in MIPOM and ROMS, respectively. Moreover from the Shelf Current a large part peels off and follows the bottom topography into the Norwegian trench in the MIPOM model where most of the Shelf Current in ROMS continues further northeastward in this area. However, the Norwegian Coastal Current has similar strength in both model simulations.

To demonstrate the difference between and eddy-permitting (4 km) and an eddy-resolving (1.5 km) resolution, the mean kinetic energy (MKE) and eddy kinetic energy (EKE) is calculated. The higher frequencies are filtered out by taken 24-hour averaged currents. The MKE is determined for 30-day averaged currents and the EKE is based on the current deviations from these 30-day mean currents. The results are depicted in Figure 46 and Figure 47. The mean currents at 50 m depth are stronger in ROMS, which as a result is more energetic than MIPOM in both the inflow from water from the central North Sea near Denmark as within the Norwegian Coastal Current. Increasing the resolution from 4 to 1.5 km leads to increasing energy levels in both models, however, the patterns of the MKE is similar in all four model results. The variability in the 27-year simulation is well described by the EKE. As with MKE, EKE levels in ROMS are higher than in MIPOM, which is mostly related to the higher order advection scheme used in ROMS, which essentially increases the theoretical resolution. In addition, extra numerical dissipation in MIPOM to suppress numerical instabilities may dissipate horizontal gradients and reduce EKE variability. As with MKE, the EKE increases with increasing model resolution. However, EKE patterns change significantly from lower to higher resolution. In the low resolution simulation the band of high EKE is confined to a small band close to the Norwegian coast, whereas in the high resolution cases the band of EKE is much broader and extends much further out into the Norwegian trench.

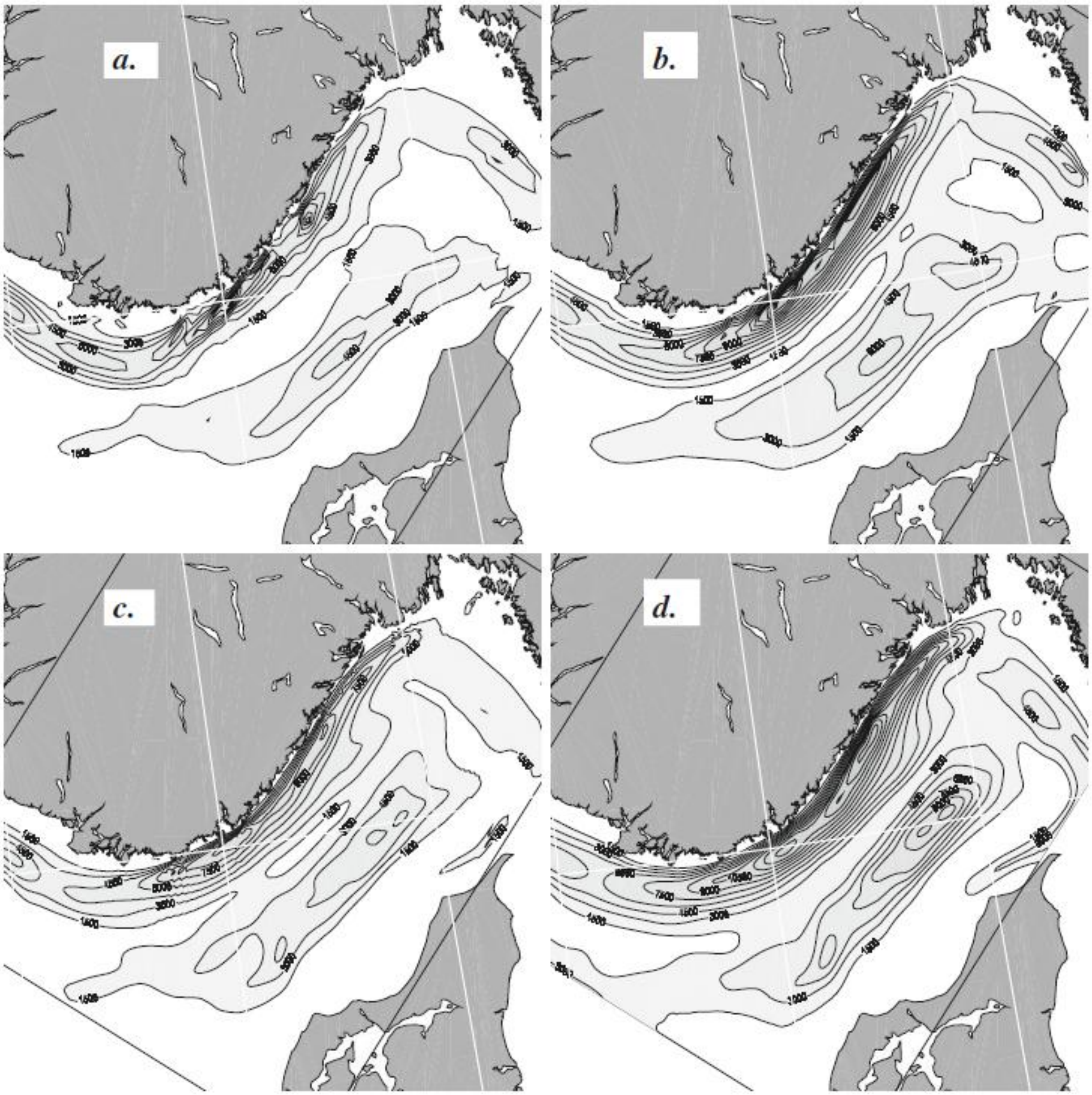

Figure 46: Depth averaged mean kinetic energy calculated from four experiments with the focus on the Skagerrak. The values are averaged from 1981 to 2007 and the contour interval is 1500 J/m^2. The panels show the mean kinetic energy level from a) MIPOM 4 km, b) ROMS 4 km, c) MIPOM 1.5 km and d) ROMS 1.5 km, reprinted from Figure 13 on page 950 of Albretsen and Røed (2010).

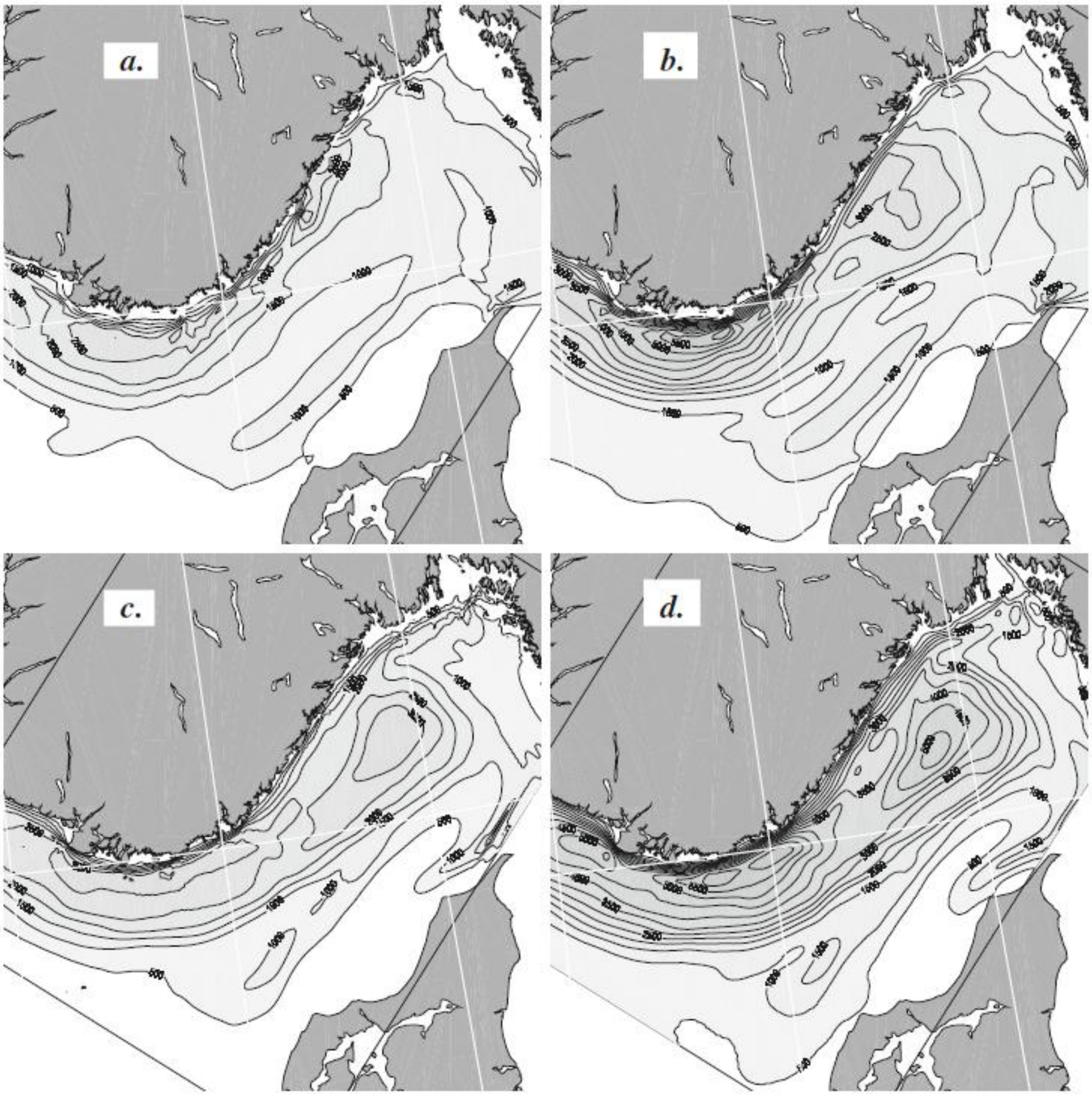

Figure 47: Depth averaged eddy kinetic energy calculated from four experiments with the focus on the Skagerrak. The values are averaged from 1981 to 2007 and the contour interval is 1500 J/m^2. The panels show the mean kinetic energy level from a) MIPOM 4 km, b) ROMS 4 km, c) MIPOM 1.5 km and d) ROMS 1.5 km, reprinted from Figure 14 on page 951 of Albretsen and Røed (2010).

Albretsen and Røed (2010) conclude that it is vital to correctly simulate the actual mesoscale pattern in order to be able to track particles using the hydrodynamics of that particular numerical model. Based on several long, validated model runs, in particular LaCasce et al. (2007), the met.no now uses ROMS as the operational forecast model (l. P. Røed, personal communication). ROMS was shown to be more energetic than MIPOM and below the mixed layer ROMS was even found to be too energetic in the intermediate layers. The MKE patterns in the model runs were comparable for both the 4 and the 1.5 km resolution simulations of the models. However, the maximum in EKE in the deepest and inner part of the

Norwegian Trench in the 1.5-km models is not seen in the 4-km models. This may indicate that it is necessary to have an eddy-resolving resolution model to capture the mesoscale eddy activity properties. This may be essential to simulate pathways of particles released in the eastern (or central) part of the North Sea. Moreover, hydrographic measurements in the Norwegian Coastal Current are used to estimate the baroclinic current component of the geostrophic current. A realistic flow is only reproduced with 1.5 km resolution. The main conclusion is that ROMS behaves more satisfactory than MIPOM in most regions and at most depths.

Summary Hydrodynamic models

This section on 3D hydrodynamic models has shown that there are many different models that have been run in the North Sea setting. All 16 models described perform well with respect to the hydrodynamics in the North Sea. Although all models use the same set of basic transport equations, distinct differences are present due to numerical discretization in the vertical (z-coordinates, σ-coordinate, hybrid coordinates or adaptive coordinates), but also in the discretization of the non-linear advection terms. Besides this, the turbulence closure that is chosen to represent turbulent processes in the vertical can have many different forms and shapes, from very simple zero-th order closures, in which the turbulent processes are related in a simple way to the large scale flow, all the way to second order moments in which a large number of turbulence equations are solved to estimate the turbulent fluxes.

The comparison studies have first of all revealed that it is very hard to make a sound comparison between different models. In the first NOMADS study (Proctor et al. (1997) Tartinville et al. (1998) an attempt was made to compare the spatial and temporal coherence of realistic simulations of the North Sea hydrodynamics. The main results of the study were that all models could generally reproduce acceptable features of the circulation in the North Sea, but that significant differences between the models were found. However, it was found impossible to quantify these differences with a relatively small set of parameters or forcing function. The variability between the models was as large as the variability within the models and the major difference between the models were caused by the different forcing data applied in each model. Thus, in a second study, NOMADS2 (Proctor (2000) Delhez et al. (2004) inputs were chosen to be identical and model results were compared with in-situ observations. A statistical tool was developed to measure the variability, sensitivity studies were performed and the modeled variability was assessed against natural variability. In this study, suitable in-situ measurements proved to be the most crucial problem. The main conclusion from the NOMADS2 study was that the models behave similarly, that the higher resolution models perform a bit better, but that the differences between for instance the model transport through a section is as large as the volume flux itself and the that the error in the temperature and salinity cost function is nearly 100%. As the temperature and salinity distribution are qualitatively good representations of the mean current structure, this indicates the large inherent variability of the models. Moreover, based on the study no single parameter, such as resolution, turbulence closure scheme or model domain, could explain the differences.

In three later studies, newer models, OPYC, ISPRAMIX and GETM, were bench-marked against the HAMSOM (ZM) model, which was claimed to belong to the best models amongst the ones compared in the NOMADS1 and 2 studies. OPYC was immediately disqualified from this review, as it was run in 2D mode, which is unsuitable for reproducing the seasonal stratification in the northern North Sea.

In Ouberdous et al. (2002), ISPRAMIX was shown to display a more pronounced stratification during summer and even though temperature and salinity in the surface layer was comparable, large differences were found beneath the thermocline and attributed to the different turbulence modules used in both models, being a second order algebraic closure in HAMSOM and the more advanced second order k-L scheme in ISPRAMIX. The simulations of the models agree reasonably well, suggesting that the improved turbulence closure scheme has not significant contribution to the eventual simulation with ISPRAMIX.

A comparison between HAMSOM and GETM, which essentially differ in the turbulence closure: algebraic vs. 2nd order closure and the vertical discretization: z- vs. hybrid coordinates, is thoroughly described by Stips et al. (2004). Simulations show that GETM belongs to the models in the NOMADS consortium with the strongest summer stratification, which is due to the higher order turbulence scheme used in GETM. With respect to the mean kinetic energy (MKE) GETM belongs to the middle range of the models in NOMADS, similar as HAMSOM. A simulation with GETM, in which a higher order advection scheme is chosen, shows a more pronounced, more realistic, summer stratification, but still the lower layer heats up to quickly, leading to too large temperatures in the lower layer during the stratified period. Small scale variation observed in SST satellite imagery could not be reproduced, but in a simulation with a higher order advection scheme the small-scale frontal behavior is much better reproduced than with the low-order advection scheme implemented in HAMSOM. The main conclusion is that GETM is able to reproduce the temperature and salinity observations of the North Sea at least as well, if not better than HAMSOM, especially if advanced features, such as the higher order advection scheme, are used.

A comparison between NEMO or FOAM and POLCOMS (PO) in O'dea et al. (2012) shows significant improvement in the skill of SSH predictability. POLCOMS displays a warm bias in summer, whereas FOAM experiences such a bias in winter. POLCOMS appears to be over stratifying in summer. The bias in FOAM is due to a combination of the turbulence scheme (second-moment algebraic), the simple light attenuation scheme and the prescribed fluxes. If SST assimilated in a run with FOAM, the results with respect to SST improve significantly and the location of the seasonal tidal mixing fronts in the southern part of the North Sea is better reproduced. However, the deep waters in the Norwegian Trench become too low. A comparison between the FOAM-AMM free and assimilative runs shows an improvement of the assimilated temperatures and no significant change in the salinity profiles. All in all, FOAM appears to perform better than POLCOMS.

In the CONMAN comparison between ROMS and HYCOM on the one hand and MIPOM on the other, LaCasce et al. (2007) evaluated which of the former models could replace the MIPOM models as operational forecast model in the Norwegian Waters at the met.no. Since very recent, ROMS is used as operational model, which already implies that it is the best available model of the three involved in the study. ROMS displays a more realistic current structure at the entrance in the northern North Sea than MIPOM, probably due to the use of a third order advection scheme, a higher vertical resolution and an advanced turbulence closure model. Climatological mean speeds show that HYCOM has extremely weak currents compared with MIPOM and ROMS and consequently also weaker variability. In a more recent study by Albretsen and Røed (2010), ROMS and MIPOM are compared and it is investigated whether one needs an eddy-resolving model to capture the mesoscale statics correctly, which is essential for reproducing the correct frontal structure and associated eddies, current jets and filaments, which are necessary for reproducing correct pathways of particles or water masses. For the eddy-resolving models the energy levels are higher, although the structure for the MKE remains the same. The EKE patterns, however, changes significantly depending on resolution. Thus, Albretsen and Røed (2010) conclude that is vital to run on eddy resolving resolution to be able to track particles correctly.

In general, hybrid coordinate models, with higher order advection schemes, and higher order turbulence closures perform the best. There is also a strong impact by the horizontal and vertical resolution. But particularly, a higher order advection scheme and an improved turbulence scheme have the most influence of the setup and destruction of the seasonal stratification. Improved turbulence models affect the thermocline during the summer stratification. Moreover, higher order advection schemes cause a sharper thermocline, which brings the simulation closer to reality. Moreover, assimilating the SST to satellite observations hardly affects the stratification, but improves the location of the seasonal fronts.

From the above intercomparison studies it can be concluded that HAMSOM and POLCOMS belong to the best models in the NOMADS 1 and 2 studies. In later studies, ISPRAMIX was shown to be as good as HAMSOM, or in other words, did not show significant improvement; that GETM with advanced features in operation performs significantly better than HAMSOM and that FOAM is superior to POLCOMS. Moreover, ROMS appears to be much better in the Norwegian Waters compared to both MIPOM and HYCOM. Based on this literature review, this lists the top three models to be GETM, FOAM and ROMS (not necessarily in that order). However, it should be noted that the other models, such as for instance DELFT3D, undergo and have undergone significant alterations and improvements, which should have enhanced the accuracy of the model simulations significantly. In other words, the results obtained in the relatively old NOMADS1 and NOMADS2 studies would be completely different, if a similar intercomparison would have been performed with the state-of-the-art versions of the models mentioned in these studies.

With increasing computer power, modelers can run on increasingly higher resolution and that is exactly what is being done at different institutes. For instance at CEFAS, modelers are working on a nested setup for the entire northwestern European shelf (17.5W – 13E and 46.6 – 63N) at 6-7 km resolution with GETM, for which the boundary conditions originate from a global model (J. van der Molen, personal communication). Moreover, at IOW (Leibnitz Institute for Baltic Sea Research Warnemünde), Ulf Gräwe has a setup of the North Sea running with adaptive coordinates for the period from 2003 to 2012. Figure 48 shows the temperature distribution along of a high resolution scanfish transect along 58˚N in the top panel and the modeled temperature distribution by the GETM setup with adaptive coordinates (Gräwe et al. (2013). Clearly, the sharp thermocline is well reproduced by the simulation with temperatures of about 15˚C above the thermocline and 8˚C below it. The reason why the thermocline is that sharp in the simulation is because the layer thickness near strong vertical gradients in the stratification decreases adaptively. In the region of about 10 meters above and below the thermocline the layer thickness decreases to less than 2-3 m, whereas well above and well below the thermocline and outside of the bottom and surface boundaries, the layer thickness is 6-7 meters. In this way, small scale turbulent processes that generate the sharp thermocline in reality are well resolved by the model.

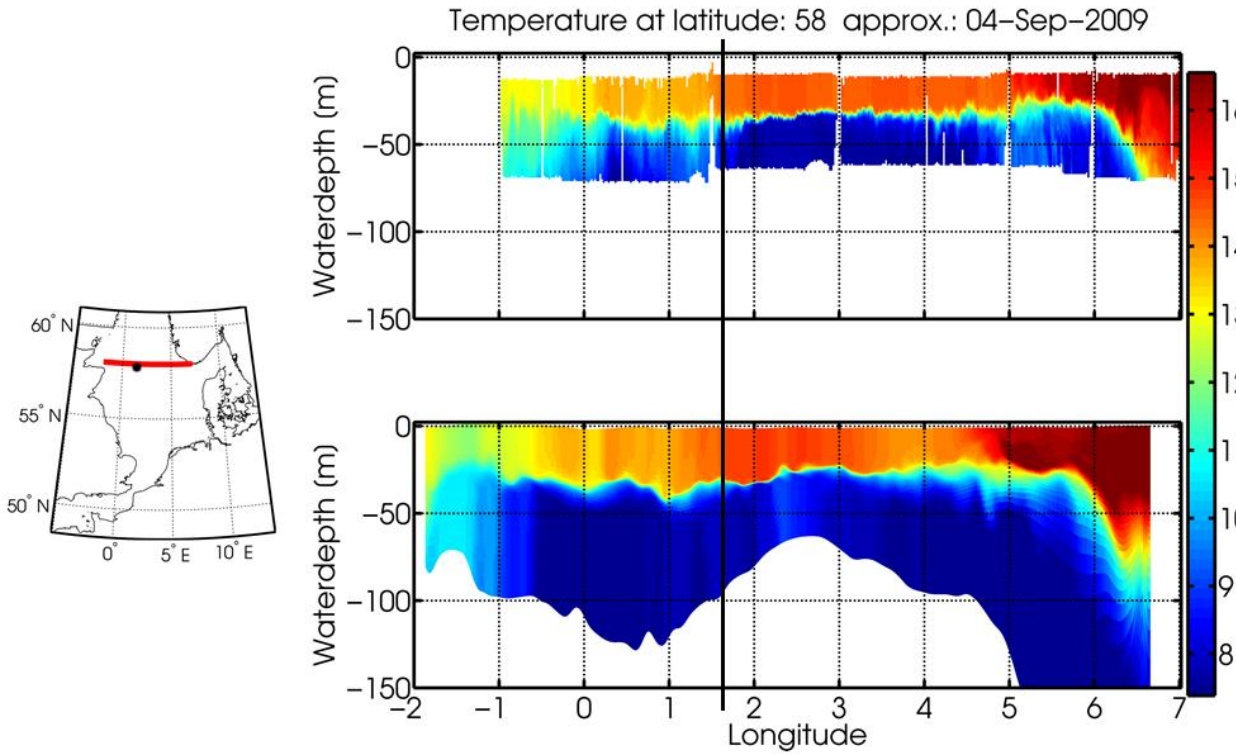

Figure 48: Temperature along a section across 58˚N of high spatial resolution in-situ measurements on 04-Sep-2009 using a scanfish (top panel) and of the GETM model simulation (bottom panel). The black line represents 1˚38'E, which is the longitude at which site 22/4b is located. Inset on the left-hand side shows the location of the transect (red) and the approximate location of site 22/4b (black dot), slightly modified from a figure to be published in Gräwe et al. (2013).

At met.no, ROMS is implemented at met.no as the Numerical Ocean Weather Prediction kernel model, since December 1, 2012 (L.P. Røed, personal communication). The model is a triple nested system (Figure 49), the largest domain, Arctic20km consist of the entire Arctic and the northern part of the North Atlantic Ocean (20 km); Nordic4 km is nested in this model and covers the northwestern part of the North Atlantic and the Atlantic sector of the Arctic at 4 km resolution and finally NoKyst800m is nested in this model and covers the entire Norwegian coast with site 22/4b located in the southwestern corner (eddy-resolving: 800 m). The outer model is forced from output from the UK met Office global FOAM model.

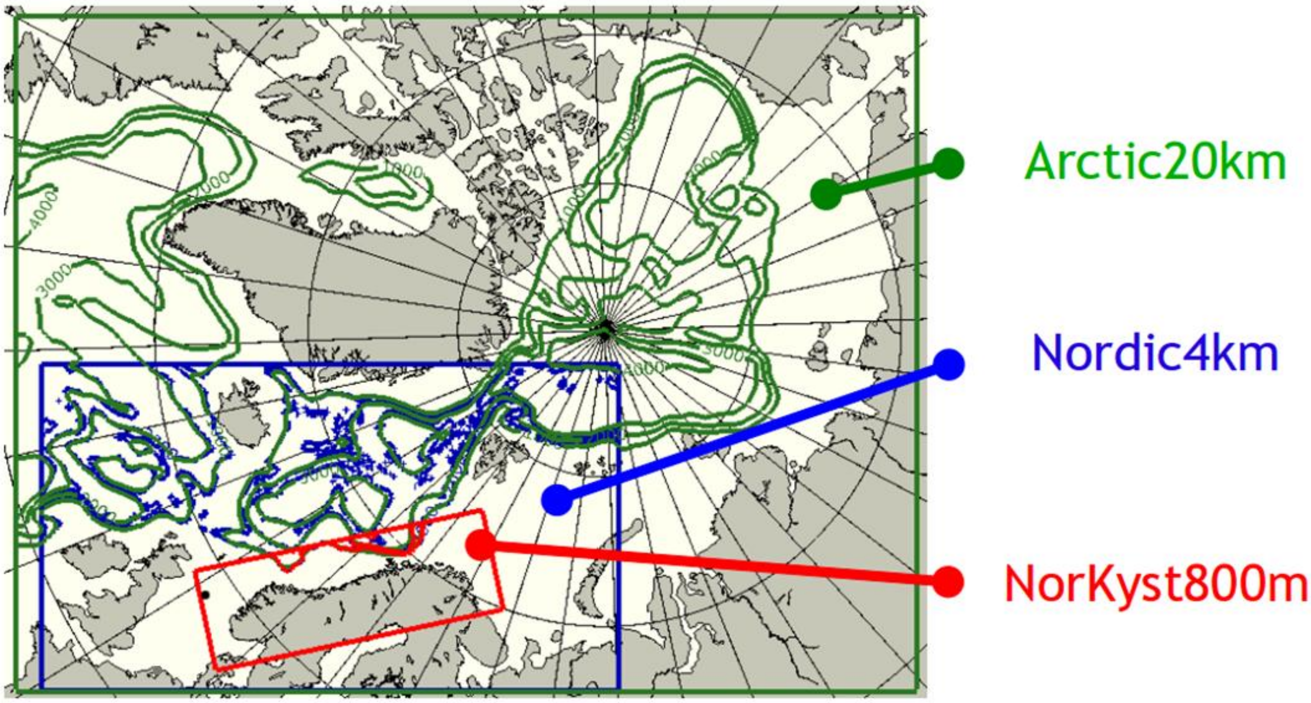

Figure 49: Nested setup of the ROMS system, currently in use as the Ocean Numerical Weather Prediction Kernel Model at the Norwegian Meteorological Institute, met.no. The large domain (green), displays the outer model of the encompassing the northern North Atlantic and the Arctic Ocean at 20 km resolution. The intermediate domain encompassing the North Sea and Norwegian Sea at 4 km resolution (blue) is forced at the boundary from the larger model. The smallest domain at 800 m resolution of the waters surrounding the coasts of Norway just incorporates site 22/4b, indicated by the black dot. This figure was obtained from Dr. L.P. Røed (met. no) through personal communication.

Fate of methane in the water column

Observations of methane bubbles released from the sea floor in various settings suggest that the release of methane in shallow water environments can occur in pulses coinciding with the changes in water pressure due to the tidal cycle and changes in current directions (Linke et al. (2010) Naudts et al. (2010) Boles et al. (2001) Torres et al. (2002) Newman et al. (2008) Greinert et al. (2006). However, also short term variations do occur which could be related to variations in internal pressure built up within local small gas pockets in the sea floor (for instance Naudts et al. (2010). Methane however not necessarily reaches the seawater as bubbles. It can also (partly) dissolve in the pore water before it reaches the sea floor.

Like any other dissolved compound, due to molecular diffusion dissolved methane migrates from high to low concentrations in the sea floor sediments and can finally reach the water column. During the diffusion through the sediments and in the water column a part of the venting methane is degraded by microbial communities. Transport along fault structures (advection) in the sea floor can result in a faster and larger volume transport of methane to the bottom water. If the methane is (partly) released as bubbles at the sea floor, the floating methane bubbles can cause the ambient water to flow upward as well (bubble-induced up-welling). This can result in an increased transport rate of methane to the upper water part of the water column and possibly into the atmosphere.

Studies in the Tommeliten field in the North Sea have shown that a large part of the methane is consumed by bacteria while it is still migrating through the sediments (Niemann et al. (2005). Only locally some of the free gas reaches the water column. Seepage of methane has also been observed or inferred from observations at other North Sea sites (for instance Håvelsrud et al. (2012) de Haas and Shipboard Scientific Crew (2011) Schroot et al. (2005). Many of these studies however do not attempt to model or quantify the flux of methane to the water column or even further into the atmosphere.

Schneider von Deimling et al. (2011), however, do attempt to quantify the flux. They conclude, after numerical modeling based on hydroacoustic, video, CTD and ROV sampling data and a gas bubble dissolution model (McGinnis et al. (2006) that of the 26 tons of methane released per year in the Tommeliten area about 4% reaches the atmosphere as methane bubbles. However, the strong seasonality of the mixing in the North Sea influences the seasonal flux. The flux is expected to increase if the mixing increases. Almost all of the methane released at the sea floor could be transferred in to the atmosphere during the stormy fall and winter seasons, while during summer dissolved methane can be trapped below the thermocline, as was also observed by de Haas et al. (2012). Schneider von Deimling et al. (2011) conclude that the total methane flux from the seabed to the atmosphere is higher than their published number, since research cruises are mostly carried out during the fair weather summer period, during which the water column is stratified and methane is trapped below the thermocline. Not enough data is available from the unstratified winter period. Methane that is trapped under the summer thermocline may be transferred horizontally over long distances to shallower areas and exchanged with the atmosphere elsewhere. Exact numbers on this process however are lacking (Schneider von Deimling et al. (2011).

Other estimates of the methane flux in this area have also been published (Hovland and Sommerville (1985) Judd and Hovland (2007), but it is not fully clear how these estimates were made. Various authors: Hovland et al. (1993), Judd (2004), Niemann et al. (2005), Wegener et al. (2008), Schneider von Deimling et al. (2010) have found gas seepage on (partly) different locations within the Tommeliten area and reported fluxes. Areas that were revisited did not show seepage during all visits, making modeling difficult. The lack of data to come to reliable transport models and flux estimates is also confirmed by Etiope (2009), not only for the Tommeliten area, but for the entire North Sea (and other regions) as well.

Tracer models and Particle tracking models

In order to determine the fate of dissolved methane in the water column a model for methane bubble dissolution, such as the one of McGinnis et al. (2006) should be coupled to a tracer dispersion or particle tracking model. As a first attempt a simple advection-diffusion model can be used in which the oxidation of methane is modeled as a sink term with a constant rate of decay determined by the methane concentration itself as in Rehder et al. (1999). This will give a first indication of the pathways that volumes of water containing a certain amount of dissolved methane will follow. In nano-molar methane concentration environments, methane may have a turnover time of one year in deep waters to several decades in the upper water column (Valentine et al. (2001). Even though methane in deeper water is subjected to microbial methane oxidation, it may travel laterally over long distances.

In general, it should be possible to use any particle tracking model with each of the hydrodynamic models that have been described in section 2.

Rehder et al. (1998) tries to explain their measurements of the near surface methane concentration along a path from the northern tip of Denmark to Scotland along 58^{o}N (passing site 22/4b) and from there to the Elbe estuary. For this purpose they used the HAMSOM model, containing 19 layers in the vertical and having a horizontal resolution of 12’ of latitude by 20’ of longitude. The model is driven by tidal data from a model covering the entire Northwest European Shelf, by weekly SST data, by climatological monthly means of fresh water discharge and by a 3-hourly wind stress distribution. Details of the model are given in Pohlmann (1996a). In this study, the water mass transport is simulated as well as the propagation of tracers and the evolution of the thermocline. The authors try to estimate the flux of methane through the section and use the water fluxes at the station positions for May 16th, 1994. They are unable to get the budget closed for the closed perimeter enclosed by the 2 sections and the northwest European mainland. The methane flux into the bounded area is estimate to be 25 mol/s, whereas the methane flux out of the bounded area is 14 mol/s. They ascribe this difference to the imbalance in the water transport in the first place.

Beside this a tracer experiment was performed, in which a tracer was continuously added to the water column at the location of the gas seep at site 22/4b and advected/diffused within the HAMSOM model in a simulations that lasted from April 1st to May 16th (time of the survey). The distribution of the tracer on May 16th is given in Figure 50, which shows a rapid surface propagation towards the north and the east.

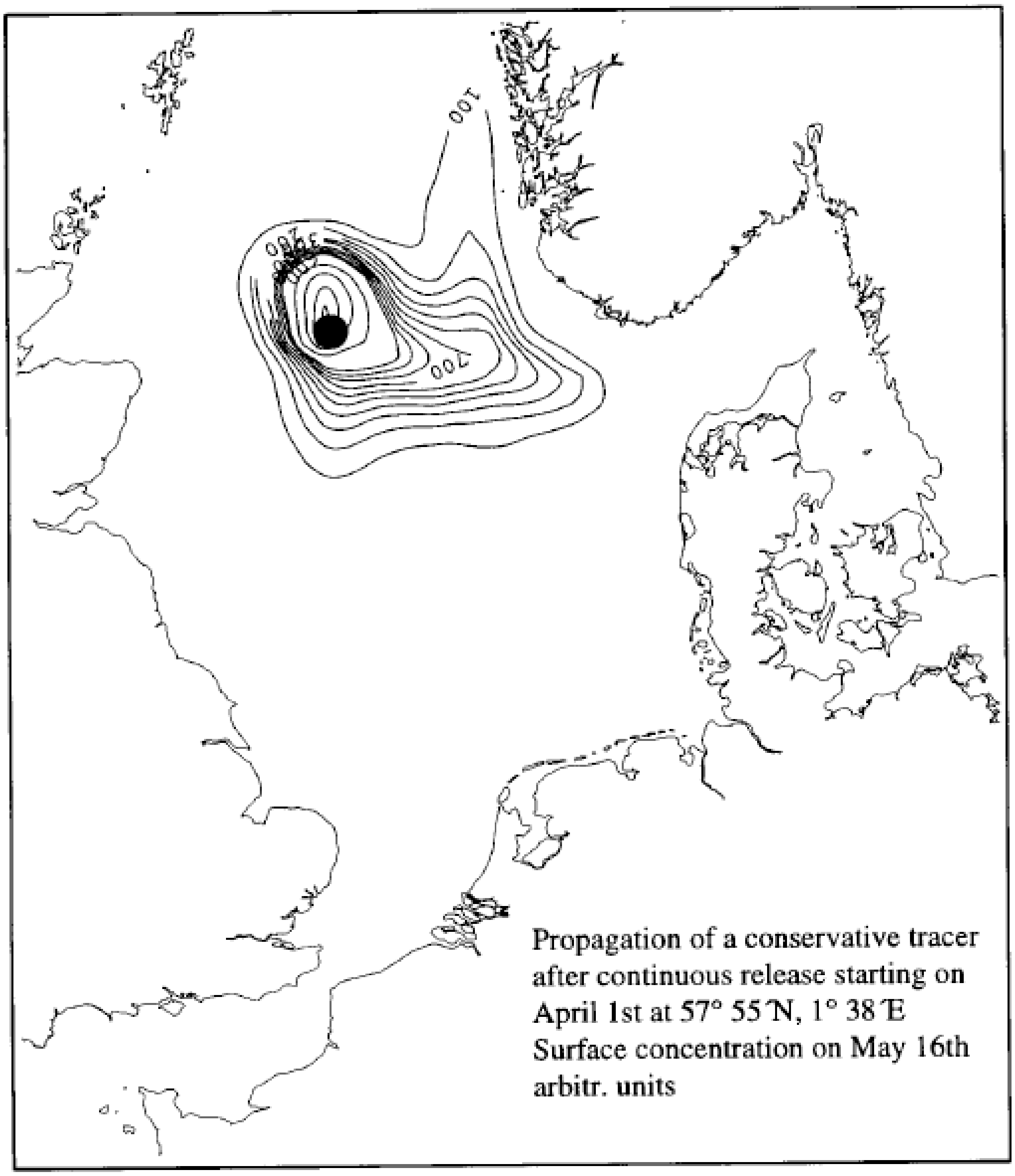

Figure 50: Surface distribution of a conservative tracer that was continuously added to the water column from April 1st, 1994; result from a simulation with the HAMSOM model. The traces is released at the black dot, which is the approximate location of site 22/4b, reprinted from Figure 10 on page 420 of Rehder et al. (1998).

Another attempt to run a particle tracking model with HAMSOM was done by Heath and Gallego (1997), Heath and Gallego (1998), Heath et al. (1999) and Gallego et al. (1999) to determine the distribution of fish larvae from the spawning area. They used the quasi-stationary solution of a nested pair of HAMSOM models with the North Sea fine (10' latitude and 20' longitude, approx. 18 km and 8 layers in the vertical) grid model nested in a coarse (20' latitude and 40' longitude) grid model of the North Atlantic. The model was run to a quasi-stationary state with climatological meteorological forcing, from initial conditions of temperature and salinity representing the spring situation of the model area. Initial conditions were from climatology. The quasi-stationary solution represents the climatological residual current generated by the climatological mean wind stress forcing and baroclinic effects, but excluding tidal residuals. The tides were incorporated artificially and parameterized as a horizontal diffusion in the particle tracking model. Particles were released from a 20' latitude x 40' longitude matrix of 240 locations covering the shelf area shallower than 200 m from 56 to 62" N and 10" W to 4" E, and tracked for 90 days (Figure 51). No diffusion was added to the model; hence tidal motion (stirring) is not incorporated in these modeled tracks. This leads to unrealistically smooth tracks as the tracks appear almost fully deterministic. And thus all tracks particles that are released at site 22/4b will travel to the Norwegian trench and exit the domain to the north along the Norwegian coast.

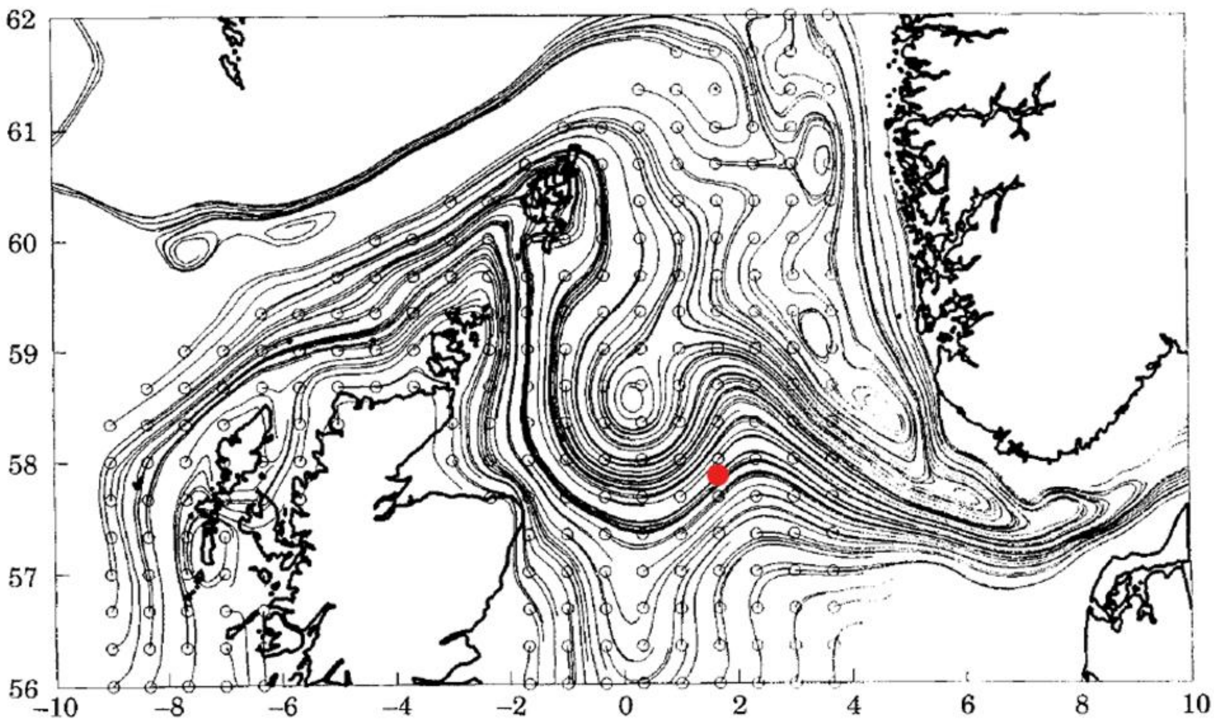

Figure 51: Deterministic trajectories of particles from each of the 240 release sites (bullets) in a 30-km matrix over the North Sea and west of Scotland shelf to a maximum depth of 200 m with no horizontal diffusion. Each trajectory s shown for maximum of 90 days or until the particle left the model domain. The red dot marks the approximate location of site 22/4b, slightly modified from Figure 4 on page 14 of Heath and Gallego (1997).

Including horizontal diffusion to parameterize the tidal motion (stirring) did not significantly alter the trajectories of the particles Figure 52. Some spread in the trajectories can be observed, but in general tracks passing site 22/4b end up in the Norwegian trench (see Figure 52a). This is because the underlying simulation is quasi-stationary (due to constant forcing) and has no tidal motion in there. This particularly unrealistic hydrodynamic simulation of the North Sea circulation leads to similarly unrealistic pathways of released particles.

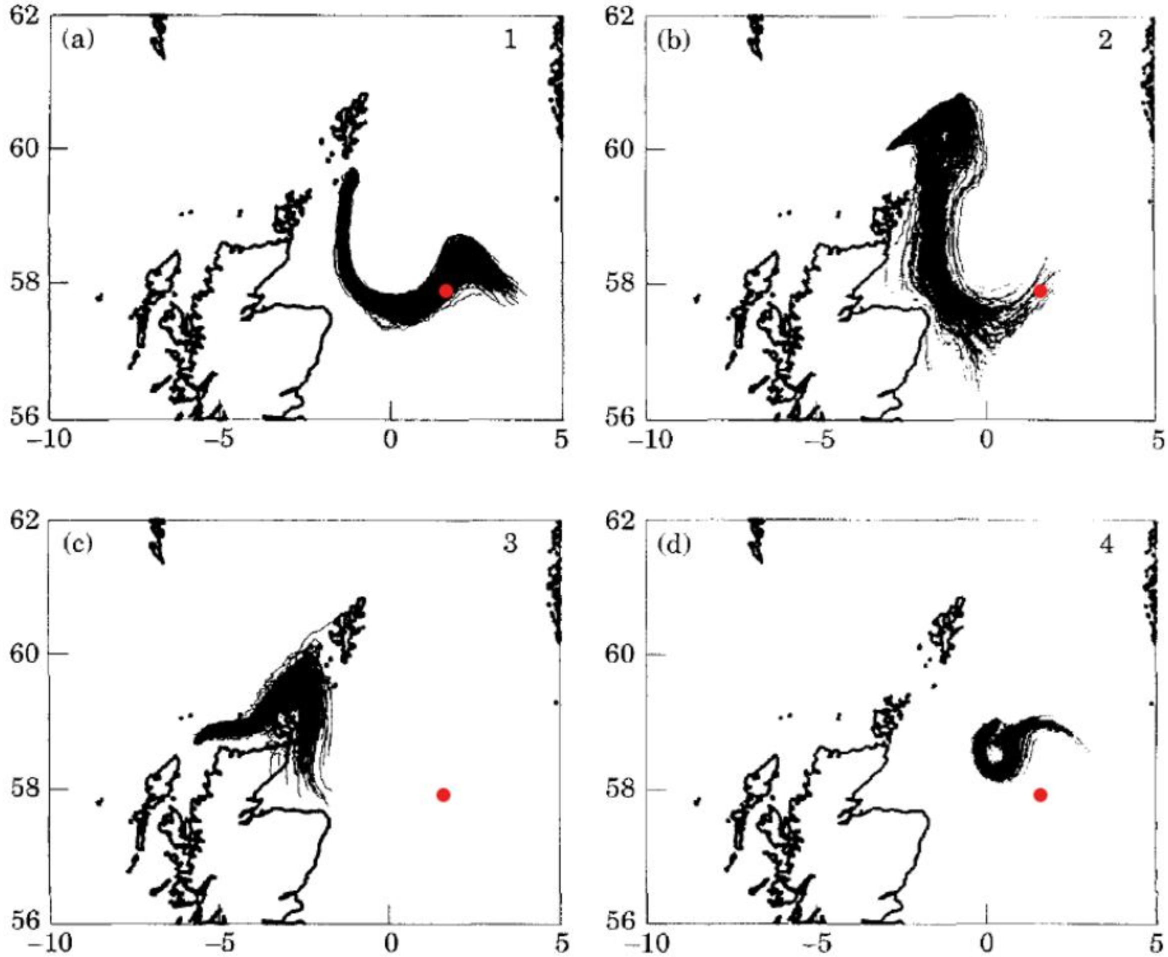

Figure 52: Ninety-day-long trajectories of 240 particles released from each of four release sites with horizontal diffusion activated. The red dot marks the approximate location of site 22/4b, slightly modified from Figure 9 on page 20 of Heath and Gallego (1997).

In Gräwe and Wolff (2010), a particle tracking model was coupled to GETM. In this particle tracking model, the particles modeled are suspended particulate matter particles, which are essential particles having a certain properties, which in the case of SPM particles is a size-dependent sinking velocity and an erosion rate based on the bottom shear stress. A similar approach can also be applied to pollutants, biology and methane concentration by changing the properties. An advection-diffusion equation for a concentration field of a passive tracer is coupled to a 3D velocity field. The model is then solved in a Lagrangian sense, i.e. the particles are followed along their path. It was shown that the model performs well with respect to SPM concentration in the Southern part of the North Sea (see Figure 53 for the nested model domain). Figure 54 shows a good correspondence between the measured and simulated SPM concentration at the time series station, even better than the Eulerian SPM module that is part of GETM.

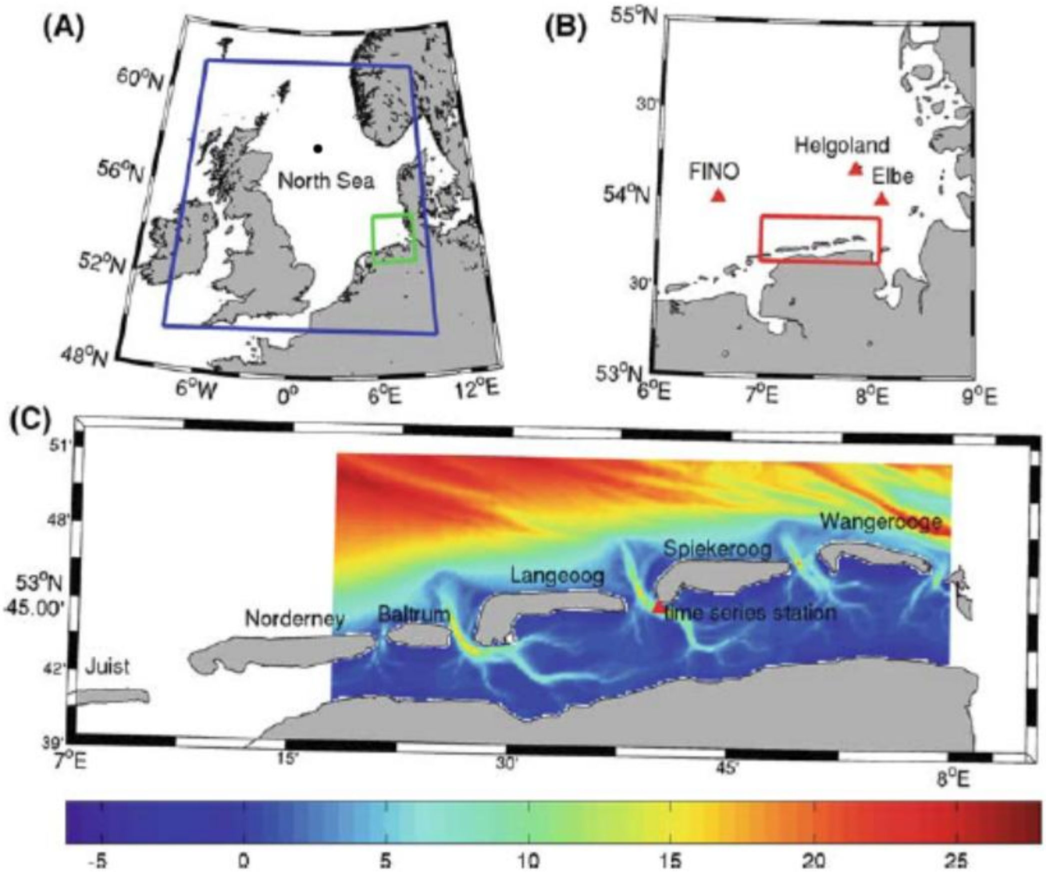

Figure 53: Location of the study site and model area. The black dot in panel a marks the approximate location of site 22/4b. The model topography (positive downward, unit is meter) of the Wadden Sea Model is shown in c. The red triangle in that panel marks the position of the time series station, form where the measured SPM concentrations in the Wadden Sea area are obtained. The blue box in a denotes the extension of the model domain used for wave modeling in the North Sea area, while the green box marks the extension of the model domain used for wave modeling in the German Bight. The red triangles in b denote the positions of the wave buoys used for validation of the model data, reprinted from Figure 5 on page 31 of Gräwe and Wolff (2010).

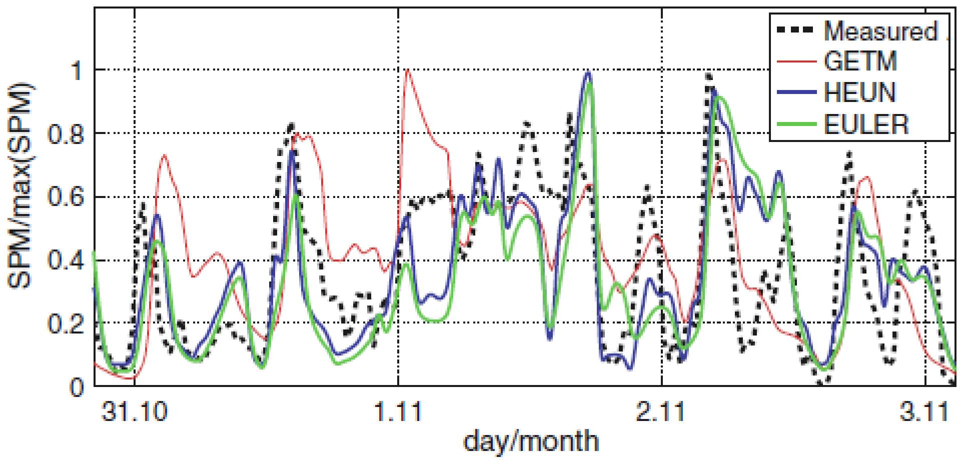

Figure 54: Modeled and measured concentrations of suspended matter at the pile station during storm Britta in November 2006. The data were normalized to indicate the temporal dynamics. Measure data using a multispectral transmissiometer are also depicted. Shown are the results of the HEUN and EULER method. Additionally a time series simulation by the Eulerian SPM module of GETM is shown, reprinted from Figure 7 on page 35 of Gräwe and Wolff (2010).

Besides the built-in particle tracking model in GETM, also an off-line version can be used to determine the pathways of the particles. In Wolk (2003), the development of a Three-dimensional Lagrangian tracer model has been described. The transport of tracers such as temperature, salinity or chemical substances has already been included in GETM using a conservation equation, which include advection, turbulent eddy diffusion (horizontal and vertical). Vertical migration of tracer concentrations, such as settling of SPM or active migration of micro-organisms can be modeled by an additional vertical velocity. Particle tracking models work in a Lagrangian sense and follow the paths of the particles. The most important benefit of a tracer model is that sources of tracers, such as the methane source at site 22/4b, are easily represented, whereas concentration models have difficulty resolving concentration fields whose spatial extent is small compared to the grid size. Moreover, sharp gradients associated with localized high tracer concentration release are difficult to represent in a Eularian framework. The model is setup in an off-line way, such that it uses the 3D velocity fields from the output-files of GETM as input. The model domain is the same as in Figure 53. The initial distribution of the particles is shown in Figure 55. After 18 tidal cycles, only 6% of the initial amount of particles is still in the Wadden Sea area and located mostly over the shallower parts, where they have settled.

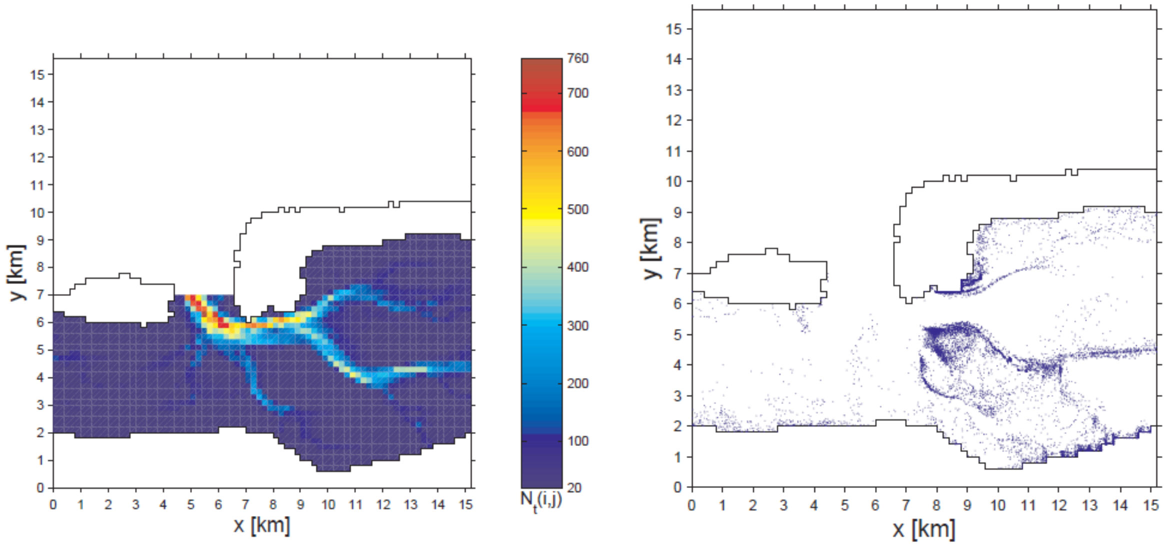

Figure 55: Left: Initial horizontal particle distribution between the islands Baltrum and Langeoog. Right: particle tracer distribution after 18 tidal periods, reprinted from Figure 4.5 and 4.6 on pages 66 and 67 of Wolk (2003).

Currently, GETM model output combined with this particle tracking model is used in a plaice larvae study a North Sea setting (Tiessen et al. (2013). The particles have certain properties, such as growth and mortality, and the objective is to determine what the dominant pathways are for plaice larvae. Figure 56 shows (part of) the results of a validation study. In 2000, the Centre for Environment, Fisheries & Aquaculture Science (CEFAS, UK) released around 30 drifters in the North Sea. Some of these drifter paths are reproduced here by the particle tracking routine. Drifters had a buoy at the surface and a drogue (big sock) at around 12 m, which means that they are hardly influenced by the wind stress at the sea surface, but mostly by the current speed at 12 m depth. Modeled particles were kept at a depth of 7.5 m. The numerical model trajectories (drawn lines in Figure 56) show the cycloid-like motion of the artificial drifters due to the tidal cyclic motion on top of a long-term mean residual circulation from the south-west to the north-east. Model results show a good agreement with drifter paths (dots). Note that these particle tracks are significantly different from the ones in Figure 51 and Figure 52. Clearly, adding a horizontal diffusion to a quasi-stationary circulation without tides, does not diverge pathways as much as the ones in the model results displayed in Figure 56. This is particularly clear for the paths of the orange and purple drifter, which are released at the same location, but diverge significantly after a few days. With the same setup, water parcels having a certain methane concentration can be released at site 22/4b. These water parcels should be advected and diffused through the system and the methane concentration should have a sink, related to the oxidation rate. Besides that, a sink should be added in case the water parcel gets into contact with the overlying atmosphere.

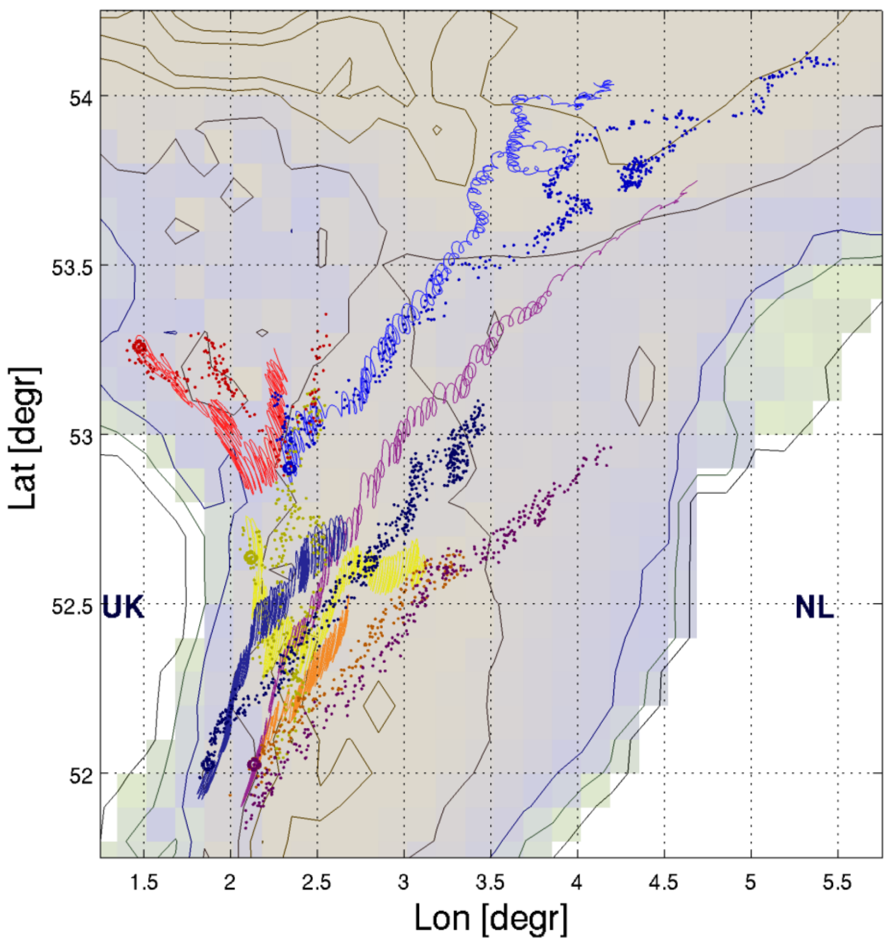

Figure 56: Three drifter paths (light colored dots) from CEFAS cruises in 2000, along with the particle tracks (dark colored lines) from the numerical model. Drifters were released on 22-01 (purple) 25-03 (yellow), 18-05 (orange, dark blue), 19-05 (red, light blue). The drifter tracks took 22 (orange), 33 (red), 39 (purple), 50 (yellow and dark blue) and 60 (light blue) days, reprinted from a figure about to be published in Tiessen et al. (2013).

Conclusions and Discussion

The North Sea displays a complicated and temporal/spatial highly variable hydrography and associated circulation. Tides, wind stress and heat fluxes dominate the setup and variability of the currents. Especially the seasonal stratification is a dominant feature in the northern part of the North Sea, which is expressed as a strong temperature gradient between the upper mixed layer and the lower layer. As the dominant part of the methane released at gas seep sites, amongst which site 22/4b, is dissolved, current may transport it for long distances before it reaches the surface and will be released to the atmosphere.

Many 3D hydrodynamic models have been used to simulate the circulation in the North Sea. In this review, 16 of these models have been discussed, which all have been part in one or more intercomparison studies. The main conclusion is that all models reproduce the general characteristics of the North Sea circulation well, as they are all based on the same fundamental set of equations. However, due to differences in discretization in the horizontal and vertical direction, but also the discretization of the advection schemes and the different ways of incorporating turbulent processes, which occur on scales smaller than the gridsize, lead to different strengths of the seasonal stratification from far too weak to close to observations. Especially, the seasonal stratification should be modeled correctly in terms of time of the onset of stratification and breakdown, but also in terms of the structure in the vertical, if it is present. The stratification has a profound influence on the circulation as the upper and lower layer are strongly separated, which may even cause the currents to be opposing. Thus the transport of methane can and will be totally different under a well-mixed or a stratified condition.

From this review, it can be concluded that any high-resolution model with sufficient layers in the vertical, having a higher order advection scheme and second order turbulence closure will give the best performance in terms of seasonal stratification, horizontal tidal fronts and overall (wind-driven) circulation. Based on these findings, the three most suitable models are GETM, FOAM and ROMS (not necessarily in that order). At this moment, CEFAS is working on a setup with GETM of the entire northwestern European Shelf at 7 km resolution. Furthermore, ROMS is currently used as the numerical ocean weather prediction model at met.no and is being run at 800 m resolution for a strip along the Norwegian Coast, which just incorporates site 22/4b.

Until recently, models where fixed in their core physics, such as the chosen advection scheme or the applied turbulent closure. Nowadays, models have become more and more modular. A nice example is GETM, which uses GOTM as a module for the physics in the vertical, giving a choice for a turbulence closure out of a suite of models that have been proposed and/or used in literature. Also with respect to the advection scheme, GETM is flexible giving a choice between fast low order advection schemes and slower higher order advection schemes. At the moment, the developers of GETM are putting in a lot of effort to make it relatively easy to couple GETM to any module, such as a sediment transport module or a passive tracer module.

As for the fate of methane in the North Sea, a first attempt to estimate its pathways is to couple a particle tracking model to any of the state-of-the-art 3D hydrodynamic models. This after a bubble model (or module) is added to the vertical column model to estimate the amount of methane that dissolves.

The microbial oxidation of methane could be modeled by a simple constant rate of decay, but eventually, a full biogeochemical module should be developed in which dissolved methane is explicitly modeled as an inorganic nutrient source for bacteria. Instead of using just a single 3D hydrodynamic model, such a biogeochemical module can be coupled to a suite of models and being run under slightly different forcing and initial conditions as is common practice in numerical weather forecasting. This provides an ensemble of possible paths that the methane will follow the most likely path.

List of Figures

List of Tables

List of Acronyms

acronym	full name
2D	2 Dimensional
3D	3 Dimensional
4DVAR	4-Dimensional Variational Data Assimilation
AMM	Atlantic Margin Model
AW^d	Atlantic Water deep (deep)
AW^u	Atlantic Water upper (shallow)
BODC	British Oceanographic Data Centre
BW	Baltic Water
CBSW	Central North Sea Water
CEFAS	Centre for Environment, Fisheries & Aquaculture Science
CFL	Courant Friedrichs Levy
COADS	Comprehensive Ocean – Atmosphere Data Set
COHERENS	COupled Hydrodynamical Ecological model for REgioNal Shelf Seas
CONMAN	Comparison of Numerical Ocean Models Applied to Norwegian waters
DA	SYSTEM3 (see Table 1)
DE	DELFT3D (see Table 1)
DJFM	December January February March
DOD	German Oceanographic Data Centre
DWD	German Weather Service
DYNOCS	Dynamics of Connected Seas
ECMWF	European Centre for Medium Range Weather Forecasting
EKASC	Quantitative description of the currents in the Barents and Kara seas in order to estimate the pathways and the fluxes of radionuclides and other environmental contaminants
EKE	Eddy Kinetic Energy
ERA-40	European Reanalysis from 09-01-1957 to 31-08-2002
ERSEM	European Regional Seas Ecosystem Model
ES1,2,3	East Shetland sections
ESAI	East Shetland Atlantic Inflow
FIC	Fair Isle Current
FOAM	Forecast Ocean Assimilation Model
GETM	General Estuarine Transport Model
GHER	GeoHydrodyncamics and Environment Research
GOTM	General Ocean Tubulence Model
HAMELS	Harmonic Analysis, Method of Least Squares
HAMSOM	Hamburg Shelf Ocean Model
HYCOM	HYbrid Coordinate Ocean Model
ICES	International Council for the Exploration of the Sea
IF	IFREMER (see Table 1)

IM	NORWECOM (see Table 1)
IOW	Leibnitz Institute for Baltic Sea Reseach, Warnemünde
ISPRAMIX	ISPRA ocean general circulation model
JCW	Jutland Coastal Water
JJA	June July August
JONSIS	JOint North Sea Information Section
KSW	Kattegat Surface Water
met.no	Norwegian Meteorological Institute
MFI	Munken – Fair Isle section
MIPOM	Meteorological Institute's revised version of the Princeton Ocean Model.
MKE	Mean Kinetic Energy
MRCS	Medium Resolution Continental Shelf
MU	COHERENS (see Table 1)
NAC	North Atlantic Current
NAO	North Atlantic Oscillation
NCW	Norwegian Coastal Water
NEMO	Nucleus for European Modelling of the Ocean
NF	Nolso-Flugga standard hydrographic section
NI/AI	North of Iceland/Arctic Intermediate Water
NODC	National Oceanographic Data Committee of the Netherlands
NOMADS	NOrth Sea Model Advection-Dispersion Study
NORWECOM	NORWegian ECOlogical Model
NS	Navier-Stokes
NSDW	Norwegian Sea Deep Water
NWECS	North Western European Continental Shelf
NWP	Numerical Weather Prediction
OPYC	Ocean and isoPYCnal coordinates
OSTIA	Operational Sea Surface Temperature and Sea Ice Analysis
PANGAEA	Data Publisher for Earth & Environmental Science
PO	POLCOMS (see Table 1)
POLCOMS	Proudman Oceanographic Laboratory Coastal-Ocean Modelling System
QU	ULTIMATE QUICKEST
R^2	coefficient of determination
RANS	Reynolds Averaged Navier-Stokes
RI	RIKZ (see table 1)
ROFI	Region of Fresh Water Influence
ROMS	Regional Ocean Modeling System
SC	Slope Current
SD	Standard Deviation
SKAGEX	SKAGerrak EXperiment
SLP	Sea Level Pressure

SNSW	Southern North Sea Water
SODA	Simple Ocean Data Assimilation
SPM	Suspended Particulate Matter
SSH	Sea Surface Height
SSS	Sea Surface Salinity
SST	Sea Surface Temperature
SSW	Skagerrak Surface Water
SU	SUPERBEE
Sv	Sverdrup
TOPAZ	Towards an Operational Prediction System for the North Atlantic European Coastal Zones
TVD	total variation diminishing scheme
UL	GHER NWECS (see Table 1)
UP	UPSTREAM
ZM	HAMSOM (see Table 1)

Acknowledgements
Jens Greinert and Theo Gerkema (NIOZ) are gratefully acknowledged for their contributions to this literature review. Jens Greinert is thanked for inviting me to attend the PERGAMOM meeting in Gent and introducing met to Ira Leifer. And Theo Gerkema is thanked for his suggestions to project plan. Besides that, Gary Robertson and Alan Judd are thanked for their comments and suggestions to the draft of this review. Moreover, it was a pleasure to have (almost) weekly telecons with Gary Robertson, Joe Smith and Ira Leifer on the progress of the project.

Bibliography

[Albretsen and Røed (2010)] Jon Albretsen and Lars Petter Røed. Decadal long simulations of mesoscale structures in the northern North Sea/Skagerrak using two ocean models. *Ocean Dynamics*, 60: 933–955, 2010. ISSN 1616-7341. doi: 10.1007/s10236-010-0296-0.

[Andersson and Rydberg (1993)] Lars Andersson and Lars Rydberg. Exchange of water and nutrients between the skagerrak and the kattegat. *Estuarine, Coastal and Shelf Science*, 36 (2): 159 – 181, 1993. ISSN 0272-7714. doi: 10.1006/ecss.1993.1011.

[Arakawa and Lamb (1977)] A Arakawa and V R Lamb. *General circulation models of the atmosphere*, chapter Computational design of the basic dynamical processes of the UCLA general circulation model, pages 173–265. New York, Academic Press, Inc, 1977.

[Baart et al. (2012)] Fedor Baart, Pieter H.A.J.M. van Gelder, John de Ronde, Mark van Koningsveld, and Bert Wouters. The effect of the 18.6-year lunar nodal cycle on regional sea-level rise estimates. *Journal of Coastal Research*, 28 (2): 511–516, 2012.

[Backhaus (1985)] Jan O. Backhaus. A three-dimensional model for the simulation of shelf sea dynamics. *Deutsche Hydrografische Zeitschrift*, 38: 165–187, 1985. ISSN 0012-0308. doi: 10.1007/BF02328975.

[Beaugrand (2004)] Grégory Beaugrand. The North Sea regime shift: Evidence, causes, mechanisms and consequences. *Progress in Oceanography*, 60 (2-4): 245 – 262, 2004. ISSN 0079-6611. doi: 10.1016/j.pocean.2004.02.018.

[Becker and Dooley (1995)] G Becker and H Dooley. The 1989/91 high salinity anomaly in the North Sea and adjacent areas. *Ocean Challenge*, 6: 52–57, 1995.

[Becker (1996)] Gerd A. Becker. Sea surface temperature changes in the North Sea and their causes. *ICES Journal of Marine Science: Journal du Conseil*, 53 (6): 887–898, 1996. doi: 10.1006/jmsc.1996.0111.

[Berx and Hughes (2009)] Barbara Berx and Sarah L. Hughes. Climatology of surface and near-bed temperature and salinity on the north-west European continental shelf for 1971-2000. *Continental Shelf Research*, 29 (19): 2286 – 2292, 2009. ISSN 0278-4343. doi: 10.1016/j.csr.2009.09.006.

[Bleck (2002)] Rainer Bleck. An oceanic general circulation model framed in hybrid isopycnic-cartesian coordinates. *Ocean Modelling*, 4 (1): 55 – 88, 2002. ISSN 1463-5003. doi: 10.1016/S1463-5003(01)00012-9.

[Blumberg and Mellor (1987)] A. F. Blumberg and G. L. Mellor. A description of a three-dimensional coastal ocean model. In N. S. Heaps, editor, *Three Dimensional Coastal Ocean Models*, pages 1–16. American Geophysical Union, 1987.

[Boles et al. (2001)] J. R. Boles, J. F. Clark, I. Leifer, and L. Washburn. Temporal variation in natural methane seep rate due to tides. coal oil point area, california. *J. Geophys. Res.*, 106 (C11): 27077–27086, 2001. ISSN 0148-0227.

[Bowers and Simpson (1987)] D.G. Bowers and J.H. Simpson. Mean position of tidal fronts in European-shelf seas. *Continental Shelf Research*, 7 (1): 35 – 44, 1987. ISSN 0278-4343. doi: 10.1016/0278-4343(87)90062-8.

[Brettschneider (1967)] G. Brettschneider. Anwendung des hydrodynamisch-numerischen Verfahrens zur Ermittlung der M2-Mitschwingungsgezeit der Nordsee. Technical Report 7, Mitt. Inst. Meereskd. Univ. Hamburg, 1967. 65 pp.

[Burchard and Bolding (2002)] H. Burchard and K. Bolding. GETM, a general estuarine transport model. Technical report, European Commission, Ispra, 2002.

[Burchard et al. (1999)] H. Burchard, K. Bolding, and M. R. Voillareal. GOTM–a general ocean turbulence model. Theory, applications and test cases. Technical Report EUR 18745 EN, European Commission, 1999.

[Burchard et al. (2006)] H. Burchard, K. Bolding, and L. Umlauf. General estuarine transport model getm - source code and test case documentation. Technical report, Baltic Sea Research Institute Warnemünde, Germany and Bolding and Burchard hydrodynamics, Germany and Denmark, 2006.

[Canuto et al. (2001)] V. M. Canuto, A. Howard, Y. Cheng, and M. S. Dubovikov. Ocean turbulence. part i: One-point closure model - momentum and heat vertical diffusivities. *J. Phys. Oceanogr.*, 31 (6): 1413–1426, June 2001. ISSN 0022-3670.

[Carton et al. (2000a)] James A. Carton, Gennady Chepurin, and Xianhe Cao. A simple ocean data assimilation analysis of the global upper ocean 1950-95. part ii: Results. *J. Phys. Oceanogr.*, 30 (2): 311–326, February 2000. ISSN 0022-3670.

[Carton et al. (2000b)] James A. Carton, Gennady Chepurin, Xianhe Cao, and Benjamin Giese. A simple ocean data assimilation analysis of the global upper ocean 1950-95. part i: Methodology. *J. Phys. Oceanogr.*, 30 (2): 294–309, February 2000. ISSN 0022-3670.

[Chassignet et al. (2003)] Eric P. Chassignet, Linda T. Smith, George R. Halliwell, and Rainer Bleck. North Atlantic simulations with the HYbrid Coordinate Ocean Model (HYCOM): Impact of the vertical coordinate choice, reference pressure, and thermobaricity. *J. Phys. Oceanogr.*, 33 (12): 2504–2526, December 2003. ISSN 0022-3670.

[Ciarlet (1978)] Phillipe G. Ciarlet. *The finite element method for elliptical problems*. North-Holland Publishing Company Amsterdam, New York, Oxford, 1978.

[Courant et al. (1928)] R. Courant, K. Friedrichs, and H. Lewy. über die partiellen differenzengleichungen der mathematischen physik. *Mathematische Annalen*, 100: 32–74, 1928. ISSN 0025-5831. doi: 10.1007/BF01448839.

[Danielssen et al. (1997)] D. S. Danielssen, L. Edler, S. Fonselius, L. Hernroth, M. Ostrowski, E. Svendsen, and L. Talpsepp. Oceanographic variability in the Skagerrak and northern Kattegat, May–June, 1990. *ICES Journal of Marine Science: Journal du Conseil*, 54 (5): 753–773, 1997. doi: 10.1006/jmsc.1996.0210.

[de Haas and Shipboard Scientific Crew (2011)] H. de Haas and 2011 Shipboard Scientific Crew. Cruise report RV Pelagia cruise 64pe340, north sea monitoring. Technical report, Royal Netherlands Institute for Sea Research, 2011.

[de Haas et al. (2012)] H. de Haas, J. Greinert, P. Urban, and P. van Gaever. Listen to the bubbles, see the bubbles, catch the bubbles: Methane seepage in the North Sea. In *11th Dutch Earth Sciences Conference*, 2012.

[Delhez and Martin (1992)] Eric Delhez and Géraldine Martin. Preliminary results of 3-d baroclinic numerical models of the mesoscale and macroscale circulations on the north-western European continental shelf. *Journal of Marine Systems*, 3 (4-5): 423 – 440, 1992. ISSN 0924-7963. doi: 10.1016/0924-7963(92)90014-Y.

[Delhez et al. (2004)] J.M Delhez, P Damm, E de Goede, J.M de Kok, F Dumas, H Gerritsen, J.E Jones, J Ozer, T Pohlmann, P.S Rasch, M Skogen, and R Proctor. Variability of shelf-seas hydrodynamic models: lessons from the NOMADS2 project. *Journal of Marine Systems*, 45 (1-2): 39 – 53, 2004. ISSN 0924-7963. doi: 10.1016/j.jmarsys.2003.09.003.

[Dickson et al. (1988)] Robert R Dickson, Jens Meincke, Svend-Aage Malmberg, and Arthur J Lee. The "Great Salinity Anomaly" in the northern north Atlantic 1968-1982. *Progress in Oceanography*, 20 (2): 103 – 151, 1988. ISSN 0079-6611. doi: 10.1016/0079-6611(88)90049-3.

[du Bois et al. (1995)] P.Bailly du Bois, J.C. Salomon, R. Gandon, and P. Guéguéniat. A quantitative estimate of English Channel water fluxes into the North Sea from 1987 to 1992 based on radiotracer distribution. *Journal of Marine Systems*, 6 (5-6): 457 – 481, 1995. ISSN 0924-7963. doi: 10.1016/0924-7963(95)00018-K.

[Egbert and Erofeeva (2002)] Gary D. Egbert and Svetlana Y. Erofeeva. Efficient inverse modeling of barotropic ocean tides. *J. Atmos. Oceanic Technol.*, 19 (2): 183–204, February 2002. ISSN 0739-0572.

[Egbert et al. (2010)] Gary D. Egbert, Svetlana Y. Erofeeva, and Richard D. Ray. Assimilation of altimetry data for nonlinear shallow-water tides: Quarter-diurnal tides of the northwest European shelf. *Continental Shelf Research*, 30 (6): 668 – 679, 2010. ISSN 0278-4343. doi: 10.1016/j.csr.2009.10.011.

[Eifler and Schrimpf (1992)] W. Eifler and W. Schrimpf. ISPRAMIX, a hydrodynamic program for computing regional sea circulation patterns and transfer processes - part 1: Description of the model equations and of the solution procedure. Technical report, Commission of the European Communities - Joint Research Centre, 1992.

[Etiope (2009)] Giuseppe Etiope. Natural emissions of methane from geological seepage in Europe. *Atmospheric Environment*, 43 (7): 1430 – 1443, 2009. ISSN 1352-2310. doi: 10.1016/j.atmosenv.2008.03.014.

[Fofonoff and Millard (1983)] Nick P. Fofonoff and Robert C. Millard. Algorithms for computation of fundamental properties of seawater. Technical report, UNESCO, 1983.

[Gallego et al. (1999)] Gallego, Heath, Basford, and Mackenzie. Variability in growth rates of larval haddock in the northern North Sea. *Fisheries Oceanography*, 8 (2): 77–92, 1999. ISSN 1365-2419. doi: 10.1046/j.1365-2419.1999.00101.x.

[Gerritsen et al. (2007)] H. Gerritsen, E.D. de Goede, F.W. Platzek, M. Genseberger, J.A.Th.M. van Kester, and R.E. Uittenbogaard. Validation document Delft3D-flow - a software system for 3d flow simulations. Technical report, Deltares, the Netherlands, 2007.

[Graham (1985)] C. Graham. Forties sheet 57°N - 00°E including part of cod 57°N - 02°E. Technical report, British Geological Survey 1:250,000 Series, SeaBed Sediments, 1985.

[Gräwe and Wolff (2010)] Ulf Gräwe and Jörg-Olaf Wolff. Suspended particulate matter dynamsics in a particle framework. *Environmental Fluid Mechanics*, 10: 21–39, 2010. ISSN 1567-7419. doi: 10.1007/s10652-009-9141-8.

[Greinert et al. (2006)] Jens Greinert, Yuriy Artemov, Viktor Egorov, Marc De Batist, and Daniel McGinnis. 1300-m-high rising bubbles from mud volcanoes at 2080 m in the black sea: Hydroacoustic characteristics and temporal variability. *Earth and Planetary Science Letters*, 244 (1-2): 1 – 15, 2006. ISSN 0012-821X. doi: 10.1016/j.epsl.2006.02.011.

[Gräwe et al. (2013)] Ulf Gräwe, Hans Burchard, Peter Holtermann, and Knut Klingbeil. Modelling the thermocline in the North Sea - advantages of adaptive vertical coordinates. *Ocean Modelling*, in prep., 2013.

[Gulev and Hasse (1999)] Sergey K. Gulev and Lutz Hasse. Changes of wind waves in the North Atlantic over the last 30 years. *International Journal of Climatology*, 19 (10): 1091–1117, 1999. ISSN 1097-0088. doi: 10.1002/(SICI)1097-0088(199908)19:10

[Heath and Gallego (1998)] Heath and Gallego. Bio-physical modelling of the early life stages of haddock, Melanogrammus Aeglefinus, in the North Sea. *Fisheries Oceanography*, 7 (2): 110–125, 1998. ISSN 1365-2419. doi: 10.1046/j.1365-2419.1998.00061.x.

[Heath and Gallego (1997)] M. Heath and A. Gallego. From the biology of the individual to the dynamics of the population: bridging the gap in fish early life studies. *Journal of Fish Biology*, 51: 1–29, 1997. ISSN 1095-8649. doi: 10.1111/j.1095-8649.1997.tb06090.x.

[Heath et al. (1999)] M.R. Heath, J.O. Backhaus, K. Richardson, E. McKenzie, D. Slagstad, D. Beare, J. Dunn, J.G. Fraser, A. Gallego, D. Hainbucher, S. Hay, S. Jónasdóttir, H. Madden, J. Mardaljevic, and

A. Schacht. Climate fluctuations and the spring invasion of the North Sea by Calanus Finmarchicus. *Fisheries Oceanography*, 8: 163–176, 1999. ISSN 1365-2419. doi: 10.1046/j.1365-2419.1999.00008.x.

[Heemink et al. (2002)] A.W. Heemink, E.E.A. Mouthaan, M.R.T. Roest, E.A.H. Vollebregt, K.B. Robaczewska, and M. Verlaan. Inverse 3D shallow water flow modelling of the continental shelf. *Continental Shelf Research*, 22 (3): 465 – 484, 2002. ISSN 0278-4343. doi: 10.1016/S0278-4343(01)00071-1.

[Hewer (1980)] R. Hewer. *Untersuchung zur Entwicklung von Extremsturmfluten an der deutschen Nordseeküste auf der Basis hydrodynamisch-numerischer Modelle*. PhD thesis, Univsity Hamburg, 1980.

[Hofmeister et al. (2010)] Richard Hofmeister, Hans Burchard, and Jean-Marie Beckers. Non-uniform adaptive vertical grids for 3D numerical ocean models. *Ocean Modelling*, 33 (1-2): 70 – 86, 2010. ISSN 1463-5003. doi: 10.1016/j.ocemod.2009.12.003.

[Hoitink et al. (2003)] A. J. F. Hoitink, P. Hoekstra, and D. S. van Maren. Flow asymmetry associated with astronomical tides: Implications for the residual transport of sediment. *J. Geophys. Res.*, 108 (C10): 3315–, October 2003. ISSN 0148-0227.

[Holt and James (2001)] J. T. Holt and I. D. James. An s coordinate density evolving model of the northwest European continental shelf, 1, Model description and density structure. , 106: 14015–14034, July 2001. doi: 10.1029/2000JC000304.

[Holt and James (1999)] Jason T. Holt and Ian D. James. A simulation of the southern North Sea in comparison with measurements from the North Sea project. part 1: Temperature. *Continental Shelf Research*, 19 (8): 1087 – 1112, 1999. ISSN 0278-4343. doi: 10.1016/S0278-4343(99)00015-1.

[Holt et al. (2001)] Jason T. Holt, Ian D. James, and J. Eric Jones. An s coordinate density evolving model of the northwest European continental shelf 2, seasonal currents and tides. *J. Geophys. Res.*, 106 (C7): 14035–14053, 2001. ISSN 0148-0227.

[Hovland and Sommerville (1985)] M. Hovland and J.M. Sommerville. Characteristics of two natural gas seepages in the North Sea. *Marine and Petroleum Geology*, 2: 319–326, 1985.

[Hovland et al. (1993)] M. Hovland, A.G. Judd, and R.A. Burke Jr. The global flux of methane from shallow submarine sediments. *Chemosphere*, 26 (1-4): 559 – 578, 1993. ISSN 0045-6535. doi: 10.1016/0045-6535(93)90442-8.

[Hulme et al. (2002)] M. Hulme, G.J. Jenkins, J.R. Turnpenny, T.D. Mitchell, R.G. Jones, J. Lowe, J.M. Murphy, D. Hassell, P. Boorman, R. McDonald, and S. Hill. Climate change scenarios for the United Kingdom: The ukcip02 scientific report. Technical report, Tyndall Centre for Climate Change Research, School of Environmental Sciences, University of East Anglia, Norwich UK., 2002.

[Hurrell (1995)] JW Hurrell. Decadal trends in the North Atlantic Oscillation: regional temperatures and precipitation. *Science*, 269 (5224): 676–679–, August 1995.

[Håvelsrud et al. (2012)]O.E. Håvelsrud, T.H.A Haverkamp, T. Kristensen, K.S. Jakobsen, and A.G. Rike. Metagenomic and geochemical characterization of pockmarked sediments overlaying the troll petroleum reservoir in the North Sea. *BMC Microbiology*, 12: 203, 2012.

[ICES (2005)] ICES. The annual ICES ocean climate status summary 2004/2005. Technical report, ICES Cooperative Research Report, No. 275. 37 pp., 2005.

[ICES 2007b (2007)] ICES 2007b. North Sea conditions – 1st quarter 2007. Technical Report ICES/EuroGOOS North Sea Pilot Project–NORSEPP, ICES/EuroGOOS Planning Group for NORSEPP (PGNSP), 2007.

[Janssen et al. (1999)] F. Janssen, C. Schrum, and J.O. Backhaus. A climatological data set of temperature and salinity for the Baltic Sea and the North Sea. *Deutsche Hydrografische Zeitschrift*, 51: 5–245, 1999. ISSN 0012-0308. doi: 10.1007/BF02933676.

[Judd and Hovland (2007)] A.G. Judd and M. Hovland. *Seabed Fluid Flow.* Cambridge University Press, New York., 2007.

[Judd (2004)] AlanG. Judd. Natural seabed gas seeps as sources of atmospheric methane. *Environmental Geology*, 46: 988–996, 2004. ISSN 0943-0105. doi: 10.1007/s00254-004-1083-3.

[Kauker and Oberhuber (1997)] F Kauker and JM Oberhuber. An isopycnal ocean circulation model of the north sea for dynamical downscaling. Technical report, GKSS Research Centre, P.O. Box 1160, D-21494 Geesthacht, Germany., 1997.

[Kauker and von Storch (2000)] Frank Kauker and Hans von Storch. Statistics of "synoptic circulation weather" in the North Sea as derived from a multiannual OGCM simulation. *J. Phys. Oceanogr.*, 30 (12): 3039–3049, December 2000. ISSN 0022-3670.

[Killworth et al. (1991)] Peter D. Killworth, David J. Webb, David Stainforth, and Stephen M. Paterson. The development of a free-surface Bryan-Cox-Semtner ocean model. *J. Phys. Oceanogr.*, 21 (9): 1333–1348, September 1991. ISSN 0022-3670.

[Kirby and Beaugrand (2009)] Richard R. Kirby and Gregory Beaugrand. Trophic amplification of climate warming. *Proceedings of the Royal Society B: Biological Sciences*, 276 (1676): 4095–4103, 2009. doi: 10.1098/rspb.2009.1320.

[Kochergin (1987)] VP Kochergin. Three-dimensional prognostic models. In *Three-dimensional ocean models.* American Geophysical Union, Washington, 1987.

[LaCasce et al. (2007)] JH LaCasce, LP Røed, L Bertino, and B Ådlandsvik. CONMAN technical report no. 2: analysis of model results. Technical report, Norwegian Meteorological Institute, P.O.Box 43, Blindern, 0313 Oslo, Norway, 2007.

[Lazure and Jegou (1998)] Pascal Lazure and Anne-Marie Jegou. 3D modelling of seasonal evolution of Loire and Gironde plumes on Biscay Bay continental shelf. *Oceanologica Acta*, 21 (2): 165 – 177, 1998. ISSN 0399-1784. doi: 10.1016/S0399-1784(98)80006-6.

[Lenhart and Pohlmann (2004)] Hermann-J. Lenhart and Thomas Pohlmann. North Sea hydrodynamic modelling: a review. *Senckenbergiana maritima*, 34: 53–88, 2004. ISSN 0080-889X. doi: 10.1007/BF03043229.

[Linke et al. (2010)] Peter Linke, Stefan Sommer, Lorenzo Rovelli, and Daniel McGinnis. Physical limitations of dissolved methane fluxes: The role of bottom layer processes. *Marine Geology*, 272: 209–222s, 2010.

[Luyten et al. (1999)] Patrick J. Luyten, John Eric Jones, Roger Proctor, Andy Tabor, Paul Tett, and Karen Wild-Allen. COHERENS - a coupled hydrodynamical-ecological model for regional and shelf seas - user documentation. Technical report, Management Unit of the North Sea Mathematical Models, 1999.

[Madec (2008)] Gurvan Madec. NEMO ocean engine. Technical report, Laboratoire d'Oceanographie et du Climat: Expérimentation et Approches Numeriques, 2008.

[McGinnis et al. (2006)] D. F. McGinnis, J. Greinert, Y. Artemov, S. E. Beaubien, and A. Wüest. Fate of rising methane bubbles in stratified waters: How much methane reaches the atmosphere? *J. Geophys. Res.*, 111 (C9): C09007–, September 2006. ISSN 0148-0227.

[Mork and Blindheim (2000)] Kjell Arne Mork and Johan Blindheim. Variations in the Atlantic inflow to the Nordic Seas, 1955-1996. *Deep Sea Research Part I: Oceanographic Research Papers*, 47 (6): 1035 – 1057, 2000. ISSN 0967-0637. doi: 10.1016/S0967-0637(99)00091-6.

[Naudts et al. (2010)] Lieven Naudts, Jens Greinert, Jeffrey Poort, Joke Belza, Elke Vangampelaere, Dries Boone, Peter Linke, Jean-Pierre Henriet, and Marc De Batist. Active venting sites on the gas-hydrate-bearing Hikurangi margin, off New Zealand: Diffusive- versus bubble-released methane. *Marine Geology*, 272 (1-4): 233 – 250, 2010. ISSN 0025-3227. doi: 10.1016/j.margeo.2009.08.002.

[Newman et al. (2008)] Kori R. Newman, Marie-Helene Cormier, Jeffrey K. Weissel, Neal W. Driscoll, Miriam Kastner, Evan A. Solomon, Gretchen Robertson, Jenna C. Hill, Hanumant Singh, Richard Camilli, and Ryan Eustice. Active methane venting observed at giant pockmarks along the U.S. mid-Atlantic shelf break. *Earth and Planetary Science Letters*, 267 (1-2): 341 – 352, 2008. ISSN 0012-821X. doi: 10.1016/j.epsl.2007.11.053.

[Niemann et al. (2005)] H. Niemann, M. Elvert, M. Hovland, B. Orcutt, A. Judd, I. Suck, J. Gutt, S. Joye, E. Damm, K. Finster, and A. Boetius. Methane emission and consumption at a North Sea gas seep (Tommeliten area). *Biogeosciences Discussions*, 2 (4): 1197–1241, November 2005.

[O'dea et al. (2012)] E.J. O'dea, A.K. Arnold, K.P. Edwards, R. Furner, P. Hyder, M.J. Martin, J.R. Siddorn, D. Storkey, J. While, J.T. Holt, and H. Liu. An operational ocean forecast system incorporating

NEMO and SST data assimilation for the tidally driven European north-west shelf. *Journal of Operational Oceanography*, 5 (1): 3–17, 2012.

[Otto et al. (1990)] L. Otto, J.T.F. Zimmerman, G.K. Furnes, M. Mork, R. Saetre, and G. Becker. Review of the physical oceanography of the North Sea. *Netherlands Journal of Sea Research*, 26 (2-4): 161 – 238, 1990. ISSN 0077-7579. doi: 10.1016/0077-7579(90)90091-T.

[Ouberdous et al. (2002)] M Ouberdous, T Pohlmann, A stips, and W. schrimpf. Comparison of two ocean numerical models: HAMSOM and ISPRAMIX for the North Sea dynamics simulation. Technical report, Joint Research Centre of the European Commission, 2002.

[Pingree (2005)] Robin Pingree. North Atlantic and North Sea climate change: curl up, shut down, NAO and ocean colour. *Journal of the Marine Biological Association of the United Kingdom*, 85 (06): 1301–1315, 2005. doi: 10.1017/S0025315405012488.

[Plag and Tsimplis (1999)] H.-P Plag and M.N Tsimplis. Temporal variability of the seasonal sea-level cycle in the North Sea and Baltic Sea in relation to climate variability. *Global and Planetary Change*, 20 (2-3): 173 – 203, 1999. ISSN 0921-8181. doi: 10.1016/S0921-8181(98)00069-1.

[Pohlmann (1996a)] Thomas Pohlmann. Simulating the heat storage in the North Sea with a three-dimensional circulation model. *Continental Shelf Research*, 16 (2): 195 – 213, 1996. ISSN 0278-4343. doi: 10.1016/0278-4343(95)00032-V.

[Pohlmann (1996b)] Thomas Pohlmann. Predicting the thermocline in a circulation model of the North Sea - part i: model description, calibration and verification. *Continental Shelf Research*, 16 (2): 131 – 146, 1996. ISSN 0278-4343. doi: 10.1016/0278-4343(95)90885-S.

[Proctor (2000)]R. Proctor. North Sea advection dispersion study: 2. assessments of model variability. In *Marine Processes, Ecosystems and Interactions*. Eurocean2000, 2000.

[Proctor and James (1996)] R. Proctor and I.D. James. A fine-resolution 3d model of the southern North Sea. *Journal of Marine Systems*, 8 (3-4): 285 – 295, 1996. ISSN 0924-7963. doi: 10.1016/0924-7963(96)00011-5.

[Proctor et al. (1997)] R. Proctor, A. Baart, P. Berg, J. Boon, E. Deleersnijder, E. Delhez, P. Garreau, H. Gerritsen, J.E. Jones, J. de Kok, P. Lazure, P. Luyten, J. Ozer, T. Pohlmann, K. Ruddick, R. Salden, J.C. Salomon, M. Skogen, B. Tartinville, and H.J. Vested. EC concerted action in the field of numerical modelling of marine systems NOMADS - North Sea Model Advection- Dispersion Study. Technical report, Proudman Oceanographic Laboratory (POL), 1997.

[Pugh (1987)] D. T. Pugh. *Tides, Surges and Mean Sea-Level*. JOHN WILEY & SONS, 1987.

[Rasmussen (1993)] E. B. Rasmussen. *Coastal, Estuarial and Harbour Engineer's Reference Book*, chapter Three-dimensional models, pages 109–116. London (Chapman & Hall), 1993.

[Rehder et al. (1998)] Gregor Rehder, Robin S. Keir, Erwin Suess, and Thomas Pohlmann. The multiple sources and patterns of methane in North Sea waters. *Aquatic Geochemistry*, 4: 403–427, 1998. ISSN 1380-6165. doi: 10.1023/A:1009644600833.

[Rehder et al. (1999)] Gregor Rehder, Robin S. Keir, Erwin Suess, and Monika Rhein. Methane in the northern Atlantic controlled by microbial oxidation and atmospheric history. *Geophys. Res. Lett.*, 26 (5): 587–590, 1999. ISSN 0094-8276.

[Reid and Edwards (2001)] P.C. Reid and M. Edwards. Long-term changes in the Pelagos, Benthos and fisheries of the North Sea. *Senckenb. Marit.*, 31: 107–115, 2001.

[Reid et al. (2001)] Philip C. Reid, Maria de Fatima Borges, and Einar Svendsen. A regime shift in the North Sea circa 1988 linked to changes in the North Sea horse mackerel fishery. *Fisheries Research*, 50 (1-2): 163 – 171, 2001. ISSN 0165-7836. doi: 10.1016/S0165-7836(00)00249-6.

[Reid et al. (2003)] Philip C. Reid, Martin Edwards, Gregory Beaugrand, Morten Skogen, and Darren Stevens. Periodic changes in the zooplankton of the North Sea during the twentieth century linked to oceanic inflow. *Fisheries Oceanography*, 12 (4-5): 260–269, 2003. ISSN 1365-2419. doi: 10.1046/j.1365-2419.2003.00252.x.

[Rio et al. (2005)] M.-H. Rio, P. Schaeffer, J.-M. Lemoine, and F. Hernandez. Estimation of the ocean mean dynamic topography through the combination of altimetric data, in-situ measurements and GRACE geoid: From global to regional studies. In *Proceedings of the GOCINA international workshop, Luxembourg.*, 2005.

[Rossiter (1954)] J. R. Rossiter. The North Sea storm surge of 31 january and 1 february 1953. *Philosophical Transactions of the Royal Society of London. Series A, Mathematical and Physical Sciences*, 246 (915): 371–400, 1954. doi: 10.1098/rsta.1954.0002.

[Rydberg et al. (1996)] L. Rydberg, J. Haamer, and O. Liungman. Fluxes of water and nutrients within and into the Skagerrak. *Journal of Sea Research*, 35 (1-3): 23 – 38, 1996. ISSN 1385-1101. doi: 10.1016/S1385-1101(96)90732-7.

[Schneider von Deimling et al. (2011)] J. Schneider von Deimling, G. Rehder, J. Greinert, D.F. McGinnnis, A. Boetius, and P. Linke. Quantification of seep-related methane gas emissions at Tommeliten, North Sea. *Continental Shelf Research*, 31 (7-8): 867 – 878, 2011. ISSN 0278-4343. doi: 10.1016/j.csr.2011.02.012.

[Schneider von Deimling et al. (2010)] Jens Schneider von Deimling, J. Greinert, N. R. Chapman, Wolfgang Rabbel, and Peter Linke. Acoustic imaging of natural gas seepage in the North Sea: Sensing bubbles under control of variable currents. *Limnology and Oceanography: Methods*, 8: 155–171, 2010.

[Schroot et al. (2005)] Barthold M. Schroot, Gerard T. Klaver, and Ruud T.E. Schüttenhelm. Surface and subsurface expressions of gas seepage to the seabed - examples from the southern North Sea. *Marine and Petroleum Geology*, 22 (4): 499 – 515, 2005. ISSN 0264-8172. doi: 10.1016/j.marpetgeo.2004.08.007.

[Schrum (1997)] Corinna Schrum. Thermohaline stratification and instabilities at tidal mixing fronts: results of an eddy resolving model for the German Bight. *Continental Shelf Research*, 17 (6): 689 – 716, 1997. ISSN 0278-4343. doi: 10.1016/S0278-4343(96)00051-9.

[Sharples et al. (2006)] Jonathan Sharples, Oliver N. Ross, Beth E. Scott, Simon P.R. Greenstreet, and Helen Fraser. Inter-annual variability in the timing of stratification and the spring bloom in the north-western North Sea. *Continental Shelf Research*, 26 (6): 733 – 751, 2006. ISSN 0278-4343. doi: 10.1016/j.csr.2006.01.011.

[Shchepetkin and McWilliams (2005)] Alexander F. Shchepetkin and James C. McWilliams. The Regional Oceanic Modeling System (ROMS): a split-explicit, free-surface, topography-following-coordinate oceanic model. *Ocean Modelling*, 9 (4): 347 – 404, 2005. ISSN 1463-5003. doi: 10.1016/j.ocemod.2004.08.002.

[Søiland and Skogen (2000)] H. Søiland and M. D. Skogen. Validation of a three-dimensional biophysical model using nutrient observations in the North Sea. *ICES Journal of Marine Science: Journal du Conseil*, 57 (4): 816–823, 2000. doi: 10.1006/jmsc.2000.0567.

[Skogen et al. (1995)] Morten D Skogen, Einar Svendsen, Jarle Berntsen, Dag Aksnes, and Kåre B Ulvestad. Modelling the primary production in the North Sea using a coupled three-dimensional physical-chemical-biological ocean model. *Estuarine, Coastal and Shelf Science*, 41 (5): 545 – 565, 1995. ISSN 0272-7714. doi: 10.1016/0272-7714(95)90026-8.

[Skogen et al. (1997)] Morten D. Skogen, Einar Svendsen, and Marek Ostrowski. Quantifying volume transports during SKAGEX with the Norwegian ecological model system. *Continental Shelf Research*, 17 (15): 1817 – 1837, 1997. ISSN 0278-4343. doi: 10.1016/S0278-4343(97)00051-4.

[Skogen et al. (2004)] Morten D. Skogen, Henrik Søiland, and Einar Svendsen. Effects of changing nutrient loads to the North Sea. *Journal of Marine Systems*, 46 (1-4): 23 – 38, 2004. ISSN 0924-7963. doi: 10.1016/j.jmarsys.2003.11.013.

[Sündermann and Pohlmann (2011)] Jürgen Sündermann and Thomas Pohlmann. A brief analysis of North Sea physics. *Oceanologia*, 53(3): 663–689, 2011.

[Stanev et al. (2003)] Emil V. Stanev, Jorg-Olaf Wolff, Hans Burchard, Karsten Bolding, and Götz Flöser. On the circulation in the east Frisian Wadden Sea: numerical modeling and data analysis. *Ocean Dynamics*, 53: 27–51, 2003. ISSN 1616-7341. 10.1007/s10236-002-0022-7.

[Stips et al. (2004)] Adolf Stips, Karsten Bolding, Thomas Pohlmann, and Hans Burchard. Simulating the temporal and spatial dynamics of the North Sea using the new model GETM (General Estuarine Transport Model). *Ocean Dynamics*, 54: 266–283b, 2004. ISSN 1616-7341. doi: 10.1007/s10236-003-0077-0.

[Tartinville et al. (1998)]B. Tartinville, E. Deleersnijder, P. Lazure, R. Proctor, K.G. Ruddick, and R.E. Uittenbogaard. A coastal ocean model intercomparison study for a three-dimensional idealised test case.

Applied Mathematical Modelling, 22 (3): 165 – 182, 1998. ISSN 0307-904X. doi: 10.1016/S0307-904X(98)00015-8.

[Tiessen et al. (2013)] M. Tiessen, P. Ruardij, H. van der Veer, and T. Gerkema. Numerical modeling of larval transport in the southern North Sea. *in prep.*, 2013.

[Tomczak (1996)] Matthias Tomczak. Lecture notes in oceanography. Flinders University, Adelaide, Australia School of Chemistry, Physics & Earth Sciences, 1996.

[Torres et al. (2002)] M.E. Torres, J. McManus, D.E. Hammond, M.A. de Angelis, K.U. Heeschen, S.L. Colbert, M.D. Tryon, K.M. Brown, and E. Suess. Fluid and chemical fluxes in and out of sediments hosting methane hydrate deposits on hydrate ridge, or, i: Hydrological provinces. *Earth and Planetary Science Letters*, 201 (3-4): 525 – 540, 2002. ISSN 0012-821X. doi: 10.1016/S0012-821X(02)00733-1.

[Turrell et al. (1996)] W. R. Turrell, G. Slesser, R. Payne, R. D. Adams, and P. A. Gillibrand. Hydrography of the east Shetland basin in relation to decadal North Sea variability. *ICES Journal of Marine Science: Journal du Conseil*, 53 (6): 899–916, 1996. doi: 10.1006/jmsc.1996.0112.

[Valentine et al. (2001)] David L Valentine, Douglas C Blanton, William S Reeburgh, and Miriam Kastner. Water column methane oxidation adjacent to an area of active hydrate dissociation, Eel River Basin. *Geochimica et Cosmochimica Acta*, 65 (16): 2633 – 2640, 2001. ISSN 0016-7037. doi: 10.1016/S0016-7037(01)00625-1.

[van den Hurk et al. (2006)] B. van den Hurk, A. Klein Tank, G. Lenderink, A. van Ulden, G.J. van Oldenborgh, C. Katsman, H. van den Brink, F. Keller, J. Bessembinder, G. Burgers, G. Komen, W. Hazeleger, and S. Drijfhout. *KNMI Climate Change Scenarios 2006 for the Netherlands*. KNMI Scientific Report WR 2006-01, 2006.

[van Velzen (2010)] N. van Velzen. *A Generic Software Framework for Data Assimilation and Model Calibration*. PhD thesis, Electrical Engineering, Mathematics and Computer Science, Delft Institute of Applied Mathematics, 2010.

[Vested et al. (1992)] Hans Jacob Vested, Peter Justesen, and Lars Ekebjærg. Advection-dispersion modelling in three dimensions. *Applied Mathematical Modelling*, 16 (10): 506 – 519, 1992. ISSN 0307-904X. doi: 10.1016/0307-904X(92)90001-J.

[Wegener et al. (2008)] G. Wegener, M. Shovitri, K. Knittel, H. Niemann, M. Hovland, and A. Boetius. Biogeochemical processes and microbial diversity of the Gullfaks and Tommeliten methane seeps (northern North Sea). *Biogeosciences*, 5: 1127–1144., 2008.

[Weijerman et al. (2005)] Mariska Weijerman, Han Lindeboom, and Alain F. Zuur. Regime shifts in marine ecosystems of the North Sea and Wadden Sea. *MARINE ECOLOGY PROGRESS SERIES*, 298: 21–39, 2005.

[Weisse and Günther (2007)] Ralf Weisse and Heinz Günther. Wave climate and long-term changes for the southern North Sea obtained from a high-resolution hindcast 1958-2002. *Ocean Dynamics*, 57: 161–172, 2007. ISSN 1616-7341. doi: 10.1007/s10236-006-0094-x.

[Winther et al. (2007)] Nina G. Winther, Yves G. Morel, and Geir Evensen. Efficiency of high order numerical schemes for momentum advection. *Journal of Marine Systems*, 67 (1-2): 31 – 46, 2007. ISSN 0924-7963. doi: 10.1016/j.jmarsys.2006.08.004.

[Wolk (2003)] F. Wolk. Three-dimensional lagrangian tracer modelling in Wadden Sea areas. Master's thesis, Carl von Ossietzky University Oldenburg, 2003.

NIOZ Royal Netherlands Institute for Sea Research is an Institute of the Netherlands Organization for Scientific Research (NWO).

NIOZ Texel
Landsdiep 4
1797 SZ 't Horntje, Texel

Postbox 59
1790 AB Den Burg, Texel
Nederland
Telephone: +31(0)222 - 369300
Fax: +31(0)222 - 319674

NIOZ Yerseke
Korringaweg 7
4401 NT Yerseke

Postbox 140
4400 AC Yerseke
Nederland
Telephone: +31(0)113 - 577417
Fax: +31(0)113 - 573616

www.nioz.nl

NIOZ Report 2013-3

The mission of NIOZ is to gain and communicate scientific knowledge on seas and oceans for a better understanding and sustainability of our planet, to manage the national facilities for sea research and to support research and education in the Netherlands and in Europe.